The American Mineralogist

Illinois U Library

Journal of the Mineralogical Society of America

Vol. 39 SEPTEMBER-OCTOBER, 1954 Nos. 9 and 10

Contents

Origin of dunites and of olivine-rich inclusions in basaltic rocks .... Clarence S. Ross, Margaret D. Foster and Alfred T. Myers 693

Solubility of albite in hydrothermal solutions .... A. F. Frederickson and Joseph E. Cox 738

Calculation of position and indices of Laue spots on Laue-photographs .... H. Kedesy 750

Relative geologic age measurements on granites by pleochroic haloes and radioactivity of the minerals in their nuclei .... Ichikazu Hayase 761

The coalescence of hexagonal and cubic polymorphs in tetrahedral structures as illustrated by some wurtzite-sphalerite crystal groups .... Richard S. Mitchell and Alice S. Corey 773

The bonding energies of some silicate minerals .... W. D. Keller 783

A new variety of antigorite (ortho-antigorite) from Unst, Shetland Islands .... G. W. Brindley and O. von Knorring 794

Determination of the crystal structure of nepheline .... M. J. Buerger, Gilbert E. Klein and Gabrielle Donnay 805

Mordenite as an alteration product of a pitchstone glass .... P. G. Harris and G. W. Brindley 819

Wisaksonite is metamict uranoan thorite .... C. Osborne Hutton 825

Notes and news: Ortho-antigorite and the tetrahedral configuration of hydroxyl ions .... Duncan McConnell 830

Allanite pegmatite, San Gabriel Mountains, Los Angeles County, California .... George J. Neuerburg 831

A modification of the Chayes point counter stage .... Melvin A. Rosenfeld 834

The chemical formula of clarkeite .... John W. Gruner 836

The indirect determination of β and 2V .... P. McL. Swift 838

Mineralogical Society (London) 841

Book reviews 843

New mineral names 848

EDITOR: WALTER F. HUNT
ASSISTANT EDITOR: LEWIS S. RAMSDELL

BOARD OF ASSOCIATE EDITORS:
MICHAEL FLEISCHER
ELBURT F. OSBORN
IAN CAMPBELL
GEORGE TUNELL (1954)
ADOLF PABST (1954–55)
BRIAN MASON (1954–56)

Published bi-monthly by the Society

Mineralogical Society of America

ASSOCIATED WITH THE GEOLOGICAL SOCIETY OF AMERICA

President: **Sterling B. Hendricks**, U. S. Department of Agriculture, Beltsville, Maryland.
Vice-President: **Harry H. Hess**, Princeton University, Princeton, New Jersey.
Secretary: **C. S. Hurlbut, Jr.**, Harvard University, Cambridge, Massachusetts.
Treasurer: **Earl Ingerson**, U. S. Geological Survey, Washington 25, D. C.
Editor: **Walter F. Hunt**, University of Michigan, Ann Arbor, Michigan.
Councillors: **George T. Faust**, U. S. Geological Survey, Washington 25, D. C.
Victor T. Allen, Institute of Geophysical Technology, St. Louis, Missouri.
C. Osborne Hutton, Stanford University, Palo Alto, California.
Felix Chayes, Geophysical Laboratory, Washington, D. C.
J. D. H. Donnay, The Johns Hopkins University, Baltimore, Maryland.

The enlarged issues of this journal for 1954 are made possible by a grant from the Penrose Fund of the Geological Society of America.

The American Mineralogist—Journal of the Mineralogical Society of America

A journal containing articles on mineralogy, crystallography, petrography, and allied sciences, is issued every two months. Contributions are invited from everyone.

Office of Publication, Mineralogical Laboratory, Ann Arbor, Mich.

The general conduct of the journal is in the hands of the editor, **Walter F. Hunt**, Ann Arbor, Michigan, to whom all manuscripts should be submitted. To assist the editor the council of the Mineralogical Society has appointed **Lewis S. Ramsdell**, Ann Arbor, Michigan, assistant editor, and the following board of associate editors:

Ian Campbell, California Institute of Technology, Pasadena 4, California.
Michael Fleischer, U. S. Geological Survey, Washington, D. C.
Brian H. Mason, American Museum of Natural History, New York, N. Y.
Elburt F. Osborn, Pennsylvania State College, State College, Pa.
Adolf Pabst, University of California, Berkeley 4, California.
George Tunell, University of California at Los Angeles, California.

It will expedite publication if two copies of each manuscript are submitted to the editor.

Contributors of leading articles are given without charge 100 reprints (without covers) of their article. If additional reprints are desired these can be purchased at the following rates:

Pages	*1–4*	*5–8*	*9–12*	*13–16*	*17–20*	*21–24*	*25–28*	*29–32*	*Covers*
Copies									
25	$3.50	$5.00	$ 8.00	$ 9.50	$11.00	$13.00	$15.00	$16.00	$4.90
50	3.80	5.55	8.80	10.40	12.10	14.20	16.40	17.50	5.50
75	4.10	6.10	9.60	11.30	13.20	15.40	17.80	19.00	6.10
100	4.40	6.65	10.40	12.20	14.30	16.60	19.20	20.50	6.70
Addl. C's	1.20	2.20	3.20	3.60	4.40	4.80	5.60	6.00	2.40

Cover Composition $1.55.

Sent to all members and fellows of the Mineralogical Society of America. Subscription price, $4.00 per year (single copies of normal issues, $1.00 plus postage).

Entered as second class matter at the post office at Menasha, Wis., under Act of March 3, 1879. Acceptance for mailing at the special rate of postage provided for in section 1103, Act of Oct. 3, 1917, paragraph 4 section 429 P. L. & R. authorized March 13, 1922.

Notice of change of address, orders, and remittances should be sent to Dr. Earl Ingerson, U. S. Geological Survey, Washington 25, D. C.

Printed by the George Banta Publishing Company, Menasha, Wisconsin
Printed in the United States of America

THE AMERICAN MINERALOGIST

JOURNAL OF THE MINERALOGICAL SOCIETY OF AMERICA

Vol. 39 SEPTEMBER-OCTOBER, 1954 Nos. 9 and 10

ORIGIN OF DUNITES AND OF OLIVINE-RICH INCLUSIONS IN BASALTIC ROCKS[1]

CLARENCE S. ROSS,[2] MARGARET D. FOSTER,[3] AND ALFRED T. MYERS.[3]

ABSTRACT

Basaltic rocks characterized by nodulelike inclusions of olivine and related minerals are of world-wide occurrence and have long been known, especially in Germany. Everywhere the nodules show a remarkable uniformity of chemical and mineral composition and in this respect are similar to dunites—intrusive rocks of equally wide distribution. This similarily in the chemical and mineral composition of the two modes of occurrence and the wide distribution of both of these, suggest the value of a detailed study. This paper gives the results of a large number of chemical and spectrographic analyses of the minerals in the nodules and in dunites and discusses the mineralogic and geologic relationships. The authors conclude that dunites have been brought up from profound depth by orogenic processes, and olivine-rich nodules have been carried up from the same source by basaltic magmas.

TABLE OF CONTENTS

Abstract 693
Introduction 695
Acknowledgments 695
Occurrences of Nodulelike Inclusions in Basaltic Rocks 696
  Localities of Analyzed Materials 697
    Hawaiian Islands 697
    Peridot Cove, Arizona 698
    Meng-Chian, Manchuria 699
    Camargo, Mexico 699
    Ludlow, California 700
    Dreiser Weiher, Eifel, Germany 700
    Kapfenstein, Austria 700
    Alaska 701
    Africa 701
  Localities of Earlier Studies 702
Occurrences of Dunite 704
  Localities of Analyzed Materials 704
    Dun Mountain, New Zealand 704

---

[1] Publication authorized by the Director, U. S. Geological Survey.

[2] Geologist, U. S. Geological Survey.

[3] Chemist, U. S. Geological Survey.

        - Webster, North Carolina ... 705
        - New Caledonia ... 705
        - Twin Sisters, Washington ... 705
    - Methods of Separation and Chemical Analysis ... 705
    - Discussion of Chemical and Mineralogical Studies ... 719
    - Relation to Host Rocks ... 721
- Origin of Dunite ... 723
    - North Carolina ... 723
        - Inclusions ... 724
        - Structure ... 724
        - Border Relationships ... 724
        - Serpentinization ... 725
    - New Zealand ... 725
    - Sweden ... 726
    - Physical and Chemical Relations ... 726
    - Orogenic Relations ... 727
    - Structures ... 727
    - Summary ... 728
- Origin of Nodulelike Inclusions in Basaltic Rocks ... 728
    - Chemical and Mineral Relations ... 729
    - Structures ... 729
    - Source and Emplacement ... 730
    - Summary ... 731
- Origin of Dunite and Nodulelike Inclusions Contrasted ... 732
- Conclusions ... 734
- References ... 735

Illustrations

1. Distribution of Major Constituents in Minerals of Nodules and Dunites ... 720
2. Distribution of Minor Constituents in Minerals of Nodules and Dunites ... 720
3. Reproduction of an illustration by Ernst (1936, p. 638, Fig. 2) showing "grain deformation and elongation in the plane of foliated structure" of the olivine ... 729

List of Tables

1. Mineral Composition of Nodules from Dreiser Weiher ... 700
2. Mineral Composition of Nodules from Finkenberg, near Bonn ... 703
3. Localities of Samples Analyzed in Tables 4 to 11 ... 706
4. Analyses of Olivines ... 707
5. Analyses of Enstatites ... 708
6. Analyses of Chromian Diopsides ... 709
7. Analyses of Chromian Spinels and Chromites ... 710
8. Spectrographic Determination of Minor Elements in Olivines ... 711
9. Spectrographic Determination of Minor Elements in Enstatites ... 712
10. Spectrographic Determination of Minor Elements in Chromian Diopsides ... 713
11. Spectrographic Determination of Minor Elements in Chromian Spinels and Chromites ... 714
12. Localities of Samples for Analyses Quoted in Tables 13 to 16 ... 715
13. Analyses of Olivines ... 715
14. Analyses of Enstatites ... 716
15. Analyses of Diopsides ... 716

16. Analyses of Picotites 717
17. Chemical Procedure for Chromian Spinels and Chromites 718
18. Mode of Olivine Melilitite from Westberges 721
19. Mode of Olivine Melilitite from Hochbol 721
20. Chemical Analyses of Nodule-bearing Rocks 722
21. Norms of Nodule-bearing Rocks 722

INTRODUCTION

Few igneous rocks present more interesting petrogenetic relationships or greater possibilities of significant conclusions based on those relationships than do the monomineralic rocks, and of these the peridotites, composed essentially of olivine, have been the most widely discussed. The geologist is interested in the distribution, mode of intrusion, and relations to tectonic processes; the mineralogist is interested in the minerals, their relationships, and the variations in their composition; and the geochemist is interested in the physical chemistry of their formation. Cosmogonists are interested in any information about the materials of the deeper portions of the earth's crust, which these rocks may reveal.

Peridotite rocks are found in two distinct modes of occurrence—as dunites and related rocks, and as olivine-rich nodules in basaltic rocks. These types, both of world-wide occurrence, are particularly significant in that they show chemical and mineralogic similarities that indicate a genetic relationship, which this paper will explore.

ACKNOWLEDGMENTS

The study of the minerals in olivine-rich nodule inclusions in basaltic rocks and of the same minerals in dunites was suggested by excellent samples submitted by Senor Carlos Sisniega from Camargo, Chihuahua, Mexico. The results of chemical analyses of the olivine, enstatite, chromian diopside, and chromian spinel from that locality indicated that a systematic study of similar materials would have geologic as well as mineralogic value.

The olivine nodules in the collections of the U. S. National Museum in Washington were made available for analysis by Dr. William F. Foshag, and represent materials from Kapfenstein, Austria; Dreiser Weiher, Germany; Peridot Cove, Arizona; and Salt Lake Crater, Oahu, Territory of Hawaii. Dr. Foshag's advice has been of great help in this study.

The writers wish to acknowledge the cooperation of Dr. Harry H. Hess of Princeton University, Dr. Hisashi Kuno of Tokyo University, Dr. Gordon A. Macdonald of the Hawaiian Volcanic Observatory, and Dr. Thomas P. Thayer of the U. S. Geological Survey. Monoclinic pyroxenes analyzed in the course of this investigation have been placed at the

disposal of Dr. Hess, and will thus contribute to his valuable studies of the pyroxene group of minerals. Through the courtesy of Dr. Kuno, samples which he collected from near Meng-Chian, east Manchuria, and from Ichinomegata, Oga Peninsula, Akita Prefecture, Japan, were made available. Dr. Kuno also provided the chemical analyses of the host rock of the nodule from Ichinomegata. Dr. Kuno is making an optical study of the orthorhombic pyroxenes analyzed in the course of this study.

Samples from several localities in Hawaii were contributed by Dr. Macdonald. The dunite and related websterite from Webster, North Carolina, were collected by the senior author, as were the dunite samples from Dun Mountain, New Zealand, and from a locality near Noumea, New Caledonia. The dunite from the Twin Sisters area of Washington was contributed by Dr. Thayer.

OCCURRENCES OF NODULELIKE INCLUSIONS IN BASALTIC ROCKS

The inclusions of olivine and related minerals in basaltic rocks, commonly called "knollen," have long been known in Germany and Austria, and many occurrences have been mentioned in the literature. Schadler (1914) has compiled a list of localities and papers that have been helpful in this study. These papers indicate that a zone of basaltic rocks, characterized by "knollen" reaches from western Poland across central Germany, in an arc beginning just west of Breslau and extending through Saxony, with a marked concentration in Hesse and the region immediately north, and seemingly ending on the west, at Luxembourg. Another zone seems to extend from the region of Graz west to the Black Forest and Kaiserstuhl regions along the north flank of the Alps.

Nodule inclusions in basaltic rocks have been reported from localities in Hungary, Bulgaria, Sweden, France, Portugal, and Sardinia. They are also known to occur in Jan Mayen—an island northeast of Iceland—Japan, Manchuria, Morocco and Nigeria in Africa, the Hawaiian Islands, New Zealand, Alaska, Mexico, and the western United States.

The type locality for dunite is South Island, New Zealand, where, together with its alteration product serpentine, dunite occurs in a zone in the rugged Southern Alps of that island. In the western Pacific, dunite and serpentine occur in great arcs and are recognized in New Caldeonia, Australia, the Celebes, and the Philippines. In eastern North America a zone extends from Newfoundland to Alabama, and in western North America another zone extends from Alaska south through California. In the West Indies a belt extends from Cuba toward Guatemala. Other occurrences are known in Sweden, Norway, Italy, and Scotland. Dunite and serpentine occur in a belt in Asia Minor that extends eastward. Hess (1939) has discussed the relation of such belts to mountain-building forces, and his paper is an excellent source of information on the relation of the distribution of dunite and serpentine to major tectonic zones.

Localities of Analyzed Materials

Hawaiian Islands: The largest group of specimens from any one locality is that from the Hawaiian Islands, contributed by Dr. Macdonald. The collection of samples from the 1801 Kaupulehu lava flow of Hualalai is especially complete, and shows a marked range in size and character of nodular inclusions. Stearns and Macdonald (1946, p. 147) describe the occurrence of these nodules as follows: "Several rivers [of lava] flowed seaward from this vent to form the Kaupulehu flow. This flow contains many thousands of angular and subangular xenoliths of dunite and gabbro mostly under a foot in diameter. . . . Apparently the magma stoped away a large precooled mass of dunite and gabbro before eruption."

Some nodules from Hawaii are nearly pure olivine with only a trace of diopside and chromian spinel. Other nodules are almost pure diopside, but many are made up of nearly equal proportions of olivine and diopside. The chromian spinel is sparse in most nodules but may comprise as much as 2 per cent. One specimen contains about equal proportions of plagioclase (An 75) and olivine, and another about the same proportion of diopside and plagioclase. The diopside is, for the most part, dark gray or gray green in the hand specimen but nearly colorless in thin section. Bright-green diopside, which is characteristic of the inclusions in other occurrences, was observed in only one specimen. The grains of olivine may be as large as 8 mm. in diameter, and the diopside grains, 12 mm. One specimen—representing a part of a single diopside crystal—is about 8 by 10 cm. in diameter.

The Kauai samples are part of the late Koloa volcanic series and came from the Grove Farm quarry near the road southwest of Lihue. The nodules are closely spaced in these samples, are subangular, and reach 5 cm. in diameter. The inclusions are dominantly olivine (Table 4, No. 9) and estatite (Table 5, No. 9). No diopside was observed, but a fraction of 1 per cent of chromian spinel (Table 7, No. 9) was noted.

An unusually interesting specimen submitted by Dr. Macdonald was collected by Rev. Walter Schilling of Hilo from a small cinder cone west of Hale Pohaku on the south side of Mauna Kea. This sample contains the four minerals that so widely characterize nodule inclusions—olivine, enstatite, chromian diopside, and chromian spinel. An analysis of the chromian diopside is presented in Table 6, No. 10, and of the chromian spinel in Table 7, No. 10

The material from Salt Lake Crater, Oahu, is represented by U.S.N.M. Specimen No. 53948. The nodules reach a diameter of 4 cm. and are subangular. The minerals present are dominantly olivine (Table 4, No. 8), enstatite (Table 5, No. 8), chromian diopside (Table 6, No. 8), and chromian spinel (Table 7, No. 8).

Another group of nodules is from stream boulders, from Kapohakukilomanu stream on the south slope of Kauai. These nodules are abundant but small—not larger than 1 to 3 cm. in diameter in the specimens observed. Many of them are subangular. Some of the nodules are almost pure olivine, but others contain pale-green chromian diopside. Enstatite is sparse in all the specimens; in fact the group is unusual in that chromian diopside is more abundant than enstatite.

Another group of samples is from the Ohia Lodge flow of 1950. The largest nodule in these specimens is 2 cm. in diameter. It is dominantly olivine but contains enstatite, chromian diopside, and chromian spinel. A slightly smaller nodule from the same source is composed of olivine, bytownite, enstatite, chromian diopside, and sparse chromian spinel.

Peridot Cove, Arizona: The locality locally known as the Peridot Cinder Cove, and described as Rice Station by Lawsen, lies in Gila County, Arizona, on the San Carlos Apache Indian Reservation, about 20 miles southeast of Globe, Arizona, and about 8 miles north of the Coolidge Dam. Subsequent to the study of the National Museum material, Ralph S. Cannon and N. P. Peterson of the U. S. Geological Survey visited the locality and collected additional specimens from about 1 mile west of the village of Peridot. Mr. Cannon reports that the material collected by them was from a scoraceous basalt layer underlying the cinder cone, and which contains abundant olivine nodules. The geologic age of the cinder cone is probably Late Pleistocene or Recent. For years the Apache Indians have collected and sold gem peridote from the area and guard it jealously. In describing the bombs, Lausen says, "The olivine bombs in the tuffs are usually ellipsoidal in shape and quite variable in size. The one shown in Fig. 1, p. 294 [of Lausen's paper], is fifteen inches in length. One was noted near the base of the cinder cone nearly thirty inches long and half as wide. . . . Invariably they are surrounded by a thin shell of vesicular basalt. . . . The surface of the bombs is rather smooth and suggests that there may have been some resorption of the olivine before it was thrown out by the explosions that gave rise to the tuffs.

"On a freshly broken surface the interiors of these bombs were found to consist of a granular mass of interlocking and glittering grains of olivine."

In a description of the diopside, Lausen states, "This material is relatively scarce. One large crystal found in the vesicular basalt was two inches in length. Usually the fragments are less than one-half inch."

Lausen describes the associated basalt flow as follows (1927, p. 295): "In close proximity to the cone the basalt flow is ten feet thick; the lower six feet of which is thickly crowded with nodules of granular olivines . . . many of these nodules are quite angular, while others are rounded . . . and many of the nodules are so closely crowded together as to touch. At one place along the present edge of the flow it was estimated that olivine nodules constituted fully 60 per cent of the lower six feet of the flow, while the remaining 40 per cent was vesicular basalt." The analysis of the olivine from Peridot Cove is presented in Table 4, No. 3; of the enstatite, in Table 5, No. 3; of the chromian diopside, in Table 6, No. 3; and of the chromian spinel, in Table 7, No. 3. Many of the olivine grains are perfectly clear, reach a diameter of 1 cm., and have been used as gem peridote.

Lausen mentions the possibility that the olivine nodules are detached blocks of a mass of dunite occurring in this region, but, he rejects this mode of origin and concludes that the olivine masses were formed as segregations in a volcanic pipe.

In the summer of 1952, Dr. Ralph S. Cannon of the U. S. Geological Survey collected additional specimens from the Peridot Cove locality. One of these specimens is a volcanic bomb that is subangular in shape, and measures about 10 by 14 cm. An outer shell of basaltic material is only a few millimeters in thickness. The mineral composition is the same as that of samples previously studied. Some of the olivines which have weathered from the bombs range up to 1 cm. in diameter and constitute a source of gem quality peridot. Another bomb fragment is composed dominantly of clinopyroxene but it is dark colored in the hand specimen, rather than green. With this is a small proportion of chromian spinel and olivine.

Meng-Chian, Manchuria: The material from the town of Meng-Chian was described by Dr. Kuno as an olivine-enstatite-diopside nodule in an olivine basalt. The material is completely unaltered and contains chromian spinel in addition to the materials mentioned. The nodules are reported to reach 20 cm. in diameter. Dr. Kuno had no opportunity to collect more than a very small specimen at the time, and although he very generously sent us all the material available, there was not enough to supply the entire group of minerals in amounts adequate for chemical analyses. An analysis of the olivine is given in Table 4, No. 6 and of the enstatite in Table 5, No. 6.

Camargo, Mexico: The material from Camargo, Chihuahua, is broken into small fragments but evidently occurs as rather large cores in volcanic bombs. The minerals are very fresh, and all four minerals characteristic of nodule inclusions are abundant. The chromian diopside (Table 6, No. 1) and chromian spinel (Table 7, No. 1) are unusually abundant and occur as crystals up to 4 mm. in diameter. The olivine (Table 4, No. 1) is in grains as much as 20 mm. in diameter, and the enstatite (Table 5, No. 1) reaches dimensions of 8 mm.

Ludlow, California: The material from Ludlow, San Bernardino County, California, was collected by Dr. Foshag of the National Museum (U.S.N.M. Specimen No. 94430). The specimen available for study is a rounded nodule about 8 cm. in diameter in an olivine basalt. The mineral grains are more uniform in size than in most materials of this type. The olivine (Table 4, No. 2) and enstatite grains (Table 5, No. 2) reach a maximum diameter of 4 mm. The green chromian diopside grains (Table 6, No. 2) are slightly smaller. Chromian spinel (Table 7, No. 2) in millimeter-sized grains is unusually abundant.

Dreiser Weiher, Eifel, Germany: Several geologists have discussed the olivine nodules that occur as cores in volcanic bombs at Dreiser Weiher in the Eifel. The latest and most detailed study of these nodules is by Frechen (1948).

The bombs, as described by Frechen (1948, p. 327) vary greatly in mineral content, as illustrated in the following table compiled from data given by him.

TABLE 1. MINERAL COMPOSITION OF NODULES FROM DREISER WEIHER

	1	2	3	4	5	6
Olivine	99	90	84	57	68	43
Enstatite	—	4	15	8	30	48
Chromian-diopside	—	2	1	30	2	4
Picotite	1	4	—	5	—	5

Frechen quotes several analyses of these minerals from various localities made by earlier workers but adds no complete new analyses of the Dreiser Weiher minerals.

Kapfenstein, Austria: In the southeastern part of Styria and adjoining parts of Hungary, along the eastern border of the Alps, a number of basaltic centers characterized by olivine nodules form part of the zone of centers. They have been described by Schadler (1914), and material from one of these centers is represented by the material from Kapfenstein, east of Gleichen. The basaltic tuff of Kapfenstein has long been known to contain typical olivine bombs. However, at other Styrian localities, like Kuruzzenkohl, south of Fehring and in Unterweissenbach, west of Feldbach, the basaltic tuff deposits are revealed through quarry-ing operations. The nodules are wanting in the nepheline basalt of the region. Olivine nodules have also been observed in limburgite from Loipersdorf near Furstenfeld.

In describing the olivine bombs, Schadler (1914, p. 486) says, "Besides rounded and irregular fragment-like forms, the Styrian olivine bombs also commonly show a regular parallel arrangement as Heritsch (1908) has already observed. The size of the bombs is variable, and ranges through all dimensions up to a diameter of half a meter. . . . Mineralogically the olivine bombs of Styrian occurrences throughout are an aggregate of olivine, bronzite, chrome-diopside, and picotite."

Alaska: David M. Hopkins of the U. S. Geological Survey has brought to our attention basaltic rocks that contain abundant olivine-rich nodules. These nodules are described by Mr. Hopkins (personal communication) who states, "The olivine nodules occur in the Imuruk Lake region, Seward Peninsula, Alaska, in a region of basaltic rocks, which range from early Pleistocene to Recent in age. The flows from a few of the numerous vents contain abundant inclusions. These are commonly angular and range up to 3 inches in greatest dimension. The flows which contain mafic inclusions are exceptionally olivine rich; I assume that much of the olivine is derived from disintegrated inclusions." The material available for study was inadequate for complete chemical analysis of the chromian spinel, but it was found to contain about 15 per cent Cr_2O_3.

In the course of studies of the rocks of the Aleutian Islands of Alaska, George D. Fraser of the U. S. Geological Survey collected olivine-rich nodules that occur in basaltic rocks from near the northwest coast on Kanaga Island, Andreanof Group.

Mr. Fraser (personal communication) states, "The host rock forms an isolated outcrop about 10 ft. by 50 ft. in an area devoid of other outcrops, so that the nature of the igneous body is in doubt. The rock is a dense, black altered basalt? with abundant, conspicuous, brown, olivine-rich inclusions up to a foot in diameter, both rounded and tabular. The age of the rock is unknown." Microscopic examination indicates that this is a fragmental rock in which limburgite is dominant.

The nodules are dominantly olivine with lesser amounts of bright-green chromian diopside, enstatite, and chromian spinel. Thus, the mineralogy of the Kanaga Island specimens is similar to all the others that have been studied. A sample of the chromian spinel was separated by heavy solutions, and chemical analysis shows the presence of 28.6 per cent of Cr_2O_3.

Africa: A group of specimens with nodular inclusions in basalt from an area near Azrou Morocco in the Middle Atlas region were secured from Abbe Gaudefroy, curator of the mineralogical museum of Rabat, Morocco. Some of these nodules were 2 to 3 cm. in diameter, but a fragment of a large nodule was 7 cm. long. The dominant mineral is very fresh olivine in grains that may be as large as 1 cm. in diameter. Enstatite grains reach 2 mm. and sparse chromian diopside and chromian spinel occur as millimeter-sized grains.

An olivine-rich nodular inclusion in basaltic rock from Rapp Hills, Durumi, Nigeria, is represented by U.S.N.M. Specimen No. 96584. This specimen is part of a rounded nodule about 8 cm. in diameter. The dominant olivine and less abundant enstatite grains reach 4 mm. in diameter. Sparse chromian diopside and spinel occur as millimeter-sized grains.

Localities of Earlier Studies

Many papers, some of which date back 100 years, have been published on the olivine-rich nodules in basaltic rocks. A few of the papers that give significant analyses or that contain significant discussions will be cited and briefly outlined.

Turner (1942, p. 299) has made valuable studies of olivine-rich nodules from basaltic rocks of New Zealand and has described them as follows: "Mineralogically the olivine nodules from New Zealand Tertiary and Pleistocene basalts are identical with lherzolites and harzburgites of plutonic origin. The constituent minerals include enstatite, chrome-diopside, picotite and chromite, none of which has been recognized in the enclosing basalt."

Olivine nodules have been reported by Lauro (1940) from Conca de Janas (Orosei), eastern Sardinia. He gives chemical analyses of carefully separated samples of olivine, green monoclinic pyroxene, bronzite, and picotite, which are cited in Tables 13 to 16, No. 11. Lauro concludes that the minerals of the nodules were concentrated by crystal settling and then dragged up by the basalt.

Schultz (1903) has described olivine nodules from numerous volcanic centers in the vicinity of Homberg, south of Kassel, Germany, where they occur both in flow rocks and as bombs in volcanic tuffs. The rocks enclosing the nodules are described as nepheline basalts, nepheline basanites, feldspar basalts, dolerites, and limburgites and are an excellent example of identical nodules occurring in very different rock types.

Ernst (1936) in a paper on the nodules derived from a melilitite basalt of Westberges, near Hofgeismar has thoroughly discussed their origin. Quotations from parts of this paper are included in the section on the origin of nodule inclusions (p. 729). He says that in mineral composition the nodules range from almost pure olivine, with less than 10 per cent of pyroxene and chromian-spinel, to a bronzite rock in which olivine is only an accessory mineral. The nodules are fresh, and serpentinization is almost never observed. An analysis of the Westberges rock is given in Table 20, No. 2.

A complete chemical analysis of the monoclinic pyroxene made by Ernst (1936, p. 652) is given in Table 15, No. 9. A complete analysis of the other minerals is not given, but the picotite was found to contain 23 per cent Cr_2O_3. Ernst also mentions a host rock characterized by olivine nodules from the locality of Hochbol, in the Swabian Alps (Ernst, 1936, p. 659), in which he calculates the presence of 44 per cent melilite.

Frechen (1948) includes a description of the occurrence of nodules in the basalt at Finkenberg in the Siebengebirge region, near Bonn. The mineral content in the Finkenberg occurrence varies widely, as shown by some of the proportions listed by Frechen (1948 p. 353).

TABLE 2. MINERAL COMPOSITION OF NODULES FROM FINKENBERG, NEAR BONN

	1	2	3	4	5	6
Olivine	95	67	70	65	—	—
Enstatite	—	20	30	30	75	100
Augite	5	10	—	2	25	—
Picotite	—	3	—	3	—	—

Many of the nodules carry the secondary minerals hornblende and biotite. The biotite shows distortion due to mechanical pressure, a relationship that led Frechen to conclude that this is the same force that produced the structures observed in the olivine.

Farsky (1876) describes "olivine nodules" in basalts from Kisakov, in Czechoslovakia, and gives analyses of the olivine, enstatite, diopside, and picotite, which occur in these rocks (see Tables 13 to 16, No. 1).

Knop (1877, p. 698) also gives analyses of olivine, orthorhombic pyroxene, clino-pyroxene, and chrome "eisenstein" (see Tables 13 to 16, No. 5) from Lutzelberges near Sasbach in the Kaiserstuhl.

Schuster (1878) describes olivine nodules in bombs from Reps, Siebenbürgen, Rumania, and describes olivine, augite, bronzite, and spinel from them. The same group of minerals from that locality has also been described by Bleibtreu (1883).

Bauer (1891, pp. 182-191) lists olivine, bronzite, chromian-diopside, and picotite, which occur at Stempel near Marburg Heisse, and gives chemical analyses reproduced in Tables 13–16, No. 9.

Zirkel (1904) discusses olivine nodules in the Rheinland region, mentioning olivine, bronzite, chrome-diopside, and picotite, and concludes that the nodules represent segregation from basalt.

OCCURRENCES OF DUNITE

Localities of Analyzed Materials

The minerals from several outstanding localities for dunite have been studied. These localities include Dun Mountain, South Island, New Zealand; Webster, North Carolina; New Caledonia; and Twin Sisters, Washington. A few descriptions of other localities are cited from the literature.

Dun Mountain, New Zealand: The Dun Mountain locality, near the city of Nelson in the northern part of South Island, New Zealand, is the type locality for the nearly pure olivine rock first called dunite by Hochstetter in 1859 (see also 1864). The dunite from the Nelson district has been briefly described by James Mackintosh Bell, and his coauthors Patrick Marshall and E. de C. Clarke (1911, p. 29–40). The dominant rocks of the area are dunite and its alteration product serpentine. The crystal fabric of this dunite has been studied by Turner (1942), and its serpentinization by Benson (1918).

Bell and associates (1911, p. 30) in discussing the dunite say, "Dunites have their most conspicuous exposure in the neighborhood of Dun Mountain. They consist almost entirely of olivine, but in all cases there are grains of a spinellid mineral which appears to vary between chromite and picotite. . . . There are occasional crystals of diopside in the dunite."

Harzburgite is described as composed of olivine, enstatite, and picotite; and in general it is strongly serpentinized. Another type of rock is composed of diallage, enstatite, and picotite and occurs in dikes that cut the dunite and harzburgite. Material of this type, collected by Ross, seems to represent partly serpentinized harzburgite or a phase intermediate between dunite and harzburgite. This rock contains olivine, bronzite or enstatite, chromian diopside, and the chromian spinel.

The nearly pure dunite mass resists erosion more effectively than the serpentinized phases, and forms bold outcrops of rocks which are red brown on the surface, thus giving the name to Dun Mountain and later the name dunite to the rock. Below a thin, outer oxidized film the dunite is remarkably fresh, and excellent material was obtained by Ross.

The most typical dunite at Dun Mountain is more than 90 per cent olivine (Table 4, No. 15), a few per cent chromian spinel (represented in Table 7, No. 15), and mere traces of the green chromian diopside. The chromian diopside was too sparse for separation in amounts adequate for chemical analysis, but the results of spectrographic study are given in Table 10, No. 15. Another type of rock from Dun Mountain is dominantly olivine but contains 10 to 15 per cent enstatite, which is represented in Table 5, No. 15. Like all specimens from Dun Mountain it contains traces of chromian diopside, whose green color contrasts so strongly with the pale color of the olivine that the merest traces are recognizable.

Webster, North Carolina: The dunite at Webster, North Carolina, is only locally serpentinized, and much of it and the associated websterite are remarkably fresh. This is the type locality for websterite, a rock composed of enstatite, chromian diopside, and sparse, disseminated chromite. This rock was the source of the minerals used in this study, of which chemical analyses are given in Tables 4 to 7, No. 13.

The geologic relations in the region are given in the section on the origin of dunites.

New Caledonia: The New Caledonia material was part of the country rock associated with a chrome ore mine near Noumea. The peridotite of this part of New Caledonia is in general thoroughly serpentinized, but a few specimens were collected by Ross that contained essential amounts of olivine and enstatite. The alteration complicated the separation of fresh minerals, but nearly pure olivine and enstatite were obtained. The alteration also obscured mineral relations, and the presence or absence of small amounts of monoclinic pyroxene could not be established. The analysis of the olivine is presented in Table 4, No. 14, and of the enstatite in Table 5, No. 14.

Lacroix (1942, p. 13–18), discussing the typical dunites of New Caledonia, says that they may be composed of olivine with or without "bronzite" and with spinel or chromite. Other phases of the peridotites are harzburgite composed of olivine, bronzite, picotite, and a mineral Lacroix calls clino-bronzite; bronzitite, a rock composed essentially of bronzite; and websterite, composed of bronzite and diopside.

Twin Sisters, Washington: One of the large dunite bodies of the world is that in the Twin Sisters area, about 20 miles east of Bellingham, Washington. It has been described by Thayer (personal communication) as follows: "The Twin Sisters dunite and olivine-rich saxonite form an oval pluton about 10 miles long by 4 miles wide. This rock is free from serpentine except around the margin and along throughgoing fracture zones. A large proportion of the rock is a pyroxene-free dunite, characterized by ragged, green olivine grains up to 5 cm. long, in a matrix of fine-grained olivine [Table 4, No. 12]. Saxonite containing 10 to 20 per cent enstatite probably forms two-thirds to three-fourths of the pluton, and pyroxene-rich peridotite probably constitutes 5 per cent or less. The chromite deposits range from small massive pods or lenses to elongate schlieren of disseminated chromite. Clinopyroxene of bright green color occurs along a well-defined fracture zone (Table 6, No. 12)."

Methods of Separation and Chemical Analysis

Chemical analyses of four minerals—olivine, orthorhombic pyroxene (enstatite), monoclinic pyroxene (chromian diopside), and chromian spinel—characteristically present in dunites and in nodules in basaltic rocks made in the course of this study are presented in Tables 4 to 7, spectrographic determinations of minor elements in the same samples are shown in Tables 8 to 11, and the localities from which the specimens were obtained are shown in Table 3. Analyses by earlier workers of the minerals in nodules are given in Tables 13 to 16, and the localities represented by these analyses are given in Table 12. It should be noted that the results of the spectrographic determinations are reported in terms of the element, whereas the results of chemical analysis are reported in terms of the oxides.

Table 3. Localities of Samples Analyzed in Tables 4 to 11

1. Camargo, Chihuahua, Mexico.
2. Ludlow, California.
3. Peridot Cove near Globe, Arizona (Lausen, 1927).
4. Dreiser Weiher, Eifel, Germany (Frechen, 1948).
5. Kapfenstein, Styria, Austria (Heritsch, 1908).
6. Near Meng-Chian, Tun-hua State, east Manchuria.
7. Ichinomegata, Akita Prefecture, Japan.
8. Salt Lake Crater, Oahu, Hawaiian Islands.
9. Kauai, Hawaii, Grove Farm Quarry, southwest of Librue.
10. Hale Pohaku, south flank of Mauna Kea, Hawaii (Stearns and Macdonald, 1946, p. 163).
11. 1801 Kaupulehu flow, Hualalai, Hawaii (Stearns and Macdonald, 1946, p. 147).
12. Twin Sisters, northern Whatcom County, Washington.
13. Webster, North Carolina.
14. Noumea, New Caledonia, 10 miles southeast of.
15. Dun Mountain, New Zealand (Turner, 1942).

The separation of essentially pure material for chemical analysis involved much tedious work and the adaptation of methods suitable to the different minerals. Olivine was so abundant and occurred in such large grains in all the samples—except in those from New Caledonia—that it was possible to inspect and hand-pick each grain individually. The New Caledonia olivine was concentrated from a partly serpentinized rock by means of heavy solutions. Enstatite could be hand-picked in several of the samples; but, in some, selected fragments were crushed and further concentrated by means of heavy solutions. The chromian diopside was least abundant of the silicate minerals and occurred as the smallest grains. Fragments of rock in which it was most abundant were selected by hand-picking, then crushed and further concentrated by means of the Frantz isodynamic separator, and finally hand-picked. The mineral was much more magnetic than the other silicate minerals, and high concentrations could commonly be obtained. The chromian spinel was obtained by selecting rock fragments rich in that mineral and partly con-

TABLE 4. ANALYSES OF OLIVINES

[M. D. Foster, analyst]

	From inclusions in basaltic rocks									From dunites			
	1	2	3	4	5	6	7	8	9	12	13	14	15
SiO_2	40.80	40.91	40.81	40.65	40.61	40.93	40.30	40.87	41.16	40.55	40.88	41.32	40.96
Al_2O_3	0.00	0.13	0.10	0.24	0.00	0.19	0.25	0.07	0.00	0.05	0.11	0.00	0.21
Fe_2O_3	0.00	0.00	0.00	0.00	0.00	0.00	0.00	0.00	0.00	0.00	0.00	0.30	0.00
FeO	8.61	8.96	9.46	9.30	8.96	8.86	10.26	8.72	8.89	7.99	8.28	7.49	7.86
TiO_2	0.040	0.010	0.035	0.010	0.010	0.15	0.15	0.020	0.015	0.14	0.015	0.010	0.010
Cr_2O_3	0.04	0.03	0.03	0.04	0.04	0.05	0.03	0.02	0.02	0.06	0.02	0.04	0.02
CaO	0.20	0.17	0.07	0.13	0.11	0.08	0.07	0.07	0.07	0.06	0.03	0.29	0.15
MgO	49.77	48.95	49.12	49.55	49.88	49.52	48.60	49.78	49.56	50.57	50.10	49.56	50.45
Na_2O[1]	0.00	0.02	0.01	0.02	0.01	0.03	0.04	0.01	0.03	0.06	0.02	0.01	0.01
K_2O[1]	0.00	0.00	0.00	0.00	0.00	0.03	0.03	0.00	0.00	0.04	0.00	0.00	0.00
MnO	0.13	0.15	0.15	0.13	0.12	0.11	0.09	0.15	0.15	0.12	0.15	0.15	0.13
CoO	0.02	0.01	0.013	0.013	0.012	—	—	0.013	0.010	—	0.013	0.011	0.010
NiO	0.38	0.34	0.28	0.28	0.32	0.30	0.41	0.34	0.30	0.28	0.32	0.31	0.25
V_2O_5	—	—	—	—	—	—	—	—	—	—	—	—	—
H_2O	0.29	0.20	0.11	0.07	0.05	—	0.33	0.05	0.10	0.13	0.23	0.60	0.29
Total	100.28	99.88	100.19	100.43	100.12	100.25	100.56	100.11	100.30	100.05	100.17	100.09	100.35
Specific gravity at 4° C	3.338	3.337	3.349	3.347	3.324	3.342	3.349	3.333	3.334	3.321	3.331	3.293	3.313

---

[1] Alkalies determined with flame photometer by S. M. Berthold.

TABLE 5. ANALYSES OF ENSTATITES

[M. D. Foster, analyst]

	From inclusions in basaltic rocks									From dunites		
	1	2	3	4	5	6	7	8	9	13	14	15
SiO_2	55.04	54.40	53.84	53.92	55.70	54.86	54.78	55.38	54.85	56.33	54.82	51.56
Al_2O_3	3.91	4.10	4.80	5.32	2.56	2.66	3.50	2.97	2.18	1.28	1.00	1.60
Fe_2O_3	0.00	0.00	0.16	0.00	0.00	0.00	0.00	0.00	0.00	0.00	0.00	0.00
FeO	5.93	6.83	6.21	6.10	5.77	6.32	6.86	5.66	5.99	7.75	5.28	6.72
TiO_2	0.10	0.003	0.03	0.007	0.02	0.28	0.15	0.05	0.033	0.020	0.030	0.16
Cr_2O_3	0.34	0.76	0.90	0.94	0.73	0.80	0.55	0.80	0.80	0.58	0.80	0.63
CaO	1.02	0.82	1.00	1.36	0.75	0.60	0.62	0.74	1.72	1.03	0.60	0.93
MgO	33.56	32.84	32.48	32.45	33.86	34.14	33.28	34.19	33.72	32.74	35.62	37.88
Na_2O[2]	0.00	0.04	0.15	0.08	0.11	—	0.07	0.06	0.08	0.02	—	—
K_2O[2]	0.00	0.00	0.00	0.00	0.00	—	0.03	0.00	0.07	0.00	—	—
MnO	0.15	0.13	0.12	0.12	0.10	0.12	0.13	0.12	0.09	0.12	0.09	0.12
CoO	—	0.005	—	0.005	—	—	—	0.005	—	0.005	—	—
NiO	0.07	0.07	0.07	0.07	0.10	—	0.09	0.07	0.08	0.04	0.05	0.15
V_2O_5	0.02	—	—	—	—	0.01	0.01	—	—	—	—	—
H_2O	0.20	0.15	—	0.08	0.10	—	0.13	0.14	0.18	0.19	—	—
Total	100.34	100.14	99.76	100.44	99.80	99.79	100.07	100.18	99.79	100.10	98.29[1]	99.75
Specific gravity at 4° C	3.304	3.305	3.279	3.312	3.297	3.298	3.304	3.278	3.291	3.302	3.211	3.302

[1] May be partly serpentinized.

[2] Alkalies determined with flame photometer by S. M. Berthold.

Table 6. Analyses of Chromian Diopsides

[M. D. Foster, analyst]

	From inclusions in basaltic rocks									From dunites	
	1	2	3	4	5	7	8	9	11	12	13
SiO_2	51.78	51.42	50.36	51.17	52.48	51.41	52.12	51.87	50.24	53.88	53.89
Al_2O_3	5.14	5.97	6.58	6.46	3.56	4.69	4.08	1.72	4.57	0.68	0.72
Fe_2O_3	1.75	1.43	1.53	0.85	1.13	0.69	0.82	1.61	2.53	0.16	0.00
FeO	2.14	2.57	2.66	2.87	2.52	2.64	2.24	3.66	4.04	2.11	2.42
TiO_2	0.38	0.24	0.79	0.28	0.62	0.33	0.80	0.65	0.72	0.14	0.13
Cr_2O_3	0.95	0.80	0.92	1.20	2.12	1.03	1.44	1.07	1.22	0.87	0.69
CaO	20.32	19.95	18.78	18.27	19.00	21.63	19.34	20.92	19.96	22.38	23.56
MgO	16.04	16.17	16.59	17.65	17.03	16.32	16.48	17.94	16.53	18.84	17.84
Na_2O[1]	1.06	1.36	1.41	1.20	—	0.72	2.14	0.33	0.58	0.78	0.52
K_2O[1]	0.08	0.10	0.08	0.08	—	0.04	0.08	0.02	0.04	0.04	0.10
MnO	0.12	0.15	0.09	0.16	0.15	0.11	0.09	0.06	0.13	0.07	0.12
CoO	—	—	—	—	—	—	—	—	—	—	—
NiO	0.041	0.045	0.037	0.036	0.034	0.040	0.041	0.040	—	0.039	0.028
V_2O_5	0.04	0.03	0.03	0.03	0.04	0.05	0.03	—	—	0.02	0.01
H_2O	—	—	—	0.14	—	0.11	—	0.08	—	0.14	0.10
Total	99.84	100.24	99.86	100.40	98.53	99.81	99.70	99.97	100.39	100.15	100.13
Specific gravity at 4° C	3.322	3.329	3.323	3.311	3.332	3.311	3.312	3.320	3.305	3.271	3.303

---

[1] Alkalies determined with flame photometer by S. M. Berthold.

TABLE 7. ANALYSES OF CHROMIAN SPINELS AND CHROMITES

[M. D. Foster, analyst]

	From inclusions in basaltic rocks										From dunites		
	1	2	3	4	5	7	7a[1]	8	9	10	11	12	15
SiO_2	0.46	0.44	—	0.43	—	4.10	—	—	0.22	0.18	0.50	0.86	0.40
Al_2O_3	47.63	41.68	—	27.81	—	48.06	53.43	—	19.29	24.06	26.93	8.81	13.37
Fe_2O_3	2.67	7.96	27.86[2]	7.84	29.81[2]	14.29[2]	0.00	20.62[2]	15.62	18.22	16.48	5.72	8.51
FeO	9.86[3]	8.64[3]	—	6.81[3]	—	—	13.15[3]	—	16.68[3]	15.65[3]	15.37	17.96	13.90[3]
TiO_2	0.44	2.71	—	2.11	8.50	1.25	1.39	4.80	1.60	1.40	2.20	1.40	1.65
Cr_2O_3	19.24	18.34	11.47	14.05	32.87	11.00	12.23	28.29	34.87	27.30	24.54	55.17	48.48
CaO	0.20	0.00	—	0.04	—	0.55	0.60	—	0.08	0.12	0.00	0.20	0.04
MgO	19.22	19.71	—	20.69	—	21.30	18.29	—	12.14	12.92	13.66	10.02	13.23
Na_2O	0.00	—	—	—	—	—	—	—	—	—	—	—	—
K_2O	0.00	—	—	—	—	—	—	—	—	—	—	—	—
MnO	0.15	0.13	—	0.12	—	0.11	0.11	—	0.18	0.15	0.15	0.16	0.07
CoO	—	—	—	—	—	—	—	—	—	—	—	0.002	—
NiO	—	—	—	—	—	—	—	—	—	—	0.07	—	—
V_2O_5	0.04	—	—	—	—	—	—	—	—	—	—	—	—
H_2O	—	—	—	—	—	—	—	—	—	—	—	—	—
Total	99.91	99.61	—	99.90	—	100.66	99.20	—	100.68	99.98	99.90	100.30	99.65
Specific gravity at 4° C	3.850	3.905	—	3.913	—	3.886	—	—	4.395	4.293	—	4.289	4.396

[1] Recalculated from 7, high SiO_2 of which indicates contamination by olivine.

[2] Total iron as Fe_2O_3.

[3] Calculated to give 1:1 ratio of $RO:R_2O_3$.

TABLE 8. SPECTROGRAPHIC DETERMINATION OF MINOR ELEMENTS IN OLIVINES

[A. T. Myers, analyst]

	From inclusions in basaltic rocks									From dunites			
	1	2	3	4	5	6	7	8	9	12	13	14	15
Mn	0.14	0.12	0.12	0.12	0.10	0.10	0.12	0.11	0.13	0.14	0.11	0.12	0.11
Ni	0.44	0.25	0.25	0.30	0.30	0.30	0.35	0.35	0.35	0.25	0.30	0.25	0.25
Cr	0.028	0.015	0.015	0.025	0.020	0.040	0.010	0.010	0.015	0.035	0.010	0.035	0.015
Co	0.016	0.016	0.016	0.018	0.015	0.016	0.016	0.016	0.018	0.02	0.015	0.015	0.017
Ti	0.004	0.001	0.008	0.006	0.003	0.004	0.003	0.003	0.002	—	0.0008	0.004	0.002
V	—	—	—	—	—	—	—	—	—	—	—	0.003	0.001
Ca	0.075	0.07	0.05	0.07	0.04	0.0X	0.0X	0.05	0.05	0.02	0.02	0.2	0.07
Al	—	0.036	0.032	0.048	0.027	—	—	0.032	0.024	—	0.024	0.032	0.018

Looked for but not found: Ag, As, B, Ba, Be, Bi, Cd, Ga, Ge, In, La, Li,[1] Mo, P,[2] Pb, Sb, Sr, Y, Zn, and Zr.

[1] Li present at about the 0.000X order.

[2] Not present at 0.5 per cent or more.

TABLE 9. SPECTROGRAPHIC DETERMINATION OF MINOR ELEMENTS IN ENSTATITES

[A. T. Myers, analyst]

	From inclusions in basaltic rocks									From dunites		
	1	2	3	4	5	6	7	8	9	13	14	15
Mn	0.16	0.12	0.10	0.09	0.10	0.08	0.10	0.08	0.08	0.11	0.06	0.11
Ni	0.080	0.070	0.065	0.070	0.070	0.065	0.060	0.065	0.050	0.040	0.050	0.060
Cr	0.36	0.25	0.30	0.40	0.45	0.30	0.25	0.45	0.35	0.25	0.30	0.40
Co	0.006	0.005	0.005	0.005	0.006	0.008	0.008	0.006	0.005	0.007	0.004	0.005
Ti	0.09	0.04	0.20	0.07	0.06	0.04	0.12	0.03	0.02	0.02	0.002	0.01
V	0.010	0.007	0.007	0.008	0.006	0.008	0.007	0.008	0.008	0.004	0.003	0.010
Y	—	—	0.001	—	—	—	—	—	—	—	—	—
Ca	—	0.6	0.8	0.9	0.8	0.5	0.6	0.5	1.2	0.9	0.5	0.9

Looked for but not found: Ag, As, B, Ba, Be, Bi, Cd, Ga, Ge, In, La, Li, Mo, P,[1] Pb, Sb, Sr, Y, Zn, and Zr.

[1] Not present at 0.5 per cent or more.

TABLE 10. SPECTROGRAPHIC DETERMINATION OF MINOR ELEMENTS IN CHROMIAN DIOPSIDES

[A. T. Myers, analyst]

	From inclusions in basaltic rocks									From dunites			
	1	2	3	4	5	6	7	8	9	12	13	14	15
Mn	0.11	0.12	0.08	0.12	0.12	0.10	0.09	0.08	0.08	0.10	0.10	0.05	0.10
Ni	0.038	0.030	0.030	0.035	0.030	0.040	0.030	0.030	0.035	0.040	0.025	0.035	0.050
Cr	1.24	0.65	0.70	0.80	1.5	0.85	0.70	1.0	0.75	0.8	0.45	0.75	0.65
Co	0.005	0.004	0.005	0.005	0.004	0.004	0.004	0.004	0.005	0.004	0.005	0.005	0.005
Ti	0.30	0.2	0.6	0.2	0.2	0.15	0.45	0.1	0.1	0.02	0.01	0.08	0.01
V	0.044	0.02	0.02	0.02	0.02	0.02	0.04	0.02	0.02	0.02	0.008	0.008	0.02
Y	—	0.004	0.005	0.004	0.001	0.002	0.004	0.002	0.002	—	—	0.002	—
Sr	—	0.002	0.01	0.002	0.008	0.002	Tr.	0.02	0.0007	0.003	0.001	0.0004	0.002
Ba	—	—	—	—	—	0.000X	0.000X	—	—	—	—	0.00X	—
Zr	—	—	0.00X	—	0.00X	—	—	0.00X	0.X	—	—	—	—

Looked for but not found: As, Ag, B, Be, Bi, Cd, Ga, In, La, Li, Mo, P,[1] Pb, Sb, and Zn.

[1] Not present at 0.5 per cent or more.

TABLE 11. SPECTROGRAPHIC DETERMINATION OF MINOR ELEMENTS IN CHROMIAN SPINELS AND CHROMITES

[A. T. Myers, analyst]

	From inclusions in basaltic rocks								From dunites		
	1	2	3	4	5	7	8	9	12	14	15
Mn	0.10	0.07	0.07	0.06	0.12	0.08	0.09	0.15	0.14	0.09	0.14
Ni	0.20	0.10	0.15	0.10	0.10	0.10	0.10	0.10	0.025	0.08	0.06
Co	0.010	0.010	0.009	0.008	0.010	0.010	0.010	0.020	0.02	0.02	0.020
Ti	0.1	0.02	0.3	0.1	0.4	0.04	0.1	0.4	0.06	0.02	0.2
V	0.03	0.01	0.01	0.01	0.03	0.005	0.02	0.04	0.02	0.02	0.02
Ga	—	0.002	0.002	0.002	0.002	0.002	0.002	0.002	0.001	0.002	0.002
Ca	—	0.05	0.05	0.05	—	0.0X	0.04	0.07	0.4	0.2	0.04
Zr	—	—	—	—	—	—	—	0.0X	—	—	—

Looked for but not found: Ag, As, B, Ba, Bi, Cd, Ge, In, La, Li, Mo, P,[1] Pb, Sb, Sr, Y, and Zn.

[1] Not present at 0.5 per cent or more.

TABLE 12. LOCALITIES OF SAMPLES FOR ANALYSES QUOTED IN TABLES 13 TO 16

Locality	Author
1. Kosakov, Czechoslovakia	Farsky, 1876, pp. 207–208.
2. Buchberg, near Klein-Iser, Czechoslovakia	Braun, 1922, p. 278.
3. Unterweissenbach, Styria, Austria	Schadler, 1914, p. 491.
4. Kapfenstein, Styria, Austria	Schiller, 1905, p. 316.
5. Lutzelberges, near Sasbach, Kaiserstuhl, Germany	Knop, 1877, pp. 697, 698, 699.
6. Finkenberg, Siebengebirge, near Bonn, Germany	Bleibtreu, 1883, p. 520.
7. Kreuzberg, Rohn, Hesse, Germany	H. Link, 1887, p. 100.
8. Westberges, north of Kassel, W. Germany	Ernst, 1936, p. 652.
9. Stempel, near Marburg, W. Germany	Bauer, 1891, pp. 182, 186.
10. Reichenweiler, Alsace, France	G. Link, 1891, p. 663.
11. Conca de Janas (Orosei), eastern Sardinia	Lauro, 1940, pp. 186. 187, 190, 292.
12. Jan Mayen, an island northeast of Iceland	Scharizer, 1884, p. 708.
13. Vuoka Ruopsok, Sweden	Du Rietz, 1935, pp. 143, 144.
14. Pupuke Lake, Takopuna, New Zealand	Turner and Bartrum, 1928, p. 900

TABLE 13. ANALYSES OF OLIVINES

	1	2	3	5	9	10	11	13	14
SiO_2	41.22	41.30	40.72	41.19	40.68	41.53	40.99	41.55	41.53
Al_2O_3	0.15	0.17	—	—	—	2.33	—	0.01	0.42
Fe_2O_3	—	0.55	—	—	—	0.58	0.38	7.34	0.10
FeO	9.0	9.81	9.47	8.54	9.19	10.27	8.58	—	8.51
TiO_2	—	—	—	—	—	—	Trace	—	0.08
Cr_2O_3	0.05	—	—	—	—	—	Trace	—	0.20
CaO	—	0.02	—	—	—	—	0.11	0.03	0.31
MgO	49.42	47.96	49.88	50.27	49.58	43.60	50.00	50.83	47.33
Na_2O	—	—	—	—	—	—	—	—	0.11
K_2O	—	—	—	—	—	}1.69	—	—	None
MnO	0.18	—	—	—	—	—	0.20	—	0.15
CoO	—	—	—	—	0.02	—	—	—	None
NiO	0.29	0.38	—	—	0.50	—	Trace	—	0.44
CuO	—	—	—	—	0.08	—	—	—	
H_2O	—	—	—	—	—	—	—	0.24	+0.24 −0.21
Total	100.31	100.19	100.07	100.00	100.05	100.00	100.16	100.00[1]	99.70[2]

[1] Calculated after allowing for 6 per cent of enstatite.

[2] Includes 0.02 S, tr. P_2O_5, NoSrO, no BaO, no V_2O_3.

TABLE 14. ANALYSES OF ENSTATITES

	1		3	4	5	6	9	10	11	13
SiO_2	56.23	53.29	53.40	54.39	52.50	54.16	55.45	52.67	53.79	55.80
Al_2O_3	2.62	2.77	3.66	1.89	2.29	4.51	4.66	4.84	2.19	4.02
Fe_2O_3	—	—	4.66	2.49	—	—	—	2.07	2.50	0.76
FeO	6.67	15.43	4.04	4.52	6.07	7.63	6.47	5.11	5.99	4.85
TiO_2	—	—	—	0.12	—	—	—	0.60	Trace	None
Cr_2O_3	0.34	—	0.34	—	0.00	0.48	Trace	—	0.26	0.20
CaO	0.96	1.79	0.75	0.05	4.35	1.97	1.07	1.55	2.08	None
MgO	32.27	27.01	33.16	34.88	32.23	32.46	32.97	32.82	32.20	34.70
Na_2O	—	—	—	—	—	—	—		—	—
								0.94		
K_2O	—	—	—	—	—	—	—		—	—
MnO	0.23	—	—	0.21	—	—	—	—	—	—
CoO	—	—	—	—	—	—	—	—	—	—
NiO	—	—	—	—	—	—	—	—	—	—
CuO	—	—	—	—	—	—	—	—	—	—
H_2O	0.95	0.35	0.26	1.71	—	0.28	—	—	0.20	0.23
Total	100.28	100.64	100.27[1]	100.26		101.49	100.62		100.21	100.56

[1] Includes 2.00 per cent residue.

TABLE 15. ANALYSES OF DIOPSIDES

	1	3	5	7	8	9	11	12
SiO_2	53.44	49.87	51.89	54.50	52.43	52.50	52.37	51.86
Al_2O_3	3.74	5.44	4.76	6.47	4.16	5.19	6.11	1.56
Fe_2O_3	—	2.75	—	—	2.66	—	1.44	2.44
FeO	4.70	2.50	4.40	4.00	3.53	2.31	2.01	3.46
TiO_2	—	—	—	—	0.37	—	0.29	—
Cr_2O_3	0.75	1.76	1.09	1.98	1.06	2.43	0.05	0.73
CaO	19.90	20.74	19.73	17.87	16.56	19.52	20.88	22.15
MgO	16.19	16.26	15.47	14.58	18.19	18.01	16.72	17.40
Na_2O	—	—	—	—	0.90	—	—	—
K_2O	—	—	—	—	0.07	—	—	—
MnO	0.31	—	0.54	0.70	0.12	—	0.10	Trace
CoO	—	—	—	—	—	—	—	—
NiO	—	—	—	—	0.08	—	—	—
CuO	—	—	—	—		—	—	—
H_2O	—	0.55	—	—	[1]	—	0.09	0.12
Total	99.03	99.87	100.18[2]	100.33[3]	100.37[4]	99.96	100.06	99.72

[1] H_2O-, 0.11; H_2O+, 0.09.

[2] Includes 2.30 per cent residue.

[3] Includes 0.23 per cent BaO, 0.01 per cent V_2O_5.

[4] Includes 0.03 per cent BaO and 0.01 per cent V_2O_5.

TABLE 16. ANALYSES OF PICOTITES

	1	5	9	11	11*a*[1]
SiO_2	1.25	—	—	4.30	—
Al_2O_3	52.47	20.06	39.91	31.43	34.92
Fe_2O_3	21.42	—	—	22.60	15.38
FeO	—	12.98	26.64		10.27
TiO_2	—	—	—	—	—
Cr_2O_3	7.01	46.87	30.33	19.50	21.67
CaO	Trace	—	—	—	—
MgO	18.23	20.55	3.26	21.33	17.76
Na_2O	—	—	—	—	—
K_2O	—	—	—	—	—
MnO	—	—	—	—	—
CoO	—	—	—	—	—
NiO	—	—	—	—	—
H_2O	—	—	—	—	—
Total	100.38	100.46	100.14	99.06	—

[1] High SiO_2 content in sample 11 indicates contamination (olivine); sample recalculated in 11*a*.

centrating it with the Frantz isodynamic separator. This fraction was then crushed to a very fine size and briefly treated with sulfuric acid. The spinel was completely unattacked, but the surface alteration of the admixed olivine made it possible to float off the chromian spinel in methylene iodide.

Previous writers have commonly referred to the orthopyroxene as bronzite, and that name appears in most of the quotations cited. However, magnesium is strongly dominant over ferrous iron (about 33 per cent MgO to 6 per cent FeO) and enstatite is the better name. The chromian spinel has commonly been called picotite, but chromian spinel seems the best name where Cr_2O_3 is a dominant constituent.

The analyses were made according to the usual methods of rock analysis as described by Hillebrand and Lundell (1929) except for sodium and potassium, which were determined with the flame photometer by S. M. Berthold. Because of the small amount of material available for analysis on some of the samples, it was not always possible to determine Na_2O, K_2O, and H_2O, and for all the samples it was necessary to adopt a scheme of analysis that would permit the determination of as many constituents as possible on a single fraction. Thus, in the analysis of the olivines and pyroxenes, Cr_2O_3, V_2O_5, and CoO, as well as TiO_2, were determined on the SiO_2/R_2O_3 fraction (see Foster 1946, p. 15–18). After titration of total iron, subsequent to reduction in the Jones reductor, R_2O_3 was again precipitated. Separation of Fe_2O_3, TiO_2, and CoO from Cr_2O_3

and V_2O_5 was effected by fusion of this second R_2O_3 precipitate, after drying, in a porcelain crucible with Na_2O_2 followed by a water leach and filtration.

Because spectrographic determinations showed TiO_2 to be very low, iron was removed by ether extraction before determination of TiO_2 with H_2O_2. After removal of H_2O_2, CoO was determined on the same solution, using NH_4CNS and acetone. CaO and MnO were separated and determined on the magnesium precipitate after ignition and weighing; and NiO was determined on the fraction used for determination of ferrous iron, subsequent to titration of ferrous iron and removal of HF and H_2SO_4.

As sodium carbonate, used to break down the olivines and pyroxenes, is not effective for the breakdown of chromian spinels and chromites, a different method of attack was required. The scheme of analysis used for these minerals is shown in Table 17.

TABLE 17. CHEMICAL PROCEDURE FOR CHROMIAN SPINELS AND CHROMITES

Fuse 0.5 sample with $NaHSO_4$, dissolve fusion in 1:5 H_2SO_4,
evaporate to fumes, dilute, digest, and filter

<table>
<tr><td rowspan="3"><i>Precipitate:</i>
SiO_2 ignite and weigh.</td><td colspan="3"><i>Filtrate:</i>
Sulfates of R_2O_3 group, Ca, Mg and Mn. Make double NH_4OH precipitation; filter.</td></tr>
<tr><td colspan="2"><i>Precipitate:</i>
Hydroxides of Al, Fe, Ti, Cr. Ignite and weigh, fuse in porcelain crucible with Na_2O_2, leach, didigest, filter.</td><td rowspan="2"><i>Filtrate:</i>
Sulfates of Ca, Mg, and Mn. Precipitate and weigh as pyrophosphates, dissolve in dilute H_2SO_4 and determine CaO and MnO; obtain MgO by difference.</td></tr>
<tr><td><i>Precipitate:</i>
Oxides of Fe and Ti. Dissolve in H_2SO_4, dilute, reduce in Jones reductor and titrate to obtain total iron, add H_2O_2, determine TiO_2 colorimetrically.</td><td><i>Filtrate:</i>
Na_2CrO_4—Boil to eliminate H_2O_2, acidify with H_2SO_4, titrate with $FeSO_4$ and $KMnO_4$.
Al_2O_3 by difference: Total weight R_2O_3 minus Fe_2O_3, TiO_3, Cr_2O_3.</td></tr>
</table>

On those chromian spinel samples for which less than 0.2 was available for analysis, only Fe_2O_3, TiO_2, and Cr_2O_3 were determined.

The chemical and spectrographic results were in good agreement for all the minor elements except titanium. The tendency for discrepancies in the determination of titanium has been recognized previously, and the causes are to be the subject of further study.

Discussion of Chemical and Mineralogical Studies

The distribution of the major constituents in the four minerals—olivine, enstatite, chromian diopside, and chromian spinel—from olivine inclusions in basaltic rocks and from dunites is shown in Fig. 1. The high, low, and average values obtained for each constituent are shown enclosed in brackets, except those values that are so nearly the same that they are represented by two points, or only one. Both ferrous and ferric iron are included in the value shown as Fe_2O_3, although in the olivines and enstatites iron was present as ferrous iron only.

The small range in the values for the different constituents in the silicate minerals from inclusions and from dunites—olivine, enstatite, and chromian diopside—is striking. This is particularly true of the olivines, in which, for all the specimens analyzed regardless of source, there is a range of not more than 1 per cent in the silica content, not more than 2 per cent in the magnesia content, and not more than 3 per cent in FeO content. With regard to the FeO content, however, a slight differentiation may be made between the olivines from inclusions and those from dunites, in that the FeO content of the dunite olivines falls in the lower part of the range, and the FeO content of olivines from inclusions falls in the upper part. All the iron in the olivines is present as ferrous iron. The average aluminum content of the olivines is 0.10 per cent.

In the enstatites from dunite the range between high and low values for silica and magnesia is about 5 per cent, but in the enstatites from inclusions the range for these constituents is not more than 2 per cent. All the values for silica in enstatites from inclusions lie in the upper part of the range of values for silica in enstatites from dunites. On the other hand, the values for MgO in enstatites from inclusions lie in the lower part of the range of values for MgO in enstatites from dunites. The range between high and low values for FeO in all the enstatites is not more than 3 per cent, with the values for FeO in enstatites from dunites falling in the median part of the range. One enstatite contains 0.16 per cent of Fe_2O_3; in the others, all the iron is present as ferrous iron. Al_2O_3 in the enstatites from inclusions averages 3.55 per cent and ranges from 2.18 per cent to 5.32 per cent; in the enstatites from dunites, it averages only 1.30 per cent and ranges from 1.00 per cent to 1.60 per cent.

The chromian diopsides from dunites are slightly higher in SiO_2 and CaO content and slightly lower in total iron content—as Fe_2O_3—than the chromian diopsides from inclusions. The range between high and low values for these constituents in all the chromian diopsides, however, is less than 4.50 per cent. For MgO the range is less than 3 per cent. The greatest divergence in average content between diopsides from inclusions and diopsides from dunites appears in the Al_2O_3; in the inclusions the average Al_2O_3 content is 4.80 per cent; in the dunites it is only 0.70 per cent.

Much greater differences were found in the composition of the chromite and chromian spinels than in the composition of the three silicate minerals. The disseminated type of chromite was obtained in sufficient amounts for analysis in only two of the dunite samples. These two samples were similar in composition and were much higher in Cr_2O_3 content than any of the chromian spinels from the inclusions. In fact they may be classified as true chromites, whereas none of the spinels from the nodules could be so classified. The nodules differ greatly among themselves in Fe_2O_3, Cr_2O_3, and especially Al_2O_3 content, ranging from 14.29 to 29.81 per cent in iron as Fe_2O_3, from 11.00 to 32.87 per cent in Cr_2O_3 content, and from 19.29 to 53.43 per cent in Al_2O_3 content. On the other hand, in the chromite from dunite the Al_2O_3 ranges from 8.81 to 13.37 per cent, Cr_2O_3 from 48.48 to 55.17 per cent, and MgO from 10.02 to 13.23 per cent.

The distribution of the minor constituents —NiO, MnO, and Cr_2O_3— is shown in Fig. 2, plotted on a scale 25 times that used in Fig. 1. The amounts of the minor constituents in the olivines from the nodules are almost identical with the amounts of the same constituents in the olivines from dunites, and the range of values is very small. This is also true of the MnO and NiO content in the enstatites and chromian spinels. The Cr_2O_3 content of the enstatites and chromian diopsides on the other hand, is much more variable, particularly in the minerals from the nodules. The average content of Cr_2O_3 in the enstatites from the nodules is very close to the average content of Cr_2O_3 in enstatites from dunites. However, the average content of Cr_2O_3 in chromian diopsides from the nodules is about 0.4 per cent higher than the average content of Cr_2O_3 in diopsides from dunites. The Cr_2O_3 content of most of the chromian diopsides from the nodules, however, was in the lower part of the range indicated in Fig. 2; in fact, only one specimen contained more than 1.5 per cent Cr_2O_3.

The relationship of NiO to the major elements should be noted. A comparison shows that the average ratio of NiO to MgO is 0.663 in olivine, 0.023 in enstatite, and 0.002 in diopside. On the other hand, the ratio of NiO to FeO is about 0.036 in olivine, 0.02 in enstatite, and 0.015 in diopside. Therefore, the NiO does not follow the MgO but maintains roughly the same proportion to FeO in the three silicate minerals.

There is a progressive decrease in NiO content from the olivine through the enstatite to the chromian diopside. There is a marked increase in the Cr_2O_3 content in this series of minerals but the MnO content is remarkably constant throughout the whole suite of minerals.

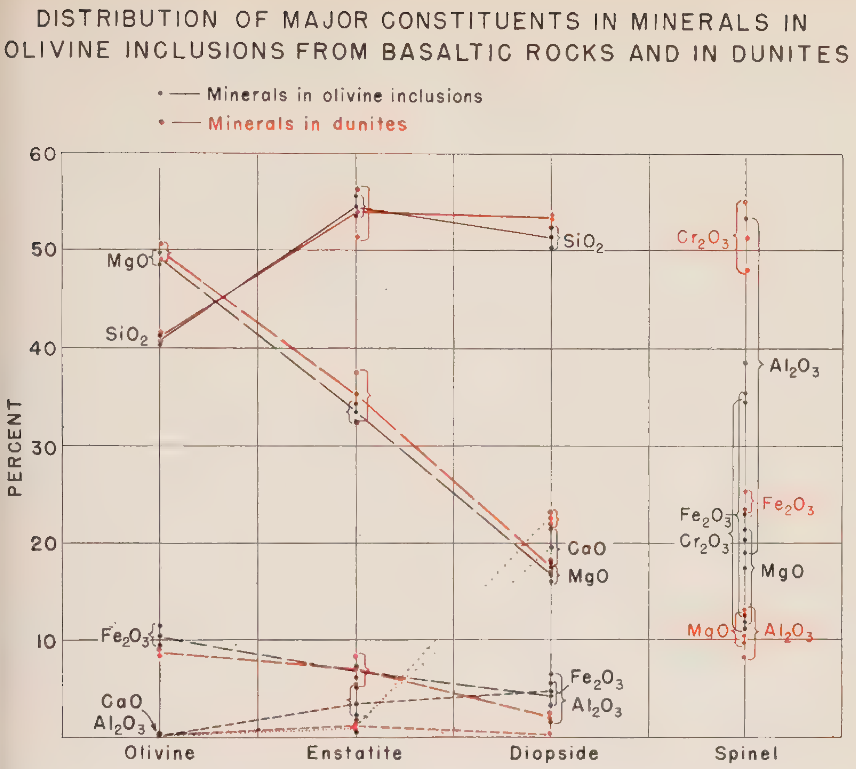

DISTRIBUTION OF MAJOR CONSTITUENTS IN MINERALS IN OLIVINE INCLUSIONS FROM BASALTIC ROCKS AND IN DUNITES

Figure 1

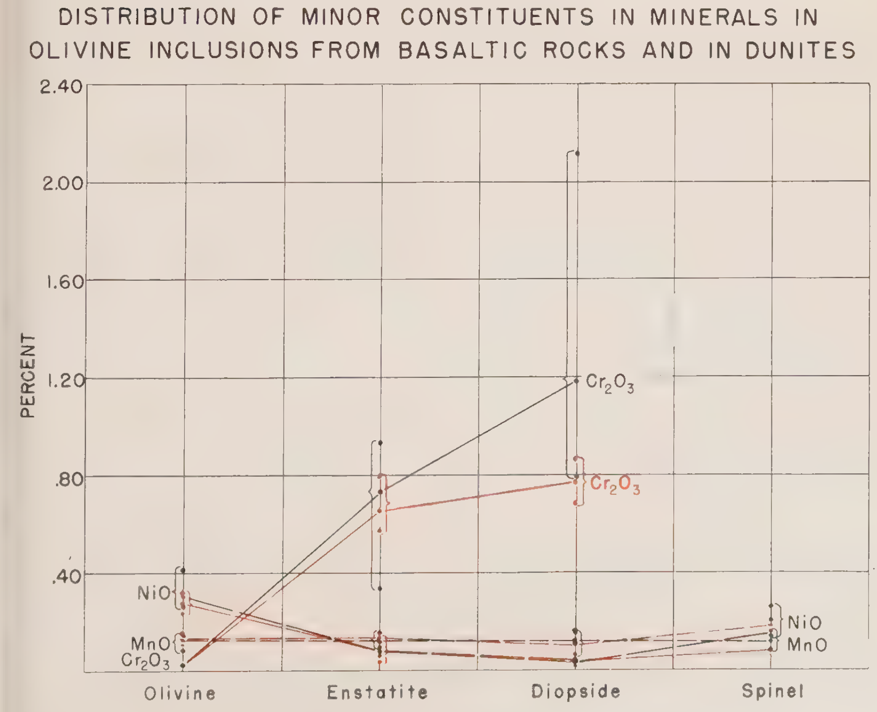

DISTRIBUTION OF MINOR CONSTITUENTS IN MINERALS IN OLIVINE INCLUSIONS FROM BASALTIC ROCKS AND IN DUNITES

Figure 2

The CoO content is very low, amounting, in general, to only 5 to 10 per cent of the NiO content.

Relation to Host Rocks

Several workers, including Ernst (1936), Frechen (1948), and Turner and Bartrum (1928, p. 899), have made important contributions to an understanding of the relationship between the nodular inclusions, and the rocks in which they occur. Chemical analyses of five of these rocks are given in Table 20. The mode of No. 2 is given in Table 18 and of No. 4 in Table 19. The norms of the five rocks are given in Table 21.

No. 1. Olivine basalt, 1801 Kaupulehu flow of Hualalai, Hawaii. Host rock of minerals listed as No. 11 in Tables 4 to 7, collected by Dr. Macdonald, analyzed by H. M. Hyman, U. S. Geological Survey. The minor elements determined by A. A. Chodos, U. S. Geological Survey, as follows:

Ni 0.03, Co 0.006, Cr 0.04, Cu 0.02, V 0.03, Ga 0.001, Sc 0.002, Ba 0.06, Sr 0.1, Y 0.004, Yb 0.0003, Zr 0.02. Looked for but not found: Pb, Be, Ag, Au, Pt, Mo, W, Ge, Sn, As, Sb, Bi, Zn, Cd, Tl, In, La, Nb, Ta, Th, U, B.

No. 2. Olivine melilitite forming matrix around olivine inclusion from Westberges near Hofgeismar, north of Kassel, Germany, analyzed by Theodor Ernst (1936, p. 647). The mode determined by Ernst as follows:

TABLE 18. MODE OF OLIVINE MELILITITE FROM WESTBERGES

Olivine	30	Apatite	3
Augite	34	Magnetite	7
Melilite	7	Chromite	
Perovskite	2	Nepheline	14
Hauyne	1	(interstitial)	

No. 3. Olivine basalt from Finkenberg, Siebengebirge, near Bonn, Germany, described by Frechen (1948, p. 321). Dr. M. Hartwig-Bendig, analyst.

No. 4. Olivine melilitite forming host rock for olivine inclusions from Hochbol Swabia, Germany. Cited by Ernst (1936, p. 659), analyzed by Wohlmann, described by Tröger (1934, p. 153).

No. 5. Basalt from Ichinomegata, Akita Prefecture, Japan. T. Katura, analyst. Analysis received through the courtesy of Dr. Kuno.

TABLE 19. MODE OF OLIVINE MELILITITE FROM HOCHBOL

Olivine	23	Biotite	4
Augite	19	Perovskite	
Melilite	44	Apatite	
Nepheline	6	Calcite	
Ores	4	Chromite	

TABLE 20. CHEMICAL ANALYSES OF NODULE-BEARING ROCKS

	1	2	3	4	5
SiO_2	46.64	37.09	41.72	36.64	51.24
Al_2O_3	14.45	8.49	13.04	7.96	17.98
Fe_2O_3	3.18	5.65	2.68	6.19	3.30
FeO	9.77	6.53	10.00	5.59	6.61
TiO_2	2.35	2.43	2.73	2.50	1.51
Cr_2O_3	—	0.13	0.06	—	—
CaO	9.86	14.09	10.82	15.11	6.98
MgO	9.33	17.36	9.00	18.15	4.62
Na_2O	2.84	2.85	3.74	2.85	5.39
K_2O	0.97	1.56	0.88	1.44	2.10
MnO	0.19	0.19	0.18	0.17	—
NiO	—	0.11	—	—	—
BaO	—	—	0.07	0.05	—
ZrO_2	—	—	0.03	0.03	—
CO_2	0.01	—	3.19	0.53	—
P_2O_5	0.34	0.99	0.58	0.91	—
H_2O-	0.00	0.45	0.27	0.03	—
H_2O+	0.06	2.16	0.92	1.56	0.35
Total	99.99	100.23[1]	100.02[2]	99.71	100.08

[1] Includes 0.15 per cent SO_3.

[2] Includes 0.11 per cent Cl.

TABLE 21. NORMS OF NODULE-BEARING ROCKS

	1	2	3	4	5
or					
ab	8.91		7.86		30.41
an	23.92	5.56	16.97	4.73	18.64
lc	4.36	7.42	3.93	6.55	9.60
ne	8.24	13.07	12.21	13.07	8.24
wo	9.64	19.28	5.34	19.51	6.74
en	23.19		22.38		11.54
fs	11.89		12.00		6.86
fo		30.39		31.56	
fa		3.06		1.02	
cs		3.63		4.48	
mt	4.63	8.10	3.94	9.03	4.86
il	4.40	4.55	5.16	4.70	2.88
ap	0.67	2.35	1.34	2.02	
hl			0.12		
cc			7.31	1.20	
	99.85	97.41	98.56	97.87	99.77

The modes and norms show that the nodules occur in rare rock types as well as in more normal olivine basalts. In four of the six rock analyses, Cr_2O_3 was determined and ranges from 0.06 to 0.19 per cent. However, even this Cr_2O_3 content is higher than that found in average basalts. Ten basaltic rocks from the Hawaiian Islands have been tested by spectrographic methods by K. J. Murata of the U. S. Geological Survey. Chromium was determined as Cr but has been recalculated to Cr_2O_3 for purposes of comparison; these rocks contain about 0.025 to 0.077 per cent Cr_2O_3. A group of rocks from the Paricutin Volcano in Mexico contain from 0.025 to 0.034 per cent Cr_2O_3. It thus seems improbable that basaltic rocks are normally high enough in chromium to produce silicate minerals and spinels that contain unusually high percentages of that element.

ORIGIN OF DUNITE

The senior author is acquainted with the dunite bodies of Pennsylvania, Maryland, and Georgia. He has also visited but not studied in detail those of Cuba, the South Island of New Zealand and New Caledonia. He has long been familiar with several dunite bodies of North Carolina, and it is on these that he bases his discussion of the bearing of the geologic relationships, upon the origin of dunites and related peridotites, particularly those of the Webster area. These bodies are the basis of comparisons with other dunite areas visited, and with the studies of other geologists.

North Carolina

The serpentinization in the dunite bodies of western North Carolina is very local, and large parts of these bodies are almost completely unaltered. Fresh and nearly pure olivine rocks are well exposed at such localities as Webster, Balsam Gap, Addy, Dark Ridge, and Democrat. In many places the contacts with the country rocks are well exposed. Much of the dunite contains 90 per cent or more of olivine, and locally disseminated chromite, rare single grains of enstatite, and conspicuous but rare grains of green chromian diopside may be present. The dunite itself in general is rather evenly granular, but in some places, notably at Addy, there is a great range in the size of the olivine grains. Crystals up to 4 cm. in diameter are commonly enclosed in a matrix of crushed grains, so that parts of the rock resemble a crush breccia. A part of a crystal unit 10 cm. in length has been observed that probably represents about half of the original crystal.

Webster is also the type locality for websterite, the orthopyroxene-diopside rock with accessory olivine. This rock forms an elongated mass parallel to the dunite with which it is associated, and of which it is evidently a phase. The pyroxene (chromian diopside) is bright yellowish green (29.GG-Yi, Ridgeway color standards) and so makes a conspicuous outcrop.

Inclusions: Lenses of chromite large enough to have been mined occur within the Webster dunite and also occur in thin stringers. Most significant, however, are rounded masses shaped like a large teardrop, which are abundant at the Dark Ridge locality. The masses are evidently blocks that have been brought up from the depths by the intrusive force of the mushlike olivine, and the tail-like ends represent partly disintegrated and dragged-out portions of the chromite blocks.

In the vicinity of Webster, blocks of almost pure enstatite up to half a meter in diameter have been observed. They form rare but large, conspicuous inclusions in the dunite and smaller inclusions in the websterite. In these masses the individual crystals may reach 30 mm. in length. Millimeter-sized olivine grains make up a small part of the rock and occupy angular spaces between the large enstatite grains; chromite and chromian diopside grains are sparse. Zones of olivine in the enclosing dunite, characterized by variable grain size, form a flow structure that sweeps around some of the enstatite blocks, indicating that at the time of emplacement these blocks were rigid masses, and the olivine was a mushlike crystalline mass that flowed into place around them.

Structure: A marked parallelism of structure is a conspicuous characteristic of the Webster mass. Parallelism is so noticeable that it led early observers to assume that the mass was sedimentary in origin. In the dunite this is caused by persistent shear zones in which the olivine grains are crushed. The shearing has exerted a close control over the degree of serpentinization, so that sheared and serpentinized zones alternate with little-sheared and unserpentinized zones.

The websterite mass is parallel to the border of the dunite, and to the structure within it. The websterite itself shows marked lineation, resulting from parallel alignment of the pyroxene grains. It is also marked by long parallel lenses of nearly pure olivine oriented with the lineation. The websterite with its marked lineation seems to have flowed into position, as did the olivine enclosing the enstatite blocks.

Border Relationships: Between dunite and the enclosing quartz schist there is a zone of hydrothermal minerals (talc, anthophyllite, and vermiculite) that ranges from a few centimeters to a meter or so in width. This zone is composed of the same minerals and shows the same zonal relations as the minerals that have formed on the borders of pegmatite lenses where the pegmatites have locally intruded the dunite at a much later geologic age. Thus, the hydrothermal borders on the dunite are evidently the result of pegmatitic solutions that penetrated along the contacts.

The dunite was intruded at a temperature and in a condition that precluded any marked reaction with the enclosing quartz schist. This condition is significant because of the marked disequilibrium that must have existed between the quartz schist and the subsilicic dunite. Any reaction between dunite and quartz schist must have been so minor that it has been entirely concealed by later hydrothermal action. This same absence of contact reactions is characteristic of the Twin Sisters body in Washington.

Serpentinization: The local character of serpentinization and its relation to shear zones in the Webster dunite have been mentioned, and a general discussion of serpentinization need not be undertaken here. However, an interesting relation between olivine and serpentinization has been observed in the vicinity of the Woods chromite mine in Pennsylvania, where olivine crystals up to 15 cm. in length have been replaced by serpentine along crystal directions in the olivine. Two distinct types of serpentine are represented—one the usual reticulate type, and the other a distinctly later one that resembles chlorite. In the Buck Creek area of North Carolina there has also been serpentinization of olivine crystals along crystal directions. In both these areas, serpentinization was controlled by the crystal structure of the olivine.

The relationships in the Webster dunite and the associated websterite and similar bodies that seem most significant are (*a*) the marked parallelism in the lineation, shear zones, parallel zones of chromite, and zones of serpentinization; (*b*) the lack of any essential reactions between dunite and country rock; (*c*) the presence of blocks of enstatite and chromite, with flow lines in the dunite that sweep around blocks; and (*d*) the remarkable size range of the olivine grains in some of the dunite masses.

New Zealand

Turner and Verhoogen (1951, p. 240) have described the New Zealand occurrences of dunite and serpentine as follows: " . . . in southern New Zealand vertical sheets of peridotite and serpentine, believed to be of late Paleozoic age, include at least three individual masses whose continuous outcrops, dissected to a relief of 5,000 to 7,000 ft.; each exceed 40 miles in length, and locally attain a width (thickness) of 3 to 5 miles." Turner states (personal communication): "Contact effects are limited or almost lacking, at least over most of the peridotite margins so far investigated. There is no indication of high-temperature metamorphism. All this fits in perfectly with Bowen's theory." In describing serpentinization, Turner says, "Most partly serpentinized peridotites that I have seen show clear evidence that serpentinization proceeds metasomatically from cracks that often are continuous through several crystals."

Sweden

Du Rietz (1935, p. 138), in discussing the origin of the dunites of Sweden, concludes that the rock was probably formed as "an intrusion of an almost crystalline phase, with a complete lack of mineralizers. . . . The author has nowhere seen any convincing trace of contact metamorphism of the peridotite on the surrounding rocks." He reports the four characteristic minerals—olivine, diopside, enstatite, and chromite, or chrome picotite. In discussing serpentinization, Du Rietz (1935, p. 233) says, "In the region described by the writer no facts supporting the derivation of the serpentinizing solutions from the peridotite magma were observed." Du Rietz describes in detail the very widespread alteration of the original dunitic rocks and concludes (p. 257) "Hydrothermal waters originating from acid intrusions have produced the transformation." An analysis of the olivine from Sweden by R. Blix is given in Table 13, No. 13, and an analysis of enstatite from the same region by I. Suckdorff in Table 14, no. 13.

Physical and Chemical Relations

The high temperature of fusion of olivine (see Bowen and Schairer, 1935, p. 204, also 1936, p. 391–396) and the previously described absence of notable contact reactions between dunite and invaded rock, are the chief reasons why geologists have in general agreed that the olivine must have been introduced at moderate temperature only. However, there is no such general agreement as to the cause of this moderate temperature. Vogt (1926, p. 232) appears to be the only one who has postulated a melt with a temperature of 1,500° to 1,600° C., but he gave no consideration to contact relationships.

Hess believes that the olivine magma contained an essential amount of H_2O at the time of introduction. Bowen (1928, p. 166) quotes Harker as also postulating an essential amount of H_2O. Bowen (1928, p. 167) in his "general consideration of ultrabasic rocks" says, "These difficulties [the problem of temperatures of formation of dunite] disappear entirely if the rocks are accepted as the result of crystal accumulation without melting." Bowen and Tuttle (1949, p. 455) made a detailed study of the system MgO-SiO_2-H_2O and reached the following conclusions: "Under certain conditions of crustal deformation, apparently involving strong overthrusting, dunitic and related materials, coming at times perhaps from a peridotite shell of the earth, at other times from a peridotite mass that has formed as a differentiate of gabbroid magma, can be intruded in a completely crystalline state into accessible levels of the earth. . . . There is no reason to suppose that the crystalline mass initially has more than a trace of water."

Orogenic Relations

The relationship of ultrabasic rocks to the profound orogenic processes in the earth's crust was pointed out by Suess (1909), has since been noted by many geologists, and is carefully reviewed by Benson (1926). Hess gives detailed consideration to the relation between belts of dunite and orogeny. Hess (1939, p. 270), says: "The strong light upper crust [about 25 km. thick] is downbuckled into the peridotite substratum which lies perhaps 60 km. below the surface. The intermediate layer [between 25 and 60 km.] of basaltic material, being considerably hotter, is not quite so strong as the upper crust so that it deforms by flowing laterally, thus allowing the upper crust at the bottom of the downbuckle to come in contact with the peridotite substratum. The differential pressures developed in the region of the bottom of the downbuckle during deformation permit the squeezing off of a product of partial fusion of the periodotite substratum."

Hess (1939 p. 263) also states that "the typical serpentinized peridotites, which occur as narrow belts paralleling island arcs, mountain systems, or eroded roots of former mountain systems, were intruded as magmas of ultramafic composition, and are not magmatic differentiates of a gabbroic [mafic] magma. This type of ultramafic is limited entirely to such strongly deformed belts, and does not occur elsewhere."

Structures

Turner (1942, p. 281) made a careful study of the structures in the dunites of New Zealand and compared them with similar material from other occurrences. In commenting on the structures in dunite he says: "Certainly of deformational origin, however, are closely spaced, discontinuous, but sharply-defined lamellae parallel to (100) that may be observed in sections of many New Zealand dunites when viewed between crossed nicols . . . translation gliding remains the most probable mode of origin for lamellar structure sub-parallel to (100) in olivine. . . . There are strong objections to any hypothesis of origin of banded structures in the unserpentinized dunites of New Zealand and the Hebridean province other than that of laminar flow in a partially, perhaps almost completely crystallized magma." Turner then gives the results of fabric studies of various types of dunites from several localities. Oriented fabric patterns were observed in all of these, and of one type, Turner (1942, p. 291) says, "The grains range from 0.5 mm. to 2 mm. in diameter, and commonly show distinct undulose extinction accompanied by translation lamellae parallel to (100) when observed between crossed nicols. No preferred dimensional orientation of grains could be detected."

The writers find translation structures in all the dunites and also in the olivine-rich inclusions in all the materials examined in the course of this study. We have made no studies similar to those of Turner of the crystal orientation in dunites. However, the lineation in the websterite phase at Webster, North Carolina, is very noticeable.

Summary

There are four distinct lines of approach to the problem of the origin of dunite and related rocks. Bowen (1928) and Bowen and Tuttle (1949) have studied the geophysical problem presented by dunites and come to the conclusion that these rocks were intruded as a largely crystalline, mushlike material. Ross, Turner (1942), Thayer, and Du Rietz (1935) are representative of those who have made field studies of the geologic relationships and conclude that the intrusion of a mushlike mass is the mechanism that best accords with the field relations. Hess (1939) has considered the relationship of dunite bodies the world over with the profound orogenic processes and concludes that the material from which dunites formed "was a water-rich product of the partial fusion of the peridotite substratum." Turner (1942) has studied the structure of dunites of New Zealand and compared them with those of Skye and believes that both these dunites must have formed by the "laminar flow of a partially, perhaps almost completely, crystalline magma." These diverse approaches to the problem of the origin of dunite and related rocks seem to present convincing evidence that the rocks were formed by the intrusion of a largely crystalline mushlike material, and that this material was made up essentially of olivine. The relations also indicate that the peridotite substratum is the most probable source of so unusual a material.

Some dunites and related rocks show relationships with basaltic rocks and evidently have had a different genetic history with those previously discussed. Hess (1938, p. 334) mentions such rocks, which are part of the Stillwater complex. The rocks of the Hebrides (Bowen 1928, p. 166, and and Harker 1904) are believed to be differentiates of basaltic rocks.

ORIGIN OF NODULELIKE INCLUSIONS IN BASALTIC ROCKS

Geologists who have discussed the origin of nodular inclusions in basaltic rocks have commonly concluded that the nodules are genetically related to the host rock, but some believe that they are derived from the peridotite shell of the earth's crust. Among those who believe in a derivation from the host rock are Lacroix (1894), Rinne (1893), Bauer (1891), Zirkel (1940) and Schwantke (1923). The most recent advocate of this origin is Frechen (1948). Heritsch (1908) postulated the derivation of the nodular inclusions from lherzolite (a peridotite composed of olivine, orthorhombic pyroxene, and monoclinic pyroxene) and Ernst (1936) has made the most thorough presentation of the theory of a derivation from the peridotite shell.

Chemical and Mineral Relations

The study of 12 olivine nodules and the data from earlier studies show that material from many widely distributed regions is characterized by the same four minerals. Some nodules contain olivine crystals that range from 1 to 3 mm. in diameter, but commonly the range is much greater. Among the specimens from Hawaii, augite grains commonly range from 1 to 12 mm. in diameter, but one individual has a cleavage surface 10 cm. across. Olivine grains are at least 15 mm. in diameter in some of the inclusions. Bauer (1891, p. 182) has described olivine crystals in nodules from Stempel, near Marburg, up to 5 cm. in diameter and "bronzite" crystals equally large. The olivine grains in specimens from Camargo, Mexico; Rice Station, Arizona; Meng-Chian, Manchuria; and Dreiser Weiher, Germany, commonly range from 1 to 10 mm. in diameter, but some are even larger. Lausen (1927, p. 298) mentions a chromian diopside crystal at Rice Station (Peridot Cove) 2 in. in length.

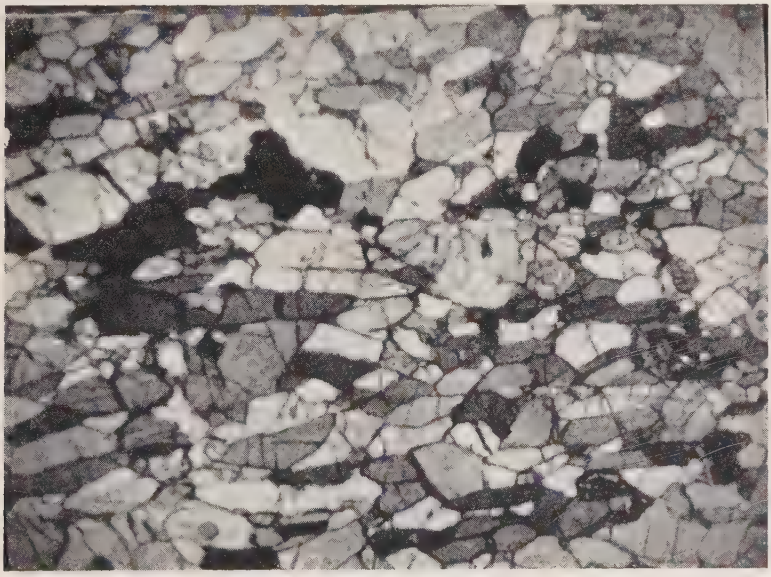

FIG. 3. Reproduction of an illustration by Ernst (1936, p. 638, Fig. 2) showing "grain deformation and elongation in the plane of foliated structure" of the olivine.

Structures

Ernst presents an excellent illustration (1936, p. 638, Fig. 2) reproduced in Fig. 3 showing "grain deformation and elongation in the plane of foliated structure" of the olivine. He also illustrates (1936, p. 640, Fig. 4) translation lamellae in olivine. He concludes (p. 640) that they show "an outstanding structural arrangement in the olivine and present strong proof that the olivine had suffered dynamic stress, in contrast with the enclosing effusives." Foliated structures in olivine-rich nodules have been described from Germany, by Schulz (1903, p. 270); from Klein-Iser, Czechoslovakia, by Braun (1922); and from Italy by Andreatta (1934, p. 241). Heritsch (1908, p. 300) discussed these structures in the olivine nodules from Kapfenstein, Austria, and concluded that they indicated that they were derived from a peridotite zone of the earth's crust.

The great range in the proportions of the characteristic minerals of the olivine-rich nodules is shown by representative occurrences in Tables 1 and 2. The range is from almost pure olivine to almost pure enstatite, and as much as 30 per cent of chromian diopside may be present. Similar relations are shown in Hawaiian material, where some nodules are pure olivine, others are pure clinopyroxene, but chromian spinel is sparse, ranging from almost none to about 2 per cent.

A careful study of the relationships in olivine inclusions of a melilite basalt from Westberges was made by Ernst (1936, p. 637), who says, "I base the evidence of the foreign nature of the olivine nodules on the following summary. There is a similarity of the nodules with lherzolitic rocks [olivine-enstatite-monoclinic pyroxene] that must seem the more remarkable if one considers the limited variability of the nodules, with the very great difference in the rocks in which the olivine nodules occur, as in the phonolites, feldspar basalts, melilite basalts and limburgites."

Turner studied several nodules derived from basaltic rocks of New Zealand in connection with his work on the structures of dunites. In describing these rocks, Turner (1942, p. 294) says, "It is therefore suggested that all three nodules are fragments torn from masses of solid peridotite, which have formed under plutonic conditions, but have never flowed in in the form of injected bodies of largely crystallized peridotite magma." And (p. 299) "The petrofabric evidence, taken in conjunction with the widespread occurrence of olivine-rich nodules, in basalts in many parts of the world, points to deep-seated solid accumulations of olivine crystals and in some cases perhaps intrusions of peridotites as the source of the nodules in question." The foregoing observations by Turner seem to summarize very effectively the evidence of a close genetic relationship between the olivine-rich inclusions in basaltic rocks and dunites.

Source and Emplacement

A definite mechanism for the intrustion of dunite has been postulated, which indicates that this material was derived directly from the peridotite zone. On the other hand, various mechanisms by which olivine-rich inclusions reached the surface have been suggested, and the problem arises as to their history after their departure from the peridotite layer. The olivine inclusions, or at least part of them, may not have come directly from the peridotite zone.

The nodules derived from basaltic rocks of New Zealand discussed by Turner had the same relation to basalts as those in other regions, but they occur in close proximity to one of the outstanding dunite areas of the world. They could thus be interpreted as having been torn from the buried dunite mass by the basalt as it made its way to the surface. The zone of nodule inclusions in basaltic rocks that extends across Germany could be related to a buried dunite zone associated with Alpine structures. That is, in these regions the inclusions might have arrived at the surface by a two-stage process. However, the profound downwarps that are believed to actuate dunite intrusion, even as buried masses, seem improbable in many of the areas where inclusions have been recognized. The Arizona and Mexico materials are from a plateau region where such downwarps are unknown, and according to Dr. Kuno (personal communication) the same is true for the Manchurian occurrence. The inclusions from the Hawaiian Islands are probably also unrelated to such profound downwarps. These facts, therefore, strongly suggest that in general the inclusions were not derived from dunite that had come part of the way from the peridotite zone.

Summary

The mineral, chemical, and physical relationships bearing on the origin of the nodulelike inclusions in basaltic rocks may be summarized as follows:

(*a*) Olivine nodules occur throughout the world and everywhere contain the same four mineral groups—olivine, enstatite, chromian diopside, and chromian spinel.

(*b*) The minerals of the nodules are the same in all occurrences; while the host rocks differ greatly in composition.

(*c*) Essentially pure olivine nodules, pure enstatite nodules, and nodules dominantly chromian diopside are improbable as simultaneously formed, direct differentiates from basaltic magmas.

(*d*) The great size of many of the individual mineral grains of the nodules does not indicate direct crystallizations from a basaltic magma.

(*e*) The high chromian content of the spinels and of the pyroxenes seem to be an improbable concentration from a basaltic magma with a few hundredths of 1 per cent of Cr_2O_3.

(*f*) The nodules show structure typical of materials that have been subjected to orogenic stress.

The most probable origin of nodulelike inclusions seems to be that they are derived from the peridotite zone of the earth's crust and that most of them at least came directly from that zone.

ORIGIN OF DUNITE AND NODULELIKE INCLUSIONS CONTRASTED

The foregoing study has brought together paragenetic, mineralogic, and chemical data on two groups of rocks –dunites and nodulelike inclusions in basaltic rocks—which superficially seem to have quite different modes of occurrence. The significant characteristics of the two groups have been summarized, and we may now review the common relationships.

A comparative summary of the significant relationships shows that dunites and nodules have the following characteristics in common:

(*a*) Similar mineralogy.
(*b*) Remarkable chemical similarity.
(*c*) World-wide occurrence.
(*d*) Great range in size of crystals.
(*e*) Similar range in variation of mineral proportions.

A few geologists have postulated a deep-seated origin for dunite, and others a deep-seated source for olivine-rich nodules in basaltic rock. However, Turner and Ernst seem to have been the only ones who have considered the origin of both these modes of occurrence.

The foregoing discussion indicates that olivine-rich nodules and dunite and related rock show a remarkable similarity in all essential relationships. Such parallelism in so varied and widely occurring a group of characteristics cannot be the result of a series of geologic accidents, and the origin of olivine inclusions in basaltic rocks and the origin of dunites must be considered together, notwithstanding the different modes of occurrence.

The most probable common genetic relationship that can be evoked seems to be derivation from the earth's peridotite shell. The dunites are believed to have been brought up from this shell by profound orogenic processes and the inclusions by eruptive processes that tapped the same profound depths.

Among the nodules of the 1801 Kaupulehu flow of Hualalai Island of Hawaii, are those composed of calcic plagioclase and olivine, or of calcic plagioclase and diopside. These nodules differ greatly in mineral composition from typical nodules, and so must have had a slightly different history. However, rocks composed only of plagioclase and olivine or of plagioclase and diopside do not present a relationship suggestive of direct crystallization from a basaltic magma. The most probable explanation seems to be that of H.H. Hess (personal communication), that they are derived from a zone in the earth's crust somewhat higher than that of the olivine-rich nodules.

In the past, many geologists believed that the olivine-rich nodules were crystal segregations from their basaltic host rock, and some believe that the common genetic relationship that must be considered is that both the dunites and the nodulelike inclusions are related to basaltic rock. This relationship would postulate that great dunite bodies as well as the "secondary" ones of Hess (1938) were related to basaltic rocks.

In view of the foregoing relationships, a direct derivation of both dunites (excluding secondary dunites) and the nodules from basaltic rocks is improbable. The dunites here considered do not show any relation to basalts and in general occur in regions quite free from other igneous activity. Rather they do show a close relationship to profound orogenic processes.

The relationship between this indicated source of the material composing dunites and inclusions and current theories about the deep zones of the earth may be considered. There is general agreement that the peridotite zone lies unusually close to the surface in the central Pacific, and Gutenberg (1951) has given reasons for believing that this zone is even shallower than previously assumed. He says (p. 434), "In this case the Mohorovicic discontinuity would be at a depth of a few kilometers. . . . "Again, "Summarizing the data, there is some indication that, in an area in the eastern Pacific Basin, the ultrabasic material with a velocity of about 8 km./sec. begins at a depth of only a few kilometers. . . ."

Hess and Maxwell (1953, p.3) state "The refraction seismatic work of R. Raitt in the Pacific and the work of Ewing, Hamilton, Hersey, Officer, Press, Worzel, and Wuenschel in the Atlantic shows material probably of peridotitic composition at a depth of 15 km. below the sea floor possibly overlain by basalt and a thin veneer of sediments. Study by Ewing and Press of surface waves from earthquakes also indicates a predominantly peridotitic oceanic crust. . . . Samples of the oceanic peridotite crust are probably available for study for examples . . . and the olivine bombs [xenoliths] found in many basaltic volcanoes. . . ."

If these are the relations in the Pacific and the Atlantic, they would impose no improbable mechanism for bringing dunitelike materials to the surface as inclusions in basalts.

The depths to the Mohorovicic discontinuity in plateau regions is much greater, as indicated by the following statement by Gutenberg (1951, p. 438), "In the continents the crust is formed by a layer of sialic rock of a thickness varying from place to place, with an average of 10 km. Below it, down to the Mohorovicic discontinuity at a depth between

30 and 40 km., but deeper in some mountain areas, are simatic rocks." Under plateau regions the depth to ultrabasic rocks would probably be of order of 50 km. and so would impose a long distance of travel if basaltic material brought olivine-rich inclusions directly from the region of the Mohorovicic discontinuity. However, some recent studies of the heat flow and chemical segregation of the mantle by Hurley (1951, p. 328) lead to the following conclusion:

"Measurements on the Oregon basalts give values too high to permit the basalt to exist as a part of a permanent extensive layer below the discontinuity, and at the same time there is difficulty in achieving the temperature of 1,100° C. or so for the molten basalt if it occurred above the discontinuity. This argument is even more pressing in the case of oceanic volcanic islands. It is therefore suggested that at least some basalts are concentrates or extracts from partial fusion at depths of at least several hundred kilometers within the mantle, brought to the surface by convection, and representing a continuing source of alumina, alkalies, and other elements of continental growth."

Verhoogen (1953, p. 329) has discussed the petrological evidence on the temperature distribution in the mantle of the earth and says, "From the maximum observed temperature of lavas and their composition it is inferred that basaltic magmas are formed by partial melting of mantle material at a depth of less than 150 km. and at an initial temperature less than 1,400° C. This suggests that the temperature at the core boundary normally does not exceed 2,400° C. Rising material at this initial temperature would have at 150 km. depth a temperature sufficiently greater than the melting point at that depth to allow partial fusion."

Conclusions

Geologic, mineralogic, and chemical studies of peridotitic material from two distinct physical modes of occurrence but of almost identical composition provide additional information about the peridotite zone of the earth's crust, a zone inaccessible for direct observation. It is a zone whose composition has fundamental bearings on the tectonics of island arcs and the great ocean deeps, its upper surface is believed to represent the Mohorovicic discontinuity, and the rate of transmission of earthquake waves within the layer has contributed to an understanding of the internal structure of the earth. The mineral composition of this zone, and its relation to the mineral composition of meteorites also concerns those investigating the composition of heavenly bodies. For these reasons, information about the peridotite zone has significance for all the earth sciences. This paper is therefore offered as a contribution to the broader aspects of earth science.

References

1. Andreatta, Ciro (1934), Analisi strutturali di rocce metamarfiche, V; oliviniti: *Periodico mineral. ann.*, **5**, 237–253.
2. Bauer, Max (1891), Der Basalt vom Stempel bei Marburg, und einige Einschlüsse desselben: *Neues Jahrb. Mineral., Geol., Band* **2**, 156–205: 231–271.
3. Becker, Arthur (1881), Über die Olivinknollen im Basalt: *Deutsche geol. gesell. Zeitsch., Band* **33**, 31–65.
4. Bell, J. M., Marshall, P., and Clarke, E. de C. (1911), The geology of the Dun Mountain Subdivision, Nelson, New Zealand: *Geol. Survey Bull.* **12**, 1–71.
5. Benson, W. N. (1918), The origin of serpentine, a historical and comparative study: *Am. Jour. Sci., 4th ser.*, **46**, 693–731.
6. Benson, W. N. (1926), The tectonic conditions accompanying the intrusion of basic and ultrabasic igneous rocks: *Nat. Acad. Sci., First Mem.* **19**, 1–90.
7. Bleibtreu, Karl (1883), Beiträge zur Kenntniss der Einschlüsse in den Basalten mit besonderer Berücksichtigung der Olivinfels-Einschlüsse: *Deutsche geol. Gesell. Zeitschr., Band* **35**, 489–556.
8. Bowen, N. L. (1928), The Evolution of the Igneous Rocks, Princeton Univ. Press, 334.
9. Bowen, N. L., and Schairer, J. F. (1935), The system MgO-FeO-SiO_2: *Am. Jour. Sci., 5th ser.*, **29**, 151–217.
10. Bowen, N. L., and Schairer, J. F. (1936), The problem of the intrusion of dunite in the light of the olivine diagram: *Geophysical Lab., Carnegie Inst. Wash. Pub., Paper* **886**, and *16th Internat. Geol. Cong.*, **1933**, Rept., vol. 1, 391–396.
11. Bowen, N. L., and Tuttle, O. F. (1949), The system MgO-SiO_2-H_2O: *Geol. Soc. Am., Bull.* **60**, 439–460.
12. Braun, H. (1922), Der Buchberg bei Klein-Iser und Seine Beziehungen zum Bohmischen Mittelgebirge: *Neues Jahrb. Mineral., Geol., Band* **2**, 277–278.
13. Du Rietz, Torsten (1935), Peridotites, serpentines, and soapstones of northern Sweden: *Geol. fören. Stockholm Förh., Band* **57**, 133–260.
14. Ernst, Theodor (1936), Der Melilith-Basalt des Westberges bei Hofgeismar, nördlich von Kassel, ein Assimilationsprodukt ultrabasischer Gesteine: *Chemie der Erde, Band* **10**, 631–666.
15. Farsky, Franz (1876), Mineralien aus den Kosakover Basalt Kugeln Austria: *Berh. K. K. geol. Reichsanstalt*, 205–208.
16. Foster, M. D. (1946), The separation of small amounts of chromium from vanadium with ethyl acetate: *U. S. Geol. Survey, Bull.* **950**, 15–18.
17. Frechen, Josef (1948), Die Genese der Olivinausscheidungen von Dreiser Weiher (Eifel) und Finkenberg (Siebengebirge): *Neues Jahrb. Mineral., Geol., Band* **79**, *Abt. A*, 317–406.
18. Gutenberg, Beno (1951), Crustal layers of the continents and oceans: *Geol. Soc. Am., Bull.* **62**, 427–440.
19. Harker, A. (1904), The tertiary igneous rocks of Skye: *Mem. Geol. Survey United Kingdom*, 1–482.
20. Heritsch, Franz (1908), Über einige Einschlüsse und vulkanische Bomben von Kapfenstein in Oststeiermark: *Centr. Mineral., Geol., Paleont.*, 297–305.
21. Hess, H. H. (1938), A primary peridotite magma: *Am. Jour. Sci., 5th ser.*, **35**, 321–344.
22. Hess, H. H. (1939) ,Island arcs, gravity anomalies, and serpentine intrusions—a contribution to the ophiolite problem: *17th Internat. Geol. Cong., Moscow,* **1937** *Rept., vol.* **2**, 263–283, English edition.

23. Hess, H. H., and Maxwell, J. C. (1953), Caribbean Research project: *Geol. Soc. Am., Bull.* **64,** 1–6.
24. Hillebrand, W. F., and Lundell, G. E. F. (1929), Applied Inorganic Analysis, John Wiley and Sons, New York, 929.
25. Hochstetter, Ferdinand von Wein (1859), Dunite: *New Zealand Govt. Gazette, No.* **39.**
26. Hochstetter, Ferdinand von Wein (1864), Dunit, korniger Olivinfels von Dun Mountain bei Nelson, Neu Seeland: *Deutsche geol. Gesell. Zeitschr., Band* **16,** 341–344.
27. Hurley, M. (1951), Heat flow and chemical segregation of the mantle: *Program for Thirty-second Ann. Meeting Nat. Research Council, Nat. Acad. Sci. Abs.*
28. Knop, A. (1877), Über die Zusammensetzung der Olivinfelsknollen im Basalte des Lutzelberges bei Sasbach im Kaiserstuhl: *Neues Jahrb. Mineral., Geol.,* 697–699.
29. Lacroix, A. (1894), Étude minéralogique de la lherzolite des Pyrenees: *Nouv. archiv du museum d'historie naturelle, 4rd ser., Paris,* 226–242.
30. Lacroix, Alfred (1942), Les Peridotites de la Nouvelle-Caledonie: *Acad. Paris, tome* **66**, 1–143.
31. Lauro, Carlo (1940), I minerali degli inclusi autigeni nel basalto di Conca de Janas (Orosei): *R. Accad. Italia, Atti, Cl. sci., Rend, ser.* **7**, *vol.* **1,** *fasc.* **6**, L'olivina e lo spinello cromifero, 186–192; *fasc.* **7**, 290–294, I pirosseni.
32. Lausen, Carl (1927), The occurrence of olivine bombs near Globe, Arizona: *Am. Jour. Sci., 5th ser.,* **14,** 293–306.
33. Link, G. (1891), Die Basalte des Elass: *Zeits. Kryst., Mineral.,* 663.
34. Link, H. (1887), Zur geologischen Kenntnis, d. südl. Rhon: Inaug-Diss. Würtzburg, 100.
35. Rammelsberg, G. F. (1876), Über dem Olivinfels vom Dreiser Weiher: *An. Phys. und Chem.,* 512–519.
36. Rinne, F., (1893), Über die Norddeutsche Basalte aus dem Gebiete der Weser und den angrenzenden Gebieten der Werra und Fulda: *Jahrb. preuss. geol. Landesanst., Band* **23,** 1–95.
37. Schadler, Joseph (1914), Zur Kenntnis der Einschlüsse in den südsteirischen Basalttuffen und iherr Mineralien: *Tschermak's min. pet. Mitt., Band* **32,** 485–511.
38. Scharizer, Rudolf (1884), Über Mineralien und Gesteine von Jan Mayen: *Jahrb. K. K. geol. Reichsanstalt, Wien, Band* **34,** 707–728.
39. Schiller, Joseph (1905), Über den Gabbro aus den Flysch bei Visegrad in Bosnien: *Tschermak's min. pet. Mitt., Band* **24,** 309–320.
40. Schultz, Walter (1903), Beiträge zur Kenntnis der Basalte aus der Gegend von Homberg a. und Efze: *Neues Jahrb. Mineral., Geol., Beilage-Band* **16,** 241–291.
41. Schuster, M. J. (1878), Über Auswurflinge im Basalttuffe von Reps in Siebenburgen: *Tschermak's min. pet. Mitt., Band* **1,** 318–330.
42. Schwantke, Arthur (1923), Differenzierungserscheinungen an hessischen Basalten: *Neues Jahrb. Mineral., Geol., Beilage-Band* **48,** 260–273.
43. Stearns, H. T., and Macdonald, G. A. (1946), Geology and groundwater resources of the Island of Hawaii: *Hawaii Terr. Div. Hydrography, Bull.* **9,** 1–363.
44. Stevens, R. E. (1944), Composition of some chromites of the western hemisphere: *Am. Mineral.,* **29,** 1–34.
45. Suess, E. (1904–1908), The Face of the Earth, translation of Das Antlitz der Erde, by Sollas, vols. **1–4.**
46. Tröger, E. (1934), Quantitative Daten einiger magmatischer Gesteine: *Min. pet. Mitt., Band* **46,** 153–173.

47. Turner, F. J. (1942), Preferred orientation of olivine crystals in peridotites, with special reference to New Zealand examples: *Roy. Soc. New Zealand, Transactions*, **72,** part 3, 280–300.
48. Turner, F. J., and Bartrum, J. A. (1928), The geology of the Takupuna-Silverdale district, Waitemata County, Auckland: *Trans. New Zealand Inst.*, **59,** 864–902.
49. Turner, F. J., and Bartrum, J. A. (1928), The geology of the Takupuna-Silverdale district, Waitemata County, Auckland: *Trans. of the New Zealand Inst.*, 864–902.
50. Turner, F. J., and Verhoogen, Jean (1951), Igneous Petrology. McGraw-Hill Book Co., New York, 174.
51. Vogt, J. H. L. (1926), Magmas and igneous ore deposits: *Econ. Geol.*, **21,** 207–233.
52. Zirkel, Ferdinand (1904), Über Urausscheidungen im Rheinischen Basalten: *Abhandl. der Math.-Phys. Klasse König. Sachs. Gesell. Wiss., Band* **22,** 103–198.

Manuscript received May 13, 1953

"SOLUBILITY" OF ALBITE IN HYDROTHERMAL SOLUTIONS*

A. F. FREDERICKSON AND JOSEPH E. COX,
Washington University, St. Louis, Missouri.

ABSTRACT

The apparent solubility of albite in pure water is determined over a limited range of temperatures at a pressure of 300 bars and compared with that of quartz. The solubilities are of the same order of magnitude suggesting that they both disintegrate or decompose according to the same mechanism. The greater "solubility" of quartz accounts for its first appearance and great persistence in natural hydrothermal solutions.

Both ions and silicate fragments result when albite is attacked under the experimental conditions used. The possibility that actual particles of silicate structures, ranging up to 1000 unit cells in size, might be transported through rocks is suggested.

An origin of certain clay minerals and the alumino-silicate fragments in shales is discussed.

INTRODUCTION

Geologists have been speculating since the earliest time concerning the manner in which materials are transported in or through rocks. The intriguing problems of the mechanism of metasomatism, granitization, vein-formation, and many others of this kind, challenge our imagination. In order to obtain a better insight into the mechanism of any of these processes, we need to formulate better or clearer ideas on

1. The solubility of silicates and other rock-forming material in hydrothermal solutions, and
2. The physical state in which material of this kind exists in these solutions.

Water is one of the most important components in most rock systems. We believe that the hydrogen ions of water are by far the most important of all elements in the earth's crust that affect geological processes. The purpose of this paper is to describe the behavior of albite in hydrothermal solutions—pure water heated to various temperatures under a pressure of 300 bars—and to speculate on the role played by hydrogen ions in this system.

PROCEDURE

An albite crystal was suspended in a bomb filled with enough distilled water to give a pressure of 300 bars when heated to the desired temperature. The system was held at the desired temperature for approximately 100 hours. Samples of the fluid in the bomb were then isolated by a series of valves and tubes using a technique described by Frederickson and Cox (1953).

---

* Contribution number 170 of the Department of Geology, Washington University, St. Louis, Missouri.

To test the homogeneity of the fluid, one sequence of samples was siphoned from the bottom of the bomb and another from near the top of the solution chamber. The apparent solubilities of albite, under these conditions, is summarized by the curves in Fig. 1.

Samples of the fluids were evaporated on collodion supports and the products examined under an electron microscope (Fig. 2).

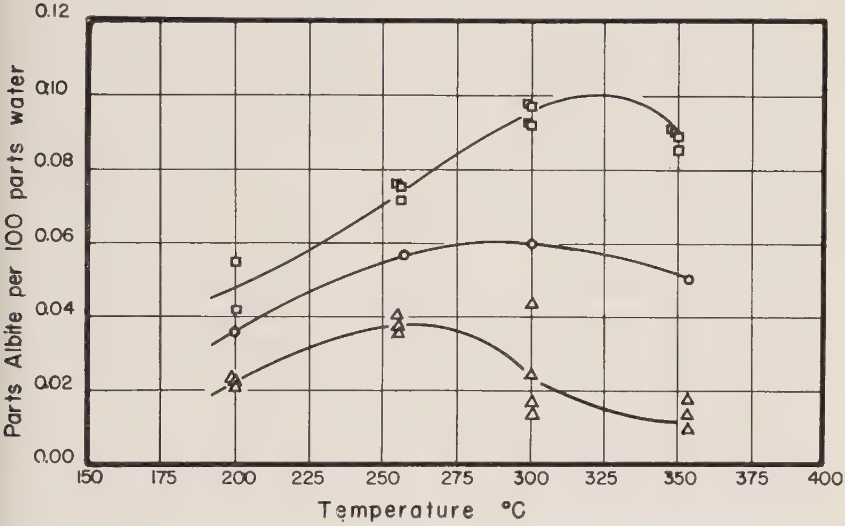

Fig. 1. Apparent solubility of albite in distilled water (pressure: 300 bars).

□ Values for bottom of bomb
△ Values for top of bomb
○ Averages of above values

The solution was electrodialyzed. The apparatus consisted of two fritted glass, Gooch-type filtering crucibles immersed in a deep Petrie dish. Graphite electrodes were operated at a potential difference of approximately 40 volts. The amount of current passing through the system was measured by use of two copper strips connected in series and immersed in a 25 ml. beaker containing $CuSO_4$. The milliequivalents of copper transferred from one electrode to the other was taken as a measure of the current. The solution accumulated in the cathode chamber was periodically removed and analyzed with a flame photometer. The electrodialysis curve for the "albite" solution is shown in Fig. 4.

Discussion

"Solubility" of Albite

The fluid in the bomb (see Fig. 1) is not homogeneous. The concentration of solids in the fluid is greater at the bottom of the bomb than at the

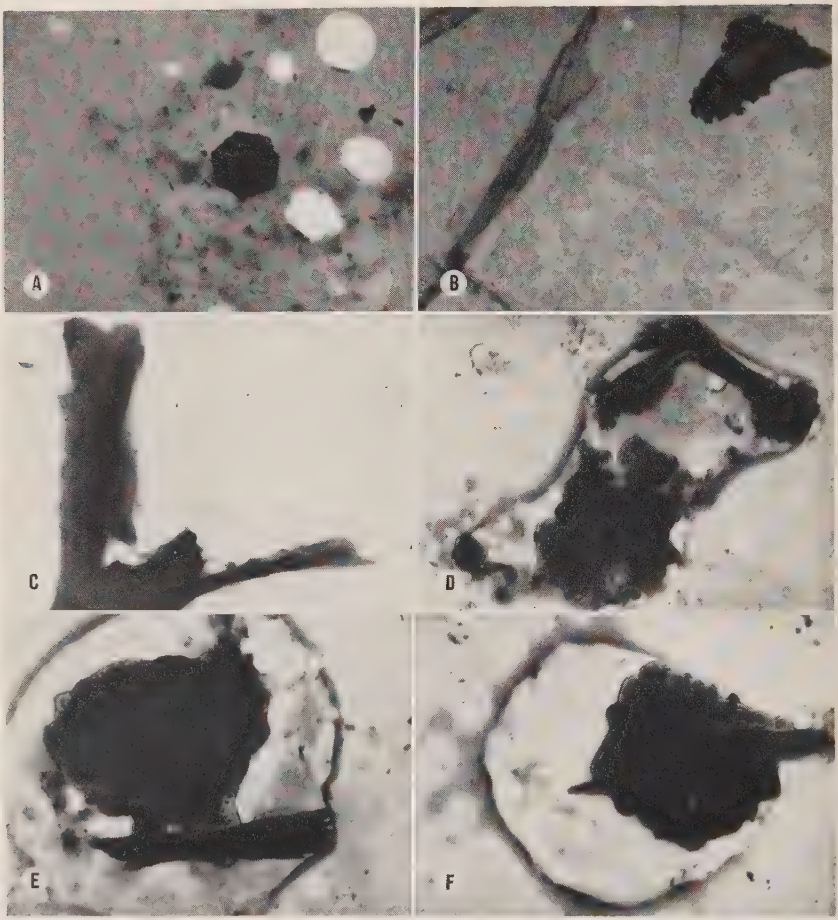

FIG. 2. Electron micrographs of "solutions" siphoned from the bottom of the bomb.

A. The comparatively large crystal with well-developed outlines is either an individual albite fragment or an aggregate of smaller albite fragments. Irregularities on the faces suggest a mosaic make-up. Smaller irregular albite granules can be seen scattered over the field. The small rod-like crystals are believed to be the zeolite detected by x-ray diffraction photographs.

B. Here the film of silica-alumina gel shows up clearly. It covers most of the field, and where broken, has curled and rolled back. The denser mass is composed of albite chunks and zeolite granules.

C. The alumina-silica gel has curled up into a series of rolls. These bear a striking resemblance to halloysite rolls or tubes. Only small changes in chemical composition and increased order within the film would be necessary to produce some of the clay minerals from this material. Perchance we have here visual evidence of the initial stages of at least one way of making a clay mineral: a sol formed during the decomposition and disintegration of the albite, gel and film formation by cross polymerization and, as seen top. This suggests that albite partially decomposes into fragments which settle toward the bottom of the bomb whereas smaller fragments or sols remain suspended in the fluid.

This conclusion is supported by the electron micrographic evidence (Fig. 2). Three products are seen:

1. Equant fragments,
2. A gel, and
3. Long fibrous and prismatic crystals.

X-ray diffraction work on these products indicates that the large, equant crystals are albite; the long, fibrous crystals are a zeolite of some kind, probably analcite.

The manner in which albite is thought to decompose is summarized in Fig. 3.

The large parent crystal contains many lineages, cracks and other crystal defects as well as a mosaic structure. After the crystal has been subjected to water at elevated temperatures and pressures, large fragments (0.1–5.0 microns) break away from the parent crystal to form the equant crystals seen in the electron micrographs (*A* and *B*, Fig. 2).

The increased solubility of the albite in water with an increase in temperature (at constant pressure) must be due to the increased activity of the hydrogen ions. The rapid increase of dissociation of water with increase in temperature results in a great increase in the number of hydrogen ions available to attack the crystals. Consequently, raising the temperature is equivalent to increasing the acidity (lowering the *p*H) of the solution.

Much of the material is reduced to particles having colloidal dimensions. When cooled, this material constitutes the gel which is the dark, mottled, gray, background material seen in most of the micrographs. Under the heat of the electron beam, the alumina-silica gel contracts, cracks, dries, and often rolls up (*B* and *C*, Fig. 2). The gel frequently shrinks into oval masses from which zeolite crystals grow.

The first zeolite to develop has a prismatic habit. If enough nutrient

---

here, generation of a tube by shrinkage and rolling of the film.

D, E, and F. Each of these micrographs illustrate the types of residue formed from an evaporated droplet of solution from the bomb. Each contains (1) gelatinous, (2) granular, and (3) fibrous or columnar material, implying that the fluid part of the "solution" when first reduced to room temperature and pressure was still quite homogeneous in composition. The zeolites, as seen with the electron microscope, appear to lie on top of most of the granular masses and films and probably formed last from some of the silica-alumina gel and sodium ions during the evaporation of the droplet. The magnification of the electron photomicrographs is 10,000×.

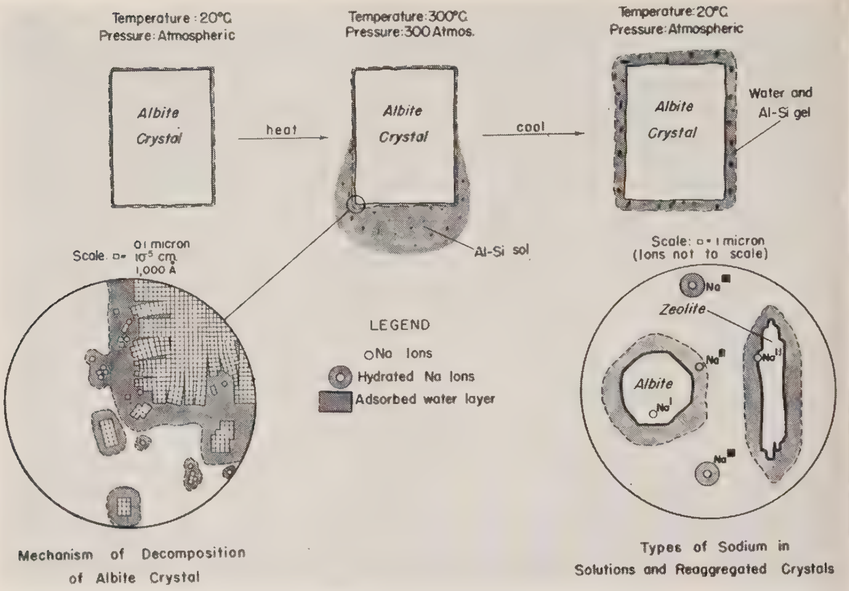

FIG. 3. Process and products of albite decomposition.

material is available, the crystals grow to a comparatively large size. The composition of the nutrient material apparently changes, or different temperature-pressure conditions cause a change in the crystal habit of the last zeolitic material to develop. The early zeolite crystals all have a long prismatic to a fibrous habit (*A*, *D*, *E*, and *F*, Fig. 2). At present, we are inclined to believe that all of the zeolite crystals grow only after the solution has been reduced to room temperature and pressure.

ELECTRODIALYSIS OF THE ALBITE "SOLUTION"

The amount of sodium transferred from the anodic to cathodic chamber is listed in Table 1 and plotted in the form of a curve in Fig. 4.

The electrodialysis experiments on the solutions taken from the bomb indicate that four different "kinds" of sodium exist. The occurrence of the sodium is indicated schematically in Fig. 3.

Large, hydrated sodium ions exist in solution (Type IIII). These are easily removed by dialysis. Extraction of this material produces the first part of the curve in Fig. 4. Increased current through the system now apparently causes a breakdown of some structure which results in a rapid release or a flood or "new" sodium. This sodium (Type III) is thought to occur as adsorbed ions around the albite fragments and on the zeolite

TABLE 1. ELECTRODIALYSIS DATA FOR THE ALBITE "SOLUTION"

Sample No.	Copper wt. change (grams)	Change in meq.	Current in meq. Cu/gm. product	Meq. Na found	Meq. Na/ Meq. Cu	Total current Meq./gm.
1	0.0010	0.0318	0.3225	0.055	1.730	0.3225
2	0.0010	0.0318	0.3225	0.079	2.484	0.6450
3	0.0035	0.1112	1.1278	0.069	0.625	1.7728
4	0.0008	0.0254	0.2576	0.020	0.787	2.0304
5	0.0005	0.0159	0.1613	0.005	0.314	2.1917
6	0.0011	0.0349	0.3540	0.005	0.143	2.5457
7	0.0054	0.1716	1.7404	0.030	0.175	4.2861
8	0.0020	0.0635	0.6440	0.015	0.236	4.9301
9	0.0018	0.0572	0.5801	0.000	0.000	5.5102
10	0.0038	0.1207	1.2241	0.003	0.025	6.7343
11	0.0027	0.0858	0.8702	0.007	0.082	7.6045
12	0.0078	0.2478	2.5132	0.000	0.000	10.1177

Initial volume of fluid: 250 ml.
Total amount of "dissolved" albite: 0.0986 gram.

crystals. The "structure" referred to above is the hydration shell adsorbed onto the albite crystal.

The first layers of this shell contain sodium ions arranged with a considerable degree of regularity and consequently can be considered to be fairly well crystallized. The removal of the sodium ions disrupts the shell which then assumes an ice structure (Frederickson, 1952) that has a lesser degree of crystallinity over a given distance from the crystal surface than did the one containing the sodium ions.

The breakdown of this layer progresses in a gradual manner as is indicated by the gradual change in slope of the dialysis curve.

The next flood of sodium is released rather abruptly and again is interpreted as being due to the breakdown of some structure; the zeolite. The amount of energy, epxressed in amount of current, necessary to break down this structure is, as would be expected, much larger than that required to wreck the less crystalline water hull.

The final, very sharp break in the curve is interpreted to mean that the remaining solid (albite) decomposes to release a small amount of sodium. The amount of sodium contained in the various postulated phases, some of which can be directly seen in the electron micrographs, is summarized in Table 2.

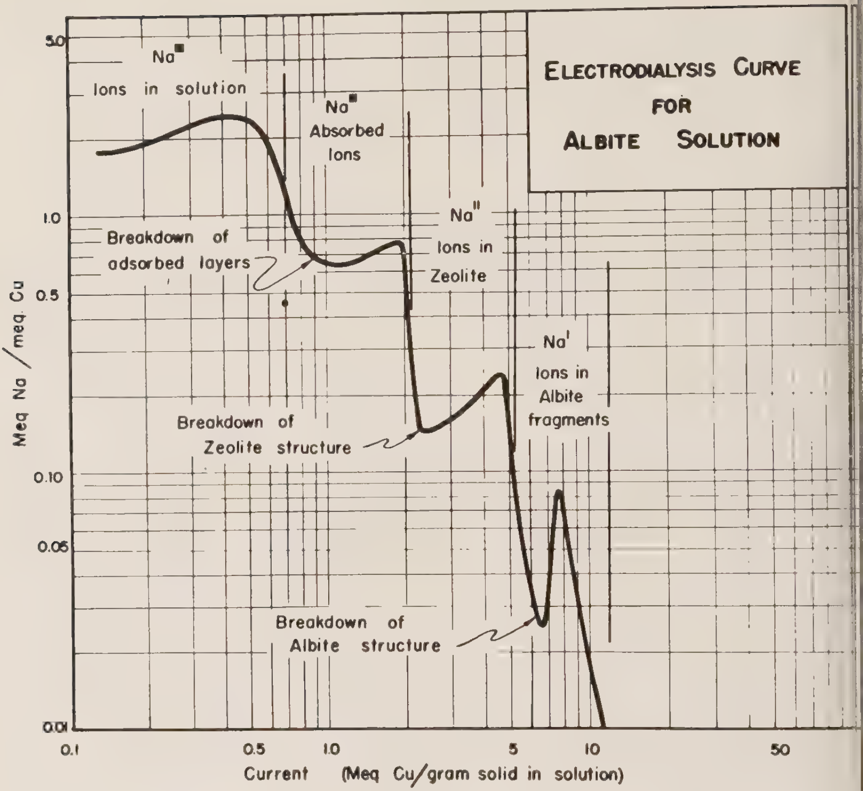

FIG. 4.

TABLE 2. AMOUNT OF SODIUM IN THE DIFFERENT PHASES IN THE ALBITE "SOLUTION"
(Calculated in per cent of the total sodium in the "solution")

Na IIII	Na III	Na II	Na I
Hydrated ions in solution 46 per cent	Ions in the zeolite 33 per cent	Ions in adsorbed water layer 18 per cent	Ions in albite fragments 3 per cent

All the various types of sodium will form a complex equilibrium. The rates at which these various equilibria will be established, however, will be considerably different; the rate at which the ions in true solution will reach an equilibrium with those adsorbed on the surface of the crystals will be very rapid. This will be in sharp contrast to the equilibrium between sodium Types I and II. The mechanism by which this equilibrium is reached was discussed in some detail by Frederickson (1952).

The dialysis procedure used here is relatively rapid; consequently equilibrium is not re-established after the first sodium is removed from the system. The current density, therefore, can be taken as a measure of how strongly the different kinds of sodium are held by the various phases.

Some Geological Implications

Silicate Paragenesis

The most surprising fact about the behavior of albite in water heated to elevated temperatures under 300 bars pressure is that its apparent solubility is almost the same as that for quartz (Frederickson and Cox, 1953). This is certainly not what one would expect. The apparent solubility curves for albite (Fig. 1) are plotted with the earlier ones obtained in Fig. 5. Although our curves for quartz solubility are not exactly the same as ones previously published by other authors, the average curve representing an arithmetical mean between the curves for solutions siphoned from the bottom and the top of the bomb corresponds almost exactly with Kennedy's (1950) data. We therefore believe that our technique and results are essentially correct or at least of the correct order of magnitude.

The apparent solubility data for quartz and albite indicate that they

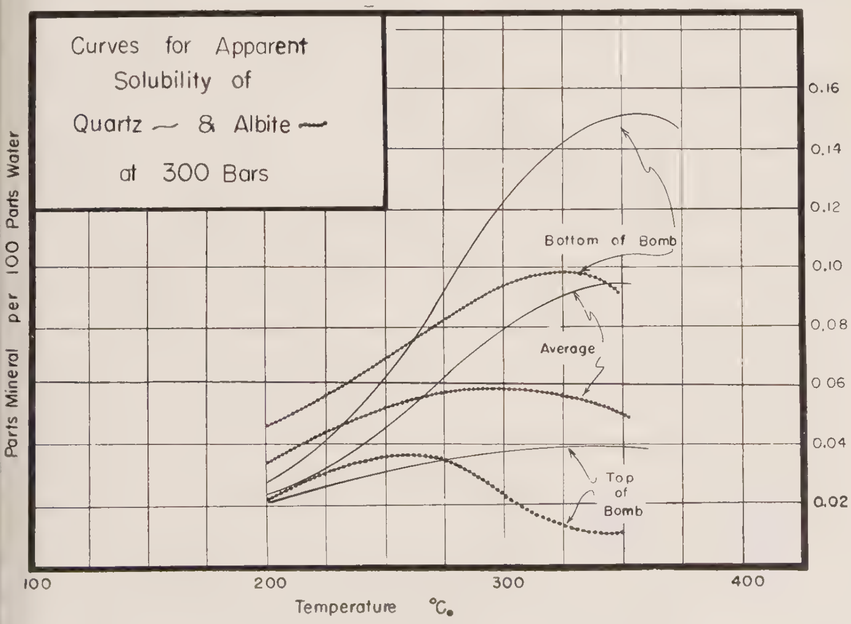

FIG. 5.

both decompose or disintegrate according to the same mechanism. The curves also indicate that quartz is appreciably more "soluble" and therefore should be selectively removed from rocks attacked by solutions of the kind used in these experiments. Not only will the quartz be selectively removed from the attacked rocks, but it will be retained in solution longer and consequently will travel farther than albite in a cooling system. Quartz should appear first in hydrothermal solutions and remain as the last component in such a system. These statements are in harmony with field observations.

The electron micrographs clearly indicate that the albite decomposes to yield both large fragments of albite and a gel material. The size of the albite fragments occurring in the "solution" can be directly measured; the largest so far seen is 5 microns in diameter, but by far the greatest percentage of these particles have a diameter closer to 0.5 micron or smaller. Some of the larger fragments may actually be aggregates of smaller ones.

In addition to these fragments, the gel material can be considered a particles of colloidal size. The large quantity of gel produced during the attack on the albite nutrient material suggests the possibility that matter can be transported in and through rocks as individual particles of considerably greater size than individual ions. Some of these particles may contain as many as 1000 unit cells of a silicate structure. The possibility of moving actual *particles* through rocks may help explain the manner in which certain preferred orientation develops in some tectonites as well as how local banding may develop by segregation (concretion and enrichment-of-the-most-stable-constituent principles of Eskola).

SIZE OF THE COLLOIDAL PARTICLES IN THE GEL

The physical state of the matter making up the gel has not been determined directly. The gel does not give an *x*-ray diffraction pattern that can be interpreted readily. Particles of albite and zeolite can be seen in the gel. These particles are so small that very little physical separation can be made with the means at our disposal; consequently the amount of the diffuse *x*-ray pattern contributed by the gel could not be assessed.*

Some idea concerning a possible size and shape of the colloidal particles can be indirectly deduced from electron micrographs of the surface of the parent albite crystal. Figure 6 is a chromium shadowed collodion replica of the surface of an albite crystal etched with distilled water at a maximum temperature of 300° C and 300 bars pressure. The crystal has been differentially etched. Relatively large pits occur on the surface. The larger pits have rude crystal outlines; the triangular terminations are usually quite regular.

---

* Standard supercentrifuge bowls require more solution than we obtain from our bombs. These small quantities, however, can be handled in an ultracentrifuge. Small-angle *x*-ray scattering experiments on the gel fraction should give useful information as to the average size of the gel particles and might also yield some information on particle shape.

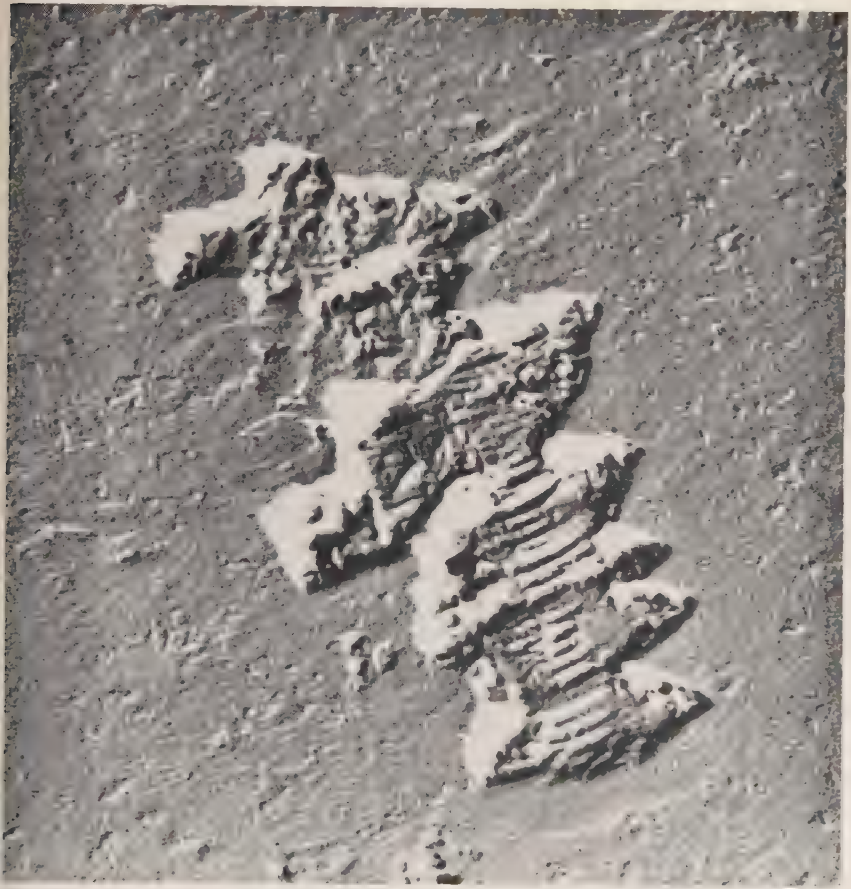

FIG. 6. Electron micrograph of a chromium shadowed collodion peel taken from the surface of an albite crystal etched with distilled water at a maximum temperature of 300° C and a pressure 300 bars. Magnification: 20,000 ×.

The most interesting features shown in Fig. 6 are the depressions within the small pits exhibiting the rude crystal outlines. It appears as if rods had been removed leaving a rod-shaped depression. The width of these rods is quite uniform and measures about 1 micron. The length of the depressions varies, but it appears as if the rods extended the full length of the crystal-shaped depression. These rods bear a striking resemblance to those of quartz (Frederickson 1953). We believe these to be the basic mosaic units contained in albite. Not enough work has been done to outline the role these rods-shaped crystallites play in gel formation. At present we believe that fragments of these rods constitute the albite fragments shown in Fig. 2. These are the mosaic units that spall off the crystal when it is attacked by the hydrothermal solutions. Both large (Fig. 2*A*) and small (Fig. 2*B*) albite fragments exist in the gel. This might be explained by assuming that albite fragments continue to spall off the parent albite crystal throughout the duration of the bomb run and that the first ones decompose almost completely to give rise to the gel. This would mean that the albite fragments shown in Fig. 2 represent mosaic units in various stages of disintegration. An argument of this kind, however, would mean that equilibrium had not been attained in the bomb and that the solubility value obtained should be a function of the duration of the bomb run. This is not the case.

The points in Fig. 1 show that the results can be closely reproduced. We therefore believe that equilibrium has been attained in the bomb. If this is accepted, some of the small crystallites must be stable in this environment.

The *x*-ray diffraction patterns of the albite fragments in the gel are quite diffuse. This can be interpreted to mean that the structure of these crystallites, although essentially the same as albite, has been greatly disturbed. This could easily result from the removal of the sodium ions. Inasmuch as albite can be considered as a coordinated network of SiO_4 and AlO_4 units slumped around the sodium ions which occcupy the interstices within the structure, a further distortion of the lattice would be expected if the sodium was removed. We believe that the lattice would actually expand (Frederickson, 1952) due to mutual repulsion of the negatively charged oxygen ions surrounding the possible sodium lattice sites. With this as a model, we visualize these fragments to be structurally similar to albite, but to also have a much larger unit cell and a different chemical composition. Particles in this condition should readily enter into chemical reactions because of their great specific surface and reactivity due to lattice distortion.

Marshall (1935) described particles found in the Putnam clay that closely resembled albite, but had slightly different indices of refraction indicating compositional changes. Bray (1937) described weathered mica products from which some of the potassium ions had been removed. The very small clay content of most shales (usually less than 5 per cent), indicates that alumino-silicate fragments, along with quartz particles, are the most important constituents of rocks of this kind. Much more work, however, must be done to establish the above presumptions as fact.

APPLICATION OF THESE RESULTS TO THE PROBLEM OF CLAY GENESIS

Experience indicates that clays can be formed in both weathering and diagenetic environments. The clays are frequently stated to be the weathering products of feldspars. Clays are essentially two-dimensional, layer-lattice structures in contrast to the three-dimensional feldspar frameworks. It is not possible to produce the clay-mineral structures from feldspar networks by a translation or displacement operation; one can be only formed from the other by a reconstructive type of transformation. What are the building blocks from which the clay structures are built? This work suggests at least two alternatives:

1. The small crystal fragments could be mortared together by aluminous or siliceous cements to form layer lattice minerals. Reaction of the cements with the fragments would produce a two-dimensional lattice and reaction products such as quartz and gibbsite. The complex layering of many clays and the common occurrence of excess silica some of which is known to exist as microcrystalline quartz, might be explained in this way.
2. The clays could be built up of the very small colloidal micelles of the gel products resulting from the decomposition of the feldspars.

Both of these possibilities are currently being tested.

ACKNOWLEDGMENTS

This work was done as part of a U. S. Army Signal Corps research contract (*No. DA-36-039 sc 5513*). Their support and encouragement is gratefully acknowledged.

REFERENCES

BRAY, R. H. (1937), Chemical and physical changes in soil colloids with advancing development in Illinois soils: *Soil Science*, **43**, 1–14.

FREDERICKSON, A. F. (1952), Mechanism of weathering: *Geol. Soc. Am. Bull.*, **62**, 221–232.

FREDERICKSON, A. F. (1953), Mosaic structure in quartz: *Am. Mineral.* (In press.)

FREDERICKSON, A. F., AND COX, J. E. (1953), "Solubility" and mechanism of decomposition of quartz under elevated temperatures and pressures: *Am. Mineral.* (In press).

KENNEDY, G. C. (1950), A portion of the system of silica-water: *Econ. Geol.*, **45**, 629–653.

MARSHALL, C. E. (1935), Mineralogical methods for the study of silts and clays: *Zeit. Krist.*, **90**, 8–34.

Manuscript received June 25, 1953

CALCULATION OF POSITION AND INDICES OF LAUE SPOTS ON LAUE-PHOTOGRAPHS

H. Kedesy, *Signal Corps Engineering Laboratories,*
Fort Monmouth, New Jersey.

Abstract

Formulae are derived for the calculation of the polar-coordinates and indices of the Lau spots on the film for the perfect crystal lattice. This calculated Laue pattern can be use as a reference pattern for any deviation of the experimental one. The formulae are given fo the cases where the incident beam is perpendicular to (001), (010), (100) or (111). An ex ample of the evaluation of a group of Laue spots of the Laue pattern of a muscovite mic will be given and discussed.

Introduction

It has been recognized for a long time that the application of the La method can serve as a powerful tool for the studies of stacking disord in the growth of layer structures, polymorphism, intergrowth and orde disorder in alloys. Furthermore, the application to problems such thermal or elastic agitation of crystals, thermal decomposition with s multaneous nucleation and oriented growth of new phases, will only mentioned here. The advantages of the Laue method over the conve tional rotating crystal methods for a study of such problems are i greater resolution power of the reflections, the non-destruction of th specimen crystal, and the much shorter exposure time of the photographic film. For a thorough study of these problems an evaluation of th Laue pattern in respect to position and indices of the spots is necessar

In the Laue method the crystal and the photographic film are hel stationary while the crystal is irradiated by a fine beam of x-rays, comprised of a wide range of wavelengths. Variables can be provided by th range of wavelengths or by the setting of the crystal in respect to th incident beam. Two techniques, the transmission- (for glancing angle $<45°$) and the back-reflection (for glancing angles $>45°$) technique ca be distinguished. The Laue spots from perfect crystals are sharp bu from imperfect or deformed crystals they are diffuse or elongated. Also a change in position and intensity, the existence of extra spots, or change in the symmetry of the pattern are indications of imperfections and represent very important experimental data for the solution o special problems and fundamental research.

The graphical methods for determining the indices of Laue spots o Laue photographs involve no difficulties as long as the crystal is free from imperfections and belongs to one of the orthogonal systems. In othe than these cases, a numerical control of at least some of the indices is necessity. For that reason and since a completely calculated Laue pattern can be used as a reference pattern for the interpretation of any deviation of the experimental one, it was decided to establish practical useful formulae for the calculation of the position and indices of Laue spots. E. Schiebold[1] in a monograph on the Laue method, published 20 years ago, has derived a formula for the general case where any crystallographic direction of a triclinic crystal can be chosen as the direction of incidence for the x-ray beam. Therefore, his formula contains too many variables and is not practical. Besides this, many extra calculations and controls, with the help of the stereographic projection, have to be included. The purpose of this paper is to present the results obtained from calculations leading to simple formulae for the calculation of positions and indices of Laue spots if the incident beam is perpendicular to one of the principal planes (001), (100), (010), or perpdendicular to the (111) plane.

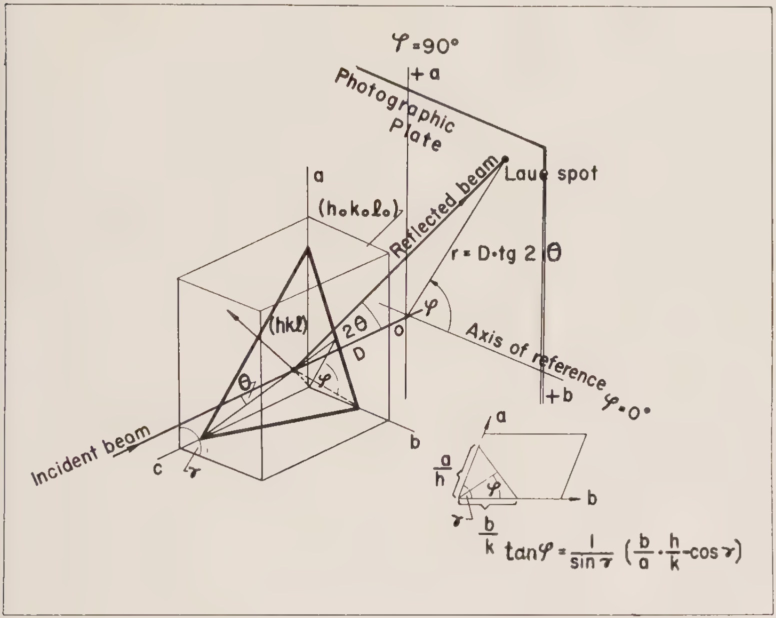

FIG. 1. Geometrical relationship between the position of the Laue spot and the reflecting plane for the case that the incident x-ray beam is perpendicular to a principal crystal plane. In the figure the (001)-plane is chosen as the plane of incidence.

In Fig. 1, the geometrical relationship between the position of the Laue spot and the reflecting crystal plane is shown for the case where the incident x-ray beam is perpendicular to one of the principal crystal planes and also perpendicular to the photographic film. For the determination of the position of the Laue spot, a polar-coordinate system in the plane of the photo-plate with its pole at the center of the Laue pattern is chosen. The azimuthal angle φ is measured from an axis, which corresponds to the direction of one of the crystal axes, parallel to the photographic plate. In this figure, the b-axis direction is chosen as the reference axis. A Laue spot on the photographic film is then determined by the radius vector r and the azimuthal angle φ. The following formulae were derived to correspond to Laue patterns as seen on the film in the direction of the incident beam. The distance r of a Laue spot from the center of the pattern is related to the corresponding Bragg angle θ by

---

[1] Schiebold, E., Die Laue Methode, Leipzig (1932).

$$r = D \cdot \tan 2\theta \tag{1}$$

where D is the distance between the crystal and the photographic plate. In the Laue method, using a white radiation, the angles φ and θ are independent of the wavelength and can be expressed in terms of the unit cell dimension, the indices of the plane of incidence $(h_0k_0l_0)$, and reflecting plane (hkl) only.

Determination of the Azimuthal Angle φ

If the incident beam is chosen perpendicular to the (001)-plane, the azimuthal angle φ of a Laue spot corresponds to the angle between the b-axis and the projection of the normal of the reflecting plane (hkl) on the (001) plane on the crystal, denoted by $(h_0k_0l_0)$. From the figure it can be seen that the intersection of the (hkl)-plane and the $(h_0k_0l_0)$-plane cuts on the a- and b-axes the section a/h and b/k. The relation between the angle φ and these sections is given by

$$\tan \varphi = \frac{1}{\sin \gamma}\left(\frac{b}{a} \cdot \frac{h}{k} - \cos \gamma\right) \tag{2}$$

where γ is the crystallographic angle between the a-and b-axes. Similar expressions can be obtained if the plane of incidence chosen is the (010) or (100)-plane. From equation 2, it can be seen that Laue spots with the same h/k-ratio of their indices, for example, spots originating from the $(21l)$, $(42l)$, $(63l)$. . . -planes lie on a straight line drawn from the center of the pattern.

Determination of the Reflection Angle θ

If the incident beam is perpendicular to a crystal plane $(h_0k_0l_0)$, the reflection angle θ from a plane (hkl) can be derived from the angle between these planes, i.e. from the angle betweeen their normals, as shown

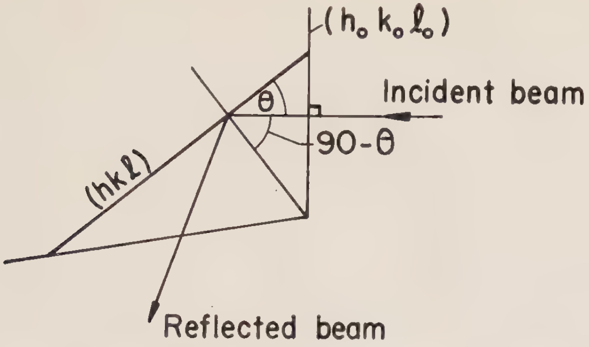

FIG. 2. Relationship between Bragg angle θ and the angle between the normals of reflecting plane and plane of incident. $(h_0k_0l_0)$ is the plane perpendicular to the incident beam, (hkl) is the reflecting plane, θ the Bragg angle, $(90-\theta)$ the angle between the normals of (hkl) and $(h_0k_0l_0)$.

in Fig. 2 Using the reciprocal lattice space the normals are vectors represented by

$$\begin{aligned} r_{hkl}^* &= a^*h + b^*k + c^*l \\ r_{h_0k_0l_0}^* &= a^*h_0 + b^*k_0 + c^*l_0. \end{aligned} \tag{3}$$

The lengths of these vectors are equal to the reciprocal of the spacings of the corresponding planes

$$\left| r_{hkl}^* \right| = \frac{1}{d_{hkl}}; \qquad \left| r_{h_0k_0l_0}^* \right| = \frac{1}{d_{h_0k_0l_0}}.$$

The angle between the vector r_{hkl}^* and $r^*_{h_0k_0l_0}$ can be found from the vector product

$$r_{hkl}^* \cdot r_{h_0k_0l_0}^* = \left| r_{hkl}^* \right| \cdot \left| r_{h_0k_0l_0}^* \right| \cdot \cos(90-\theta) = \frac{1}{d_{hkl} \cdot d_{h_0k_0l_0}} \cdot \cos(90-\theta)$$

$$\cos(90-\theta) = \sin\theta = d_{hkl} \cdot d_{h_0k_0l_0} \cdot (a^*h + b^*k + c^*l)(a^*h_0 + b^*k_0 + c^*l_0).$$

Multiplying and replacing the reciprocal unit cell dimension by the unit cell dimensions gives for a triclinic crystal:

$$\sin\theta = d_{hkl} \cdot d_{h_0k_0l_0} \cdot \frac{Q}{b^2 \cdot S} \sin\beta \tag{4}$$

where

$$\begin{aligned} Q = {} & \frac{b^2 \sin^2\alpha}{a^2 \sin^2\beta} hh_0 + kk_0 + \frac{b^2 \sin^2\gamma}{c^2 \sin^2\beta} ll_0 + \frac{b^2 \sin\alpha \cdot \sin\gamma}{ac \sin^2\beta} \cos B(hl_0 + lh_0) \\ & + \frac{b \cdot \sin\alpha}{a \cdot \sin\gamma} \cos C(hk_0 + kh_0) + \frac{b \cdot \sin\gamma}{c \cdot \sin\beta} \cos A(kl_0 - lk_0) \end{aligned}$$

with

$$\cos A = \frac{\cos\beta\cdot\cos\gamma - \cos\alpha}{\sin\beta\cdot\sin\gamma}$$

$$\cos B = \frac{\cos\alpha\cdot\cos\gamma - \cos\beta}{\sin\alpha\cdot\sin\gamma}$$

$$\cos C = \frac{\cos\alpha\cdot\cos\beta - \cos\gamma}{\sin\alpha\cdot\sin\beta}$$

$$S = 1 - \cos^2\alpha - \cos^2\beta - \cos^2\gamma + 2\cos\alpha\cdot\cos\beta\cdot\cos\gamma.$$

In order to obtain the distance of the Laue spots from the center of the pattern one has to use equation (1). In order to reduce the time in converting the sin θ-value into a tan 2 θ-value, it is useful to use a conversion graph such as shown in Fig. 3.

Azimuthal Angle φ and Reflection Angle θ if Incident Beam $\perp$ to (001), (010), (100) or (111)

The equation for sin θ is very much simplified if the plane of incident is one of the principal planes of the crystal as shown in Table 1 where, for the different crystal systems and for different cases of incidence, the corresponding formulae for tan φ and sin θ are tabulated. For each of the three cases the reference axis, from which the angle φ has to be drawn, is included. The simplicity of this set of formulae is striking and the procedure in applying it for calculation or evaluation of Laue pattern is similar to that of evaluating powder or rotation diffraction patterns.

However, one important point might be mentioned here: Because of the absence of the wavelength term in these "Laue"-formulae, no distinction between higher orders of reflection can be made; they are superimposed in the same spot. However, after having determined the indices of the Laue spot and knowing the wavelength range of the continuous radiation of the ray source, the number of reflections of higher orders contributing to the intensity in that Laue spot can be determined.

It might also be mentioned that considerations about the symmetry of the Laue pattern to be expected for each case can be predicted from the formulae.

In Table 2 the formulae for tan ϕ and sin θ are given, if the incident beam is perpendicular to the (111)-plane. The table includes only the cubic, tetragonal, and the rhombohedral systems because the Laue photographs show symmetry in the pattern only for these; a threefold symmetry for the cubic and rhombohedral and a twofold symmetry for the tetragonal. The direction corresponding to the [011]-axis in the Laue pattern is chosen as the axis from which azimuthal angle ϕ of a Laue spot is measured.

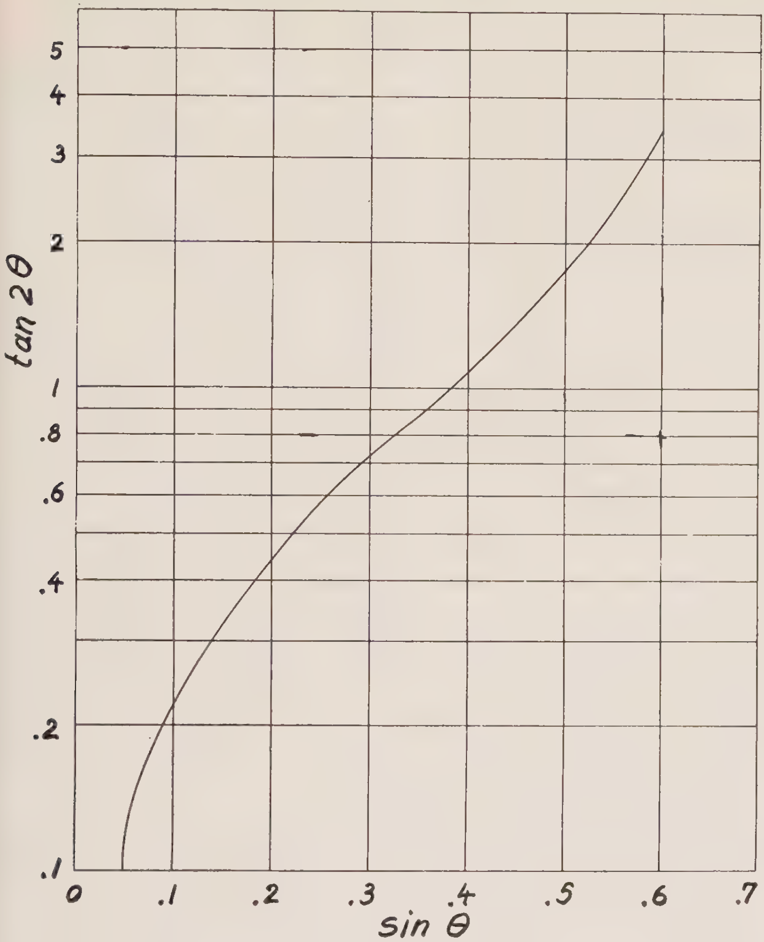

FIG. 3. Conversion of sin θ into tan 2θ.

PROCEDURE OF INDEXING LAUE PATTERN

The application of the formulae, given in Tables 1 and 2, will be demonstrated by indexing one group of Laue spots of a muscovite mica Laue pattern taken with the incident beam perpendicular to (001) and a crystal-photoplate distance $D=58.3$ mm., Fig. 4. For the calculation, the Laue spots are chosen whose indices have a h/k-ratio equal to 3, i.e. spots with the indices (31l), (62l), etc. As mentioned before, these Laue spots will lie on a straight line drawn from the center of the pattern. With the unit cell dimension of muscovite $a=5.18$ Å, $b=9.02$ Å, $c=20.04$ Å $\beta=95°\ 30'$, the azimuthal angle φ of these spots using the correspond-

TABLE 1

Crystal lattice	Incident beam perpendicular to: (001)	(100)	(010)
Cubic	$\sin\theta = d_{hkl}\cdot\frac{l}{a}$ $\tan\varphi = \frac{h}{k}$	$\sin\theta = d_{hkl}\cdot\frac{h}{a}$ $\tan\varphi = \frac{l}{k}$	$\sin\theta = d_{hkl}\cdot\frac{k}{a}$ $\tan\varphi = \frac{l}{h}$
Tetragonal	$\sin\theta = d_{hkl}\cdot\frac{l}{c}$ $\tan\varphi = \frac{h}{k}$	$\sin\theta = d_{hkl}\cdot\frac{h}{a}$ $\tan\varphi = \frac{a}{c}\cdot\frac{l}{k}$	$\sin\theta = d_{hkl}\cdot\frac{k}{a}$ $\tan\varphi = \frac{a}{c}\cdot\frac{l}{h}$
Orthorhombic	$\sin\theta = d_{hkl}\cdot\frac{l}{c}$ $\tan\varphi = \frac{b}{a}\cdot\frac{h}{k}$	$\sin\theta = d_{hkl}\cdot\frac{h}{a}$ $\tan\varphi = \frac{b}{c}\cdot\frac{l}{k}$	$\sin\theta = d_{hkl}\cdot\frac{k}{b}$ $\tan\varphi = \frac{a}{c}\cdot\frac{l}{h}$
Monoclinic	$\sin\theta = d_{hkl}\cdot\frac{1}{\sin\beta}\left(\frac{l}{c} - \frac{h}{a}\cos\beta\right)$ $\tan\varphi = \frac{b}{a}\cdot\frac{h}{k}$	$\sin\theta = d_{hkl}\cdot\frac{1}{\sin\beta}\left(\frac{h}{a} - \frac{l}{c}\cos\beta\right)$ $\tan\varphi = \frac{b}{c}\cdot\frac{l}{k}$	$\sin\theta = d_{hkl}\cdot\frac{k}{b}$ $\tan\varphi = \frac{1}{\sin\beta}\left(\frac{a}{c}\cdot\frac{l}{h} - \cos\beta\right)$
Hexagonal	$\sin\theta = d_{hkl}\cdot\frac{l}{c}$ $\tan\varphi = \frac{1}{3}\sqrt{3}\left(2\frac{h}{k} + l\right)$	$\sin\theta = d_{hkl}\cdot\frac{1}{a\sqrt{3}}(2h+k)$ $\tan\varphi = \frac{a}{c}\cdot\frac{l}{k}$	$\sin\theta = d_{hkl}\cdot\frac{1}{a\sqrt{3}}(2k+h)$ $\tan\varphi = \frac{a}{c}\cdot\frac{l}{h}$

TABLE 2

Crystal lattice	Incident beam perpendicular to (111)
Cubic	$\sin\theta = d_{hkl}\cdot\frac{1}{3}\sqrt{3}\left(\frac{h+k+l}{a}\right)$ $\tan\varphi = \frac{1}{3}\sqrt{3}\left(2\,\frac{l-h}{l-k}-1\right)$
Tetragonal	$\sin\theta = d_{hkl}\cdot\frac{(h+k)+\frac{a^2}{c^2}\,l}{a\sqrt{\frac{a^2}{c^2}+2}}$ $\tan\varphi = \frac{1}{\sqrt{2\,\frac{c^2}{a^2}+1}}\left(\sqrt{2}\cdot\sqrt{\frac{c^2}{a^2}+1}\right)\cdot\left(\frac{l-h}{l-k}-1\right)$
Rhombohedral	$\sin\theta = d_{hkl}\cdot\frac{1}{3}\sqrt{3}\cdot\sqrt{1+2\cos\alpha}\cdot\frac{(1+\cos\alpha)^2}{(1-3\cos^2\alpha+2\cos^3\alpha)}\cdot\left(\frac{h+k+l}{a}\right)$ $\tan\varphi = \frac{1}{3}\sqrt{3}\left(2\,\frac{l-h}{l-k}-1\right)$

Angle φ measured from [011].

ing formula in Table 1, is calculated to be 79°09′. The b-axis direction in the Laue pattern from which the angle φ will be measured can be found easily from the symmetry of the pattern due to the fact that the symmetry axis is along the a-axis direction. At a right angle to it the b-axis direction is found. The radius vector drawn under an angle of 79°09′ from the b-axis direction, passes through five reflections whose indices now will be determined. The equation for the reflection angle θ takes the form (Table 1):

$$\sin\theta = d_{hkl}\cdot 1.005(0.0555k + 0.0499l)$$

where

$$d_{hkl} = \frac{1}{\sqrt{0.351k^2 + 0.00251l^2 + 0.0056kl}} \qquad \text{for } h = 3k$$

and therefore

$$\sin\theta = \frac{0.0558k + 0.0501l}{\sqrt{0.351k^2 + 0.00251l^2 + 0.0056kl}}. \tag{5}$$

The next step is to calculate some values for $\sin\theta$ as a function of l for $k = 1, 2, \cdots$. After a conversion of the $\sin\theta$-values into $\tan 2\theta$-values us-

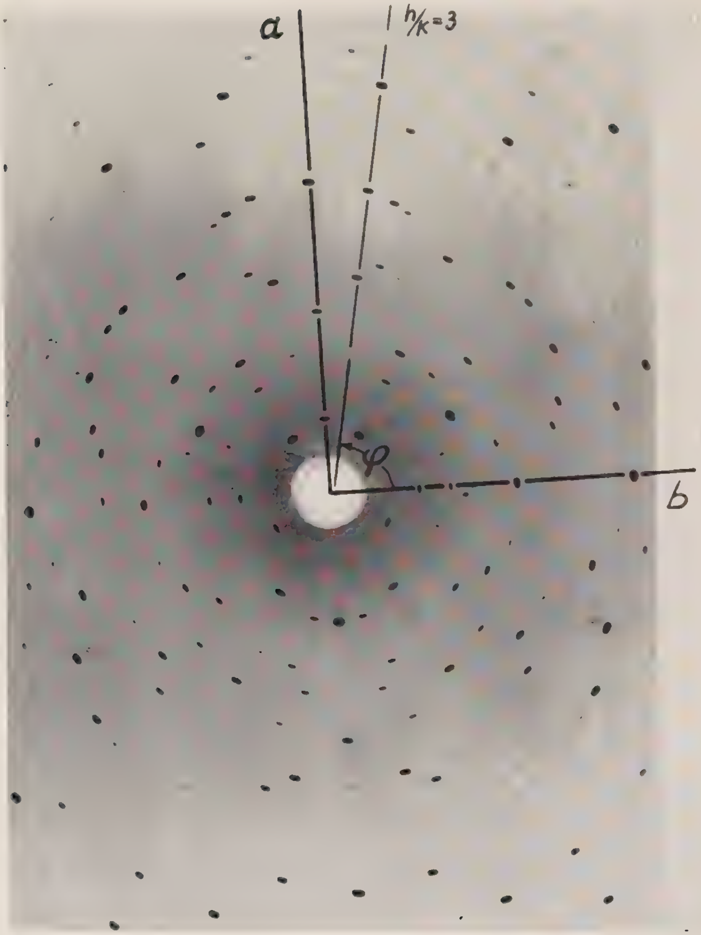

FIG. 4. Laue-photograph of muscovite mica with the incident beam perpendicular to (001). Distance crystal—photoplate $D = 58.3$ mm. Radiation: Copper target.

ing the graph in Fig. 3, $r = D \cdot \tan 2\theta$ is plotted as a function of l, for re
flections having the indices ($31l$) and ($62l$), as shown in Fig. 5. From thi
graph the indices of the five measured Laue spots, knowing their dis
tances r from the center of the pattern, can be read off directly. Tabl
3 shows the results, including the possible number of higher orders of th
reflections superimposed on the same Laue spot.

As a second example, the results from a complete evaluation of th
Laue-pattern of a phlogopite mica are shown in Fig. 6. Here the value o
a complete indexing of a Laue pattern can be recognized by the fact tha
extra spots (marked with a cross), which do not belong to the calculate

TABLE 3

Laue spots measured r [*mm*]	(*hkl*)	$n \cdot \lambda_{\text{min.}}$	n
21.5	311	0.593	1
33.2	312	0.844	1, 2
47.0	313	1.06	1, 2, 3
63.2	314	1.25	1, 2, 3, 4
73.0	629	0.666	1, 2

Cu—Radiation, E=40kv
$\lambda_{\text{min.}} = 0.308$ Å

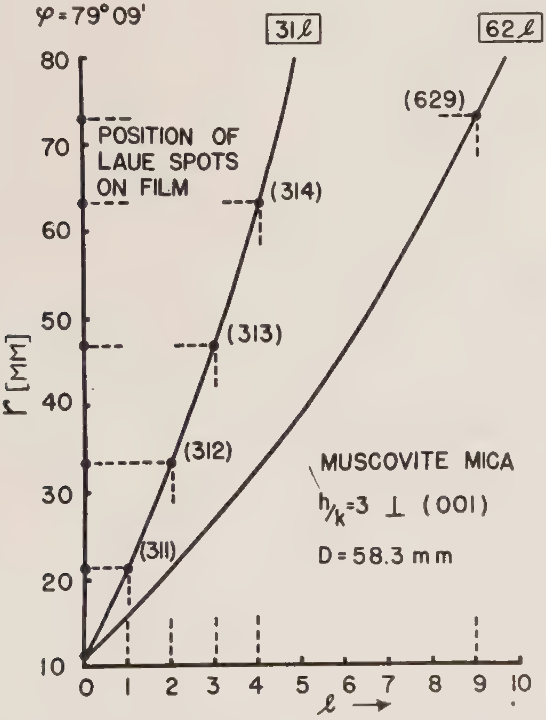

FIG. 5. Indexing of Laue spots ($h/k=3$) on a Laue photograph from muscovite mica, Fig. 4, using the distance of the Laue spots from the center of the pattern and corresponding formula from Table 1.

pattern, could be detected. The shape of these extra spots as compared with the others are different in appearance and might be due to structure defects of this phlogopite sample, caused by stacking faults of layers.

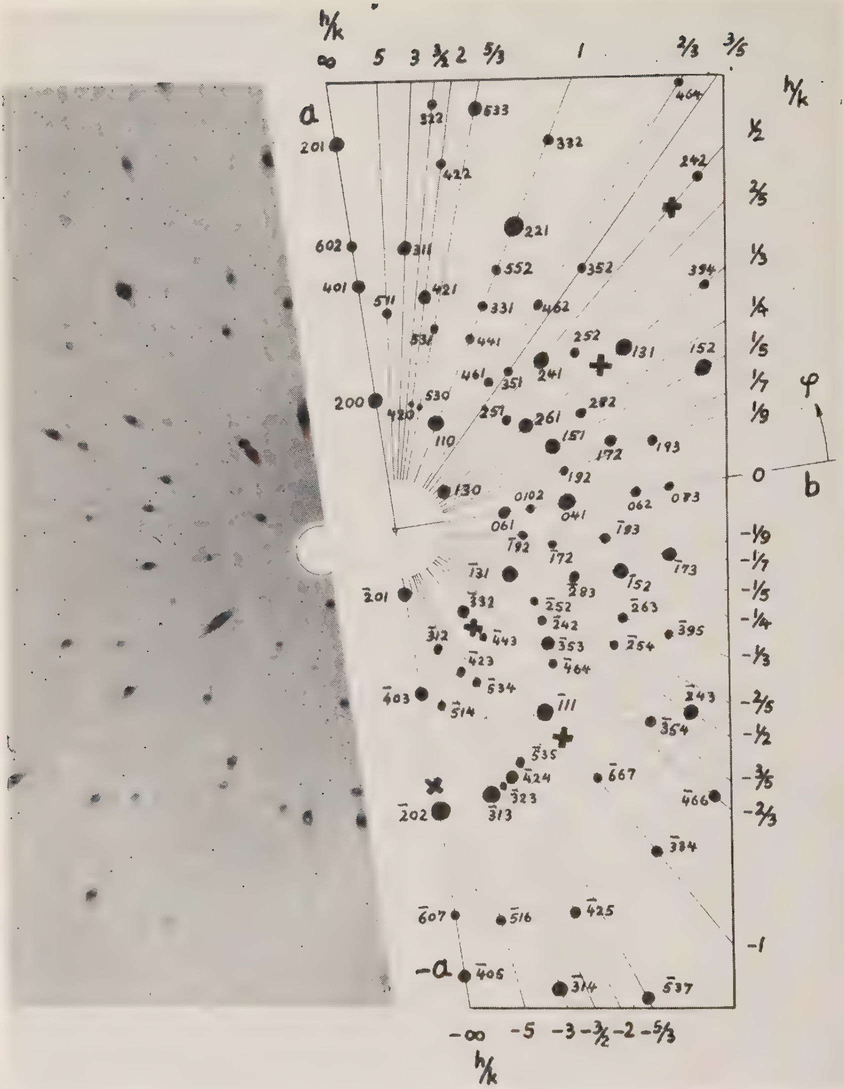

FIG. 6. Completely indexed Laue photograph of phlogopite mica with the incident x-ray beam perpendicular to (001) by the method described.

It might be worthwhile to mention that the time consumed for such a complete evaluation of a Laue pattern as shown in Fig. 6 is about 8 to 10 hours, comparable with the evaluation of crystal rotation photographs.

Manuscript received June 6, 1953

RELATIVE GEOLOGIC AGE MEASUREMENTS ON GRANITES BY PLEOCHROIC HALOES AND THE RADIOACTIVITY OF THE MINERALS IN THEIR NUCLEI

Ichikazu Hayase, *Geological and Mineralogical Institute, Faculty of Science, Kyoto University, Kyoto, Japan.*

Abstract

In each grain of the radioactive minerals contained in haloes in various Japanese granites, the radioactivity was measured by an autoradiographic method; the development of the pleochroic haloes and the radioactivity of the minerals in their nuclei were both studied in several granites. Their relative geologic ages were determined approximately.

Introduction

The method of determining the age of minerals from the amount of uranium and thorium contained in them, and the blackness of their pleochroic haloes was devised in 1913 by Joly and Rutherford (1).

The blackness of the halo in biotite increases with the number of alpha-particles emitted from the minute radioactive nuclei; and this in turn depends on the radioactivity and the age of the mineral of the nucleus. As it was impossible, however, at that time to measure the radioactivity of a single mineral grain, Joly's method could not be carried out effectively. The content of the radioactive elements in these minute mineral grains in granite is, in fact, not as uniform as Joly estimated. The result obtained by the present author indicates that grains even in the same thin section of rock are of various species with varying contents of radioactive elements. This will be dealt with in another paper.

By means of the relative blackness of pleochroic haloes, Henderson tried to measure geologic time (2). It was a suggestive method, but apparently not applicable to any rocks younger than 400 million years.

The chief difficulty in these methods of age determination lies in the bleaching or reversal phenomenon. Is this phenomenon really due alone to overexposure to alpha particles, as it has been supposed? Is it impossible to assume that it is rather due to alteration of the biotite itself?

The use of nuclear type plates (3) made the present measurement of radioactivity of minute mineral grains in a thin section much more effective, though the main process of this experiment was but a modification of autoradiography, by which process alone we may measure the radioactivity of a mineral grain so small that it is invisible to the naked eye. The author feels that this method may make some contribution to studies on petrogenesis.

Experimental Procedure

The thin sections used for autoradiography were 30 microns in thickness, as usual, but without cover-glasses. The printed mark method was adopted, as will be stated below, so that the thin section and the developed photo-plate correlate exactly with each other. To spare much of the time needed for the exact correlation of the thin section with the developed plate, the following technique is recommended.

(1) Three corners of the thin section are stained a little with black lacquer.
(2) A cross-shaped window is cut open on each of the three stains (Fig. 1 *a*).
(3) On the other side of the glass is pasted a piece of black paper (Fig. 1 *b*).

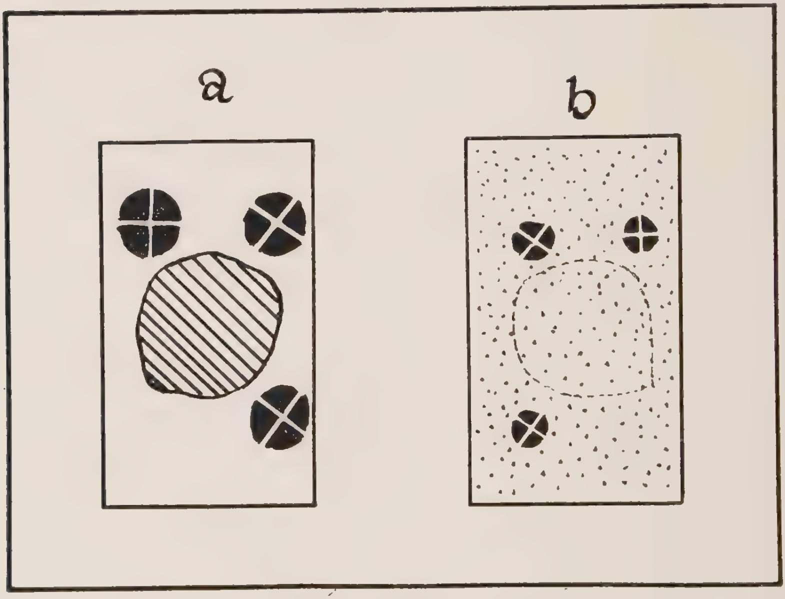

FIG. 1. (*a*). The surface of a thin section of granite with three cross-marks on it. (*b*). The black paper fixed to the reverse of the slide.

(4) Three small holes are cut in the black paper just against the three stains with the cross-shaped windows.
(5) A half-sized nuclear-type plate is fixed to the thin section thus prepared.
(6) The plate is exposed for a while to dim light through the three holes on the black paper. Thus the three cross-shaped windows on the slide are printed on the plate.
(7) The thin section and the plate are kept in contact in a dark place for some four weeks.
(8) The plate is developed with D-19 developer for 12 minutes at ordinary temperatures, and then fixed with F-5.

(9) The black paper is removed from the slide.

(10) A drop of glycerine is placed on the thin section.

(11) The photo-plate is put on this and moved until three cross-shaped marks come into coincidence with the windows on the thin section.

(12) Exact adjustment is possible only under the microscope at 150 ×, for the thickness of the photo-plate hinders the use of any higher magnification. This magnification proved to be most effective for scanning the radioactive centers.

The nuclear type plate used for this purpose was *ET-2E*, 50 microns in thickness, made by the Research Laboratory of the Fuji Photo Film Co., Ltd., of Japan, which was found little inferior in quality to Kodak *NTA*.

The number of the alpha tracks printed on the plate represents the radioactivity of each nucleus mineral grain. No thicker section than 30 microns is needed because of the short ranges of alpha particles within rock minerals.

The radius of haloes and the size of the nucleus minerals can be measured by means of a micrometer eyepiece equipped with travelling lines (Schrauben Mikrometer Okular) previously calibrated with a standard micro-scale.

The smaller the size of the nucleus mineral, the more alpha tracks per unit volume are expelled from it, owing to the small absorption of alpha particles. An extremely minute size is no doubt the most desirable, but is inapplicable to the present purpose. The reasons are as follows:

(1) In pleochroic haloes with nucleus minerals smaller than 5 microns in size, the boundary between the halo and its nucleus mineral is hardly distinguishable.

(2) Because of the lack of alpha tracks expelled during a moderate period of exposure, a nucleus mineral too small in size cannot be used.

(3) The nature of the nucleus mineral is very difficult to make out.

(4) As shown in Fig. 2*a*, the number of alpha tracks on the plate does not exactly represent the radioactivity of the nucleus mineral which has blackened the biotite, if their positions and shapes in the thin section differ.

For the determination of the relative geologic ages of two different granites, it is desirable that the greatest possible number of pleochroic haloes available be compared with the radioactivities of their nucleus minerals, which should be, of course, nearly the same in size and shape. The radioactive minerals contained in granites are usually zircon and allanite. Of these two, zircon grains especially are often found to be of moderate and nearly equal size; in radioactivity, however, these minute grains of zircon show great variations, even in the same thin section.

For the comparison, the most desirable nuclei are minute zircons 30

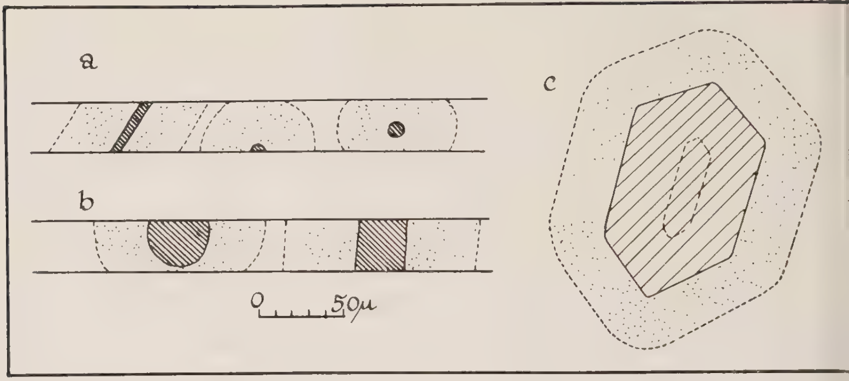

FIGS. 2. (*a*) & (*b*) The transversal section of the thin section. (Note the comparative positions of the pleochroic haloes and their nucleus minerals). (*c*) The plan of the thin sectio of a radioactive mineral with zonal halo. (The alpha particles, emitted from the centra part of the mineral, can not reach the outermost part of the halo).

microns in diameter with disk type pleochroic haloes around them. I they are of this size, not only do their positions in the thin section matte little, but also their alpha particles are not so much absorbed within th zircon grains themselves (Fig. 2*b*).

Crystals larger than 40 microns in diameter and with zonal haloes around them can also be compared with one another (Fig. 2*c*). In this case however, any calibration of the size of the nucleus minerals is unnecessary, as the mineral grain is larger than the longest range of its alpha particles. What is to be compared here between two rocks is (1) the radioactivity in unit area of the polished surfaces of the minerals, and (2) the blackness of the zonal haloes. The results derived from these two methods: disk halo and zonal halo, show a satisfactory agreement.

VARIETIES OF THE MINUTE MINERALS IN GRANITIC ROCKS

Zircon, allanite, sphene, monazite, xenotime, and the like are the ordinary radioactive accessory constituents of granite. The methods described above enabled the author to discover also in thin sections of granite, uraninite and other highly radioactive minute mineral grains. It has been known for a long time that the nucleus minerals of pleochroic haloes, even though nearly of the same size, differ greatly in the stage of development of their haloes, even in the same flake of biotite. Zircon shows remarkable variations in its radioactivity, and the more radioactive the granite as a whole, the more remarkable is the variation. The author finds that the more radioactive the granite, the more haloes it offers for comparing.

THE RELATION OF THE RADIOACTIVITY OF THE NUCLEUS MINERAL TO THE STAGE OF ITS HALOES

The blackening of biotite by alpha particles represents a complicated process, but the application of the autoradiographic technique sheds considerable light on this subject. Figure 3 illustrates the results on granite from Tanakamiyama, Siga Prefecture, Japan; the ordinate is the radii of its haloes in microns, the abscissa is the alpha particles ejected per day from one grain of the nucleus mineral.

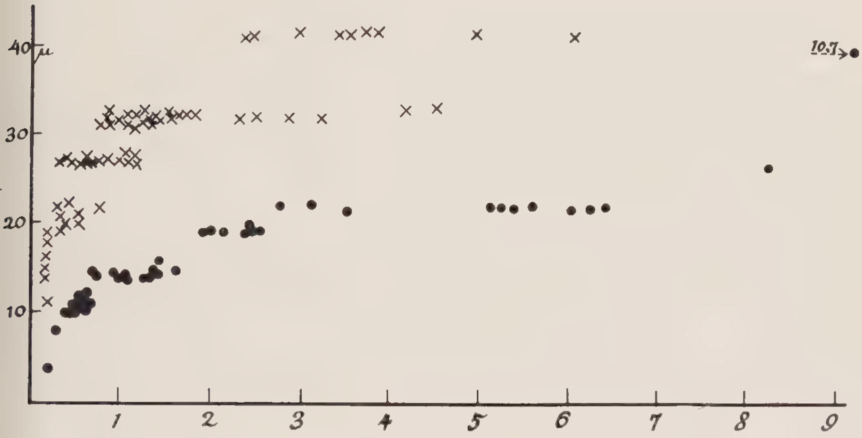

FIG. 3. The relation of halo radii and the radioactivities: Tanakamiyama granite (crosses) and Masutomi granite (solid circles). The size of nucleus mineral: about 30 microns in diameter. Ordinate: halo diameter in microns. Abscissa: alpha radioactivity from one grain of mineral per day. (All crosses from Fig. 3 to Fig. 7 represent Tanakamiyama granite).

The nucleus minerals, mostly zircon, were 25–35 microns in diameter; halo rings were measured with a micrometer ocular, using their outermost radii. The marks shown on the levels of 41, 32, and 27 microns represent the ThC′, RaC′ and ThA rings respectively; while the rings smaller than 23 microns represent complicated overlaps of the various rings. Though the density of the haloes is not given in the figure, be it noted that in the case of haloes of similar radius, the blackness is deeper on the right-hand side than on the left. The left sides of haloes are generally either embryonic or under-exposed, the right sides are over-exposed. In the semiquantitative measurement of the relative ages of two rocks, however, the best method to use is to compare the two radioactivities at the stage of the first slight appearance of their haloes. Is it possible here that, as the biotites differ, the blackness of the haloes in question may also differ? So far as the granite of Tanakamiyama, containing two sorts of biotites, is concerned, a difference of this kind appears to be negligible. One biotite is brown, with refractive index $(\gamma) = 1.64$, and is centrally located; for the other, greenish in color and myrmekitic in structure, zonally surrounding the first, and presumably containing much fluorine, $(\gamma) = 1.63$. The haloes in these two biotites show no difference in their degree of blackness. Even in the case of two different granitic rocks, a similar result also may be expected. The experimental projection of numerous alpha particles on various biotites will perhaps verify this view.

According to some investigators, the bleaching or reversal phenomenon in biotite, which is inevitable for pleochroic haloes, is extremely irregular and complicated. The radiographic studies of the author showed no such irregularity, especially in the case of granites whose age was younger than Mesozoic. Besides, it is a noteworthy fact that the reversed halo of what G. H. Henderson called "extinct halo type A" (10) is seen in the xenoliths of the Tanakamiyama granite (4). This extinct halo however, seems to the author to be due rather to the alteration of the biotite itself than to over-exposure by alpha particles from nucleus minerals, as has been believed. Though the author's results are limited in number, it seems probable that what is true of extinct haloes will some day be found true of haloes in general.

On Pleochroic Haloes in Various Japanese Granites

In South Siga there is a stock, called the Tanakamiyama granite, which outcrops in an ellipse about 14 km. long by 7 km. wide. This unconformably contributes pebbles to the Kobiwako Plio-Pleistocene formation. The granite is mostly coarse-grained, with biotite, but in its marginal phases is fine- or medium-grained, or sometimes passes into porphyritic rocks. It is generally rich in radioactive elements. According to T. Asayama's measurements (5) the radium content varies from 3.23×10^{12} g/g to 1.48×10^{-12} g/g. This radium content seems rather high for Japanese granitic rocks according to the data of Z. Hatuda (6, 7).The biotite in this district contains many pleochroic haloes and especially ThC′ haloes. On account of the slight diversity in shape and size of the minute mineral grains, some deviation from an exact linear relation is almost inevitable, for only in the case of grains of exactly the same size and shape, can exact comparison of blackening of the haloes be established. The haloes in the altered biotite are not suitable for a standard of comparison.

In Fig. 3 the dots indicate the granite in the Masutomi Spring district, Yamanashi Prefecture. Its intrusion into the Misaka formation (Miocene sediments) tells its age. The springs of this district are noted for their high radioactivity (8, 9) and the granites nearby are also fairly radioactive. With respect to the order of radioactivity of the minute crystals of accessory minerals the Masutomi and Tanakamiyama granites show no marked difference, but as far as the stages of the haloes are concerned, the former appears younger than the latter. The pleochroic haloes are, in Henderson's (10) terminology, mostly active ones; since the formation of the minerals, alpha particle ejection must have remained constant. When more than one million years have passed, the mineral has reached radioactive equilibrium.

Now let the ages of two granites A and B be Y_A and Y_B years, and the radioactivities of their nucleus minerals (similar in shape and size) be

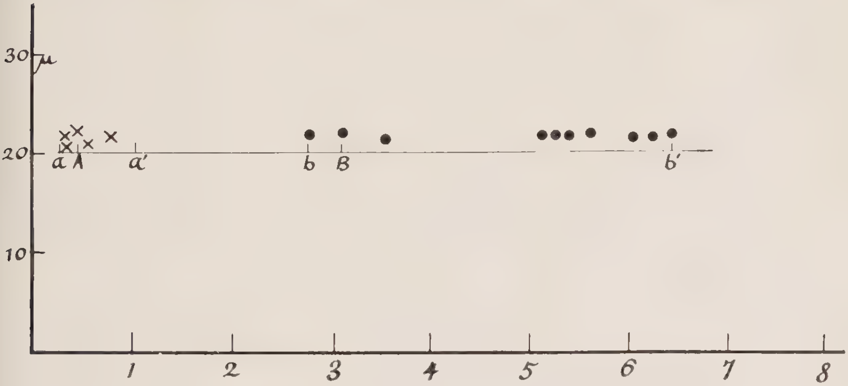

FIG. 4. Haloes about 22 microns in diameter. (See Fig. 3).

R_A and R_B (Fig. 3). If the pleochroic haloes originating from these two nucleus minerals show the same stage of blackening, then $Y_A/Y_B = R_B/R_A$.

The ratio of the two geologic ages, therefore, is inversely proportional to the radioactivity. In other words, if the stages of development of a halo and the radioactivity of its nucleus mineral can be measured, the relative geologic ages of the rocks in question can be determined. Henderson's apparatus (11), for instance, would enable us to measure the halo blackening with greater precision than is possible in the present instance. As an example, pleochroic haloes about 22 microns in radius may be considered. In Fig. 4, the aAa' group represents the Tanakamiyama granite, the bBb' the Masutomi, and the points a and b represent the faintest haloes barely recognizable under the microscope, while a' and b' are the most deeply blackened ones. The following relations are formulated, for simplicity's sake, without considering the composite haloes of the Th and U series combined:

$$a/b = A/B = a'/b' = (a' - a)/(b' - b) = Y_B/Y_A.$$

Any two corresponding points on the line aa' and bb' representing the relative blackness of haloes give the required ratio. The age is represented by $a'-a/b'-b$, hence the younger the haloes are, the greater is the difference in their radioactivities.

This tendency is not necessarily limited to certain specific haloes. RaC′ and ThC′ haloes are preferable for comparison, as they form the outermost rings of the compound haloes of the U and Th series, respectively. If a stricter comparison is necessary, the color, thickness, and orientation of the biotite in the thin section must also be considered. Halo A (Tanakamiyama granite) and halo B (Masutomi granite) are nearly the same in blackness. Hence, roughly speaking:

$$Y_A/Y_B = B/A = 3/0.5 = 6/1.$$

On this basis, because halo B belongs, as stated above, to the Miocene; using the latest geologic time scale (12), halo A should be nearly 6 times as old, and be ascribed to the middle Cretaceous. No other geological datum for the Tanakamiyama granite is in discord with this result. Figure 5 shows the San-in district granite. The data are still too scanty to tell with exactitude anything more than that its age lies between middle Cretaceous and Miocene, presumably in the oldest Tertiary.

In Fig. 6, the triangles representing the Bofu granite of Yamaguchi Prefecture are further to the right of the diagram than those representing

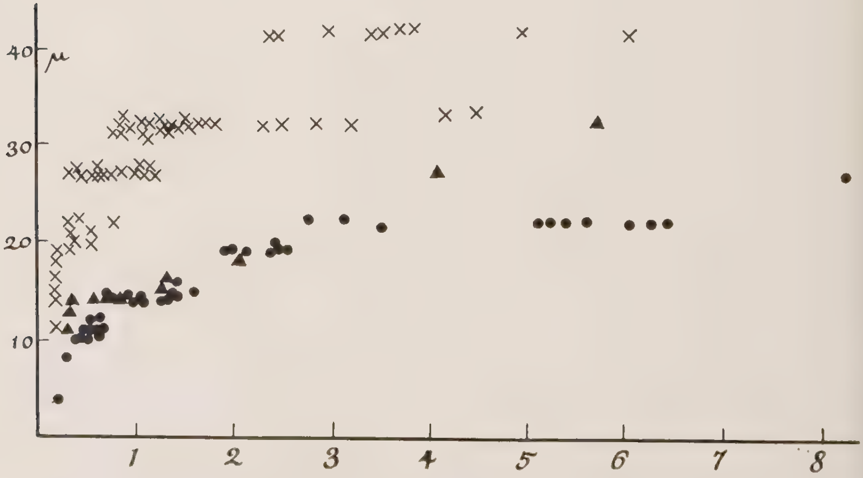

FIG. 5. San-in district granite (triangles) represents an age between Miocene and middle Cretaceous.

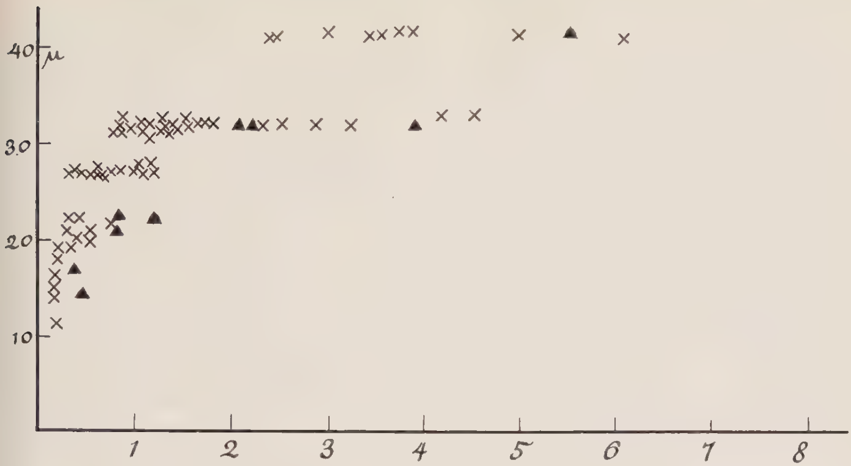

FIG. 6. Triangles: Bofu granite (Yamaguchi prefecture).

the Tanakamiyama granite, and this tells us that the intrusion of the Bofu took place a little later (upper Cretaceous?) than that of the latter. Similar results were obtained for granites from Kitashirakawa, Kyoto Prefecture; Ookawara, Shiga Prefecture; Hoki, Kyoto Prefecture; and Katanoyama, Osaka Prefecture.

The zonal halo method is applicable only to a mineral in which the radioactive elements are equally and homogeneously distributed. Such haloes are neither rare nor exceptional. This method is superior to the other one, for it requires no calibration of the size of a nucleus mineral. The results obtained by this method are shown in Fig. 7. The radioactivity is shown on the abscissa as the number of alpha particles emitted from the polished surface per day per 0.01 mm.^{2} by minerals such as coarse-grained allanite and zircon. In either method, however, great care is needed in the following:

(1) The size of the halo must be measured under the microscope as exactly as possible.

(2) No altered biotite containing pleochroic haloes can be used.

(3) In halo measurements, the position and the orientation of the radioactive mineral grains as shown in the thin section must be taken into consideration.

So far as a specimen of biotite containing a pleochroic halo is *fresh*, any two rocks may be compared to determine their relative geologic ages, whether the rock be pegmatite, volcanic rock, mica schist, or any other.

Under favorable circumstances, the order of age of two rocks can easily

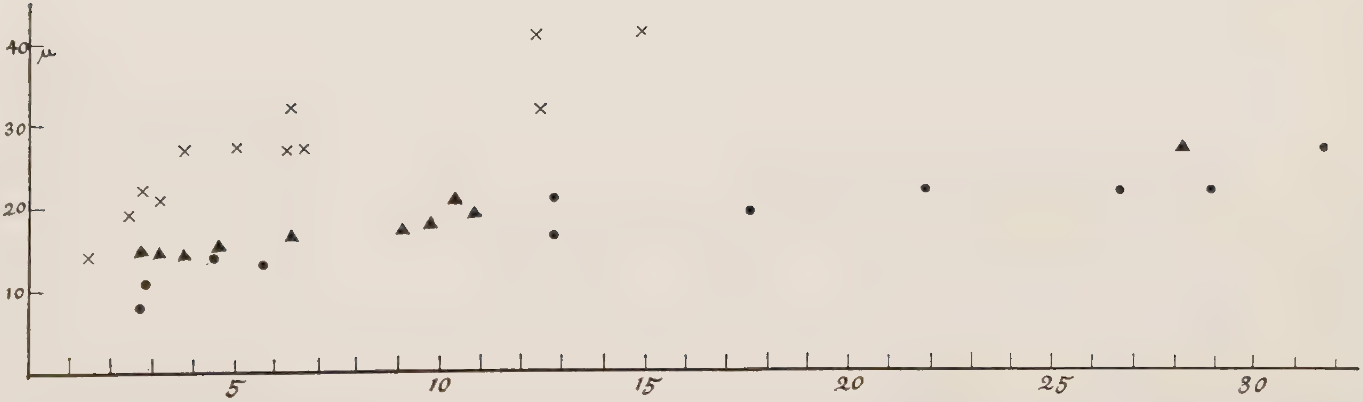

FIG. 7. The relation between width of a zonal pleochroic halo and its radioactivity. Tanakamiyama granite (crosses), San-in granite (triangles), and Masutomi granite (solid circles). Ordinate: halo width in microns. Abscissa: alpha radioactivity from the polished surface per 0.01 $mm.^2$ per day.

be determined even if they were of successive intrusions. Suppose that the same type of alpha particles gave various degrees of blackness to different biotites. If such be the case, the method of blackening the biotite artificially by exposure to a given source of alpha particles of known strength would enable us to determine not only the relative ages of two rocks, but even give us some approximation to their absolute ages. And, when autoradiographic studies become more advanced, even one pleochroic halo would, under favorable conditions, be enough to determine the age of a given rock.

Among the advantages of the author's method of measuring ages are the facts that it is freer from contamination difficulties than the lead method, and from difficulties of alteration than the helium method. Pleochroic haloes may some day be a more exact index of the age of igneous or metamorphic rocks than fossils are in sedimentary rocks.

SUMMARY

(1) Even in the same specimen of granite the minute radioactive mineral grains vary in activity.

(2) The blackness of a pleochroic halo is proportional to the product of the radioactivity and the age of the nucleus mineral.

(3) The relative geologic age of two rocks each bearing pleochroic haloes is easily determined by comparing the stages of development of the haloes in each, and by contrasting the respective radioactivities of the nucleus minerals of the haloes.

ACKNOWLEDGMENTS

The author thanks Dr. J. P. Marble, Chairman of the Committee on the Measurement of Geologic Time of the U. S. National Research Council for his kind recommendation of this paper, and for editorial assistance, and Dr. S. Fujisawa and Mr. S. Koseki of the Research Laboratory of the Fuji Photo Film Co., Ltd., for supplying him with *ET* nuclear plates.

In addition thanks are offered to Prof. A. Harumoto, and Asst. Prof. Z. Hatuda of the Geological and Mineralogical Institute, Kyoto University, for their constant aid and inspiration. The present work was carried out with the aid of the Science Research Grant conferred by the Education Ministry and of the Hattori Hôkô-kai Grant.

REFERENCES

1. JOLY, J., AND RUTHERFORD, E., The age of pleochroic halos: *Phil. Mag.*, **25,** 644–657 (1913).
2. HENDERSON, G. H., A new method of determining the age of certain minerals: *Proc. Roy. Soc. London,* **145A,** 591–598 (1934).

3. Yagoda, H., Radioactive measurements with nuclear emulsions: New York, John Wiley and Sons (1949).
4. Hayase, I., Extinct halo "type A" found in the biotite in the contact zone of Tanakamiyama, Siga prefecture, Japan. (in Japanese): *Chigaku* (The Science of the Earth), No. **3,** 19–23 (1950).
5. Asayama, T., The radium content and the chemical composition of granitic rocks in Japan, 4: *Mem. Fac. Ind. Arts, Kyoto Tech. Univ.,* **3**
6. Hatuda, Z., Radium contents in granites in Nippon (Preliminary report): *Mem. Coll. Sci. Kyoto. Imp. Univ.* Series B, **X,** 63–72, Kyoto (1934).
7. Hatuda, Z., Radium contents of rocks in Nippon, I: *Mem. Coll. Sci. Kyoto Imp. Univ.* Series B, **XII,** 1–18, Kyoto (1936).
8. Shimokata, K., Thorium contents of mineral springs in Japan. (in Japanese): *Rep. Nagoya Inst. Tech.* No. **1,** 159–164 (1949).
9. Kuroda, K., and Yokoyama, Y., The Lauritsen-type K. Y. Fontactoscope and its use in geochemistry: *Chem. Researches* (Tokyo) vol. **3,** 29, 1948.
10. Henderson, G. H., and Sparks, F. W., A quantitative study of pleochroic halos. IV: *Proc. Roy. Soc. London.,* **173,** A. 238 (1939).
11. Henderson, G. H., and Bateson, S., A quantitative study of pleochroic halos. I: *Proc. Roy. Soc. London,* **145,** A. 563–581. (1934).
12. Holmes, A., The oldest known minerals and rocks: *Trans. Edinburgh Geol. Soc.*, **14,** Pt. II, 176–194 (1948).

Original manuscript received March 23, 1953

THE COALESCENCE OF HEXAGONAL AND CUBIC POLYMORPHS IN TETRAHEDRAL STRUCTURES AS ILLUSTRATED BY SOME WURTZITE-SPHALERITE CRYSTAL GROUPS*

RICHARD S. MITCHELL† AND ALICE S. COREY,‡ *University of Michigan, Ann Arbor, Michigan.*

ABSTRACT

The structural similarities of the hexagonal and cubic polymorphs of zinc sulfide are illustrated by some unusual wurtzite-sphalerite crystal groups synthesized at this laboratory. In general these crystal groups consist of oriented overgrowths of wurtzite prisms extending from the tetrahedral faces of sphalerite nuclei. The method and theory of their growth is discussed. The coalescence of hexagonal and cubic polymorphs in other tetrahedral structures is reviewed.

INTRODUCTION

The relationship of the crystal structures of wurtzite and sphalerite has been known for some time. This relationship, first described by Bragg (1920), resembles that between cubic and hexagonal close packing. In sphalerite the zinc atoms are on a face-centered cubic lattice, whereas in wurtzite they are nearly in the position of hexagonal close packing. In both structures four sulfur atoms surround each zinc atom tetrahedrally. That the wurtzite structure can be derived from the sphalerite structure simply by rotating every other layer of atoms in sphalerite 180° (60°) around its trigonal axis [111] has been pointed out by Aminoff and Broomé (1931).

In Fig. 1, portion *ABCD* is a 110 cross section through the sphalerite structure while *AEFB* is a 11·0 cross section through the wurtzite structure. *SRHP* and *WURA* outline the unit cells of these substances. As a result of the twinning process, which takes place by a 180° rotation of every other layer of atoms (represented in Fig. 1 by the lines parallel to *AB*), the sphalerite [111] becomes the wurtzite *c* axis. From this twinning relationship wurtzite can be considered as a special form of sphalerite and might be called a polymorphic twin of sphalerite.

MORPHOLOGICAL DESCRIPTION OF SOME ZINC SULFIDE CRYSTAL GROUPS

Recently at this laboratory some crystal groups of zinc sulfide were grown which emphasize the structural relationship of these two poly-

---

* This investigation was made possible by assistance from the Office of Naval Research. Contribution from the Dept. of Mineralogy and Petrography, University of Michigan, No. 181.

† Present address Dept. of Geology, University of Virginia, Charlottesville, Va.

‡ Present address 220 S. Winter St., Yellow Springs, Ohio.

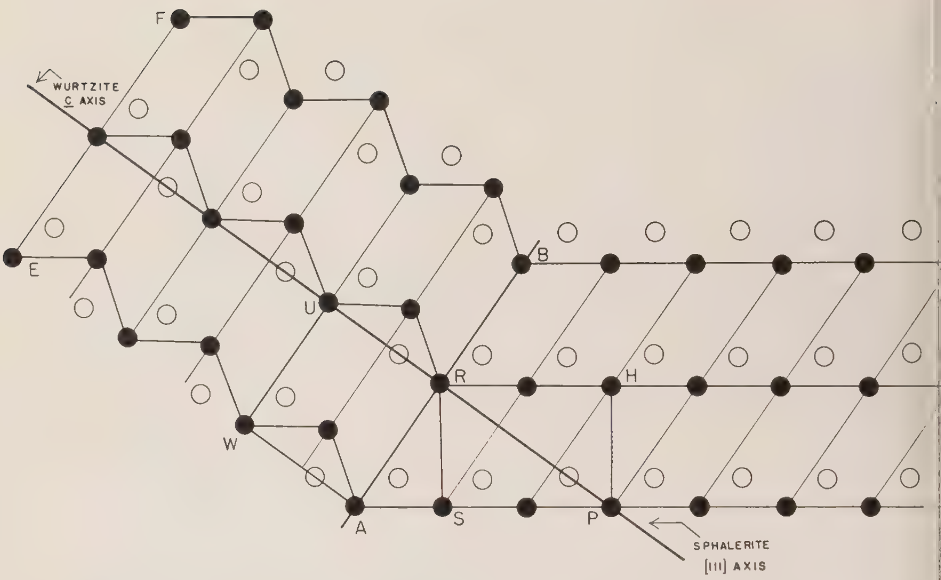

FIG. 1. The twinning relationship of the structures of sphalerite and wurtzite as shown by a section of sphalerite (*ABCD*) and 11.0 section of wurtzite (*AEFB*). Dots represent Zn (or S) and c represent S (or Zn) atoms.

morphs. These crystal groups, consisting of wurtzite prisms extending from the faces of sphalerite tetrahedrons, can be divided into three main types based upon the position of the wurtzite prisms in relationship to

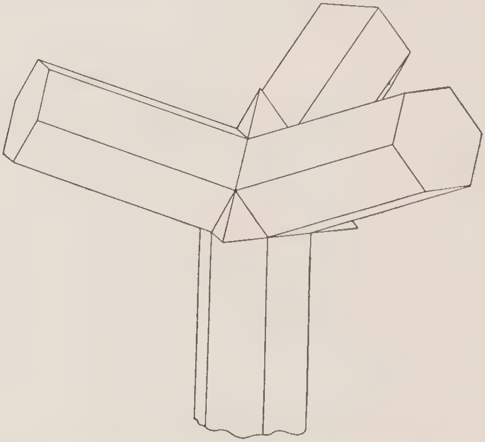

FIG. 2. Idealized drawing of simplest combination of wurtzite-sphalerite groups, showing wurtzite prisms extending from the positive tetrahedral faces of sphalerite.

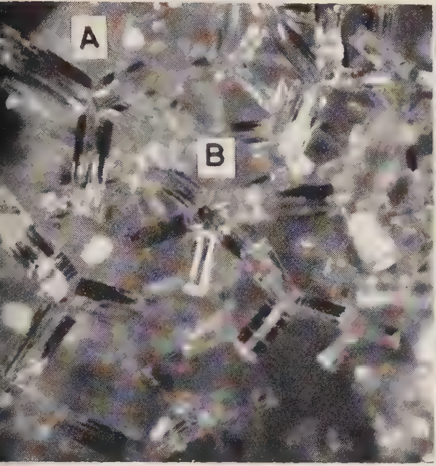

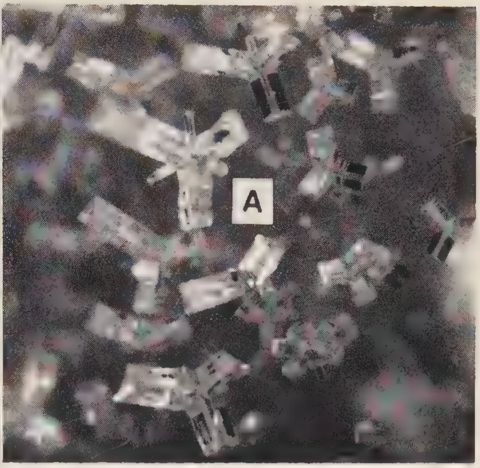

FIG. 3. Photomicrograph of wurtzite-sphalerite groups (×80). (*a*) Simplest combination showing wurtzite prisms extending from positive tetrahedral faces. (*b*) Complex group showing wurtzite prisms growing from positive tetrahedral faces of twinned sphalerite.

FIG. 4. Photomicrograph of crystal groups (×80). (*a*) Wurtzite prisms extend from both the positive and negative tetrahedral faces.

the sphalerite nucleus. The simplest combination (Figs. 2 and 3*a*) consists of four wurtzite prisms extending perpendicular to four faces of a simple sphalerite tetrahedron. The second type (Fig. 4*a*) is made up of eight wurtzite prisms, four of which protrude from the positive* tetrahedral faces and four from the negative tetrahedral faces of sphalerite. The third, a more complicated type (Figs. 5 and 3*b*), is composed of wurtzite prisms extending from the positive tetrahedral faces of sphalerite which is itself twinned on [111] by a rotation of 180°. As can be seen in Fig. 5, the twinning axis of the tetrahedron is parallel to the *c* axis of the vertical wurtzite prism. Looking down the crystal group along this twin axis, one sees six prisms radiating from the tetrahedron 60° apart. Three of these, which are 120° apart, extend out of the positive tetrahedral faces of the lower part of the twin. The other three, also 120° apart, but lying in the intermediate positions, extend from the positive tetrahedron of the upper part of the twin. Wurtzite prisms were not found protruding from the negative tetrahedral faces of the sphalerite twin, but the writers see no reason why this combination is not possible.

In each of the crystal groups mentioned above, the *a* axes of the wurtzite prisms are parallel to the edges formed by the intersections of the faces of the tetrahedrons. In addition to larger first order prisms, smaller

---

* The larger faces were considered to be positive.

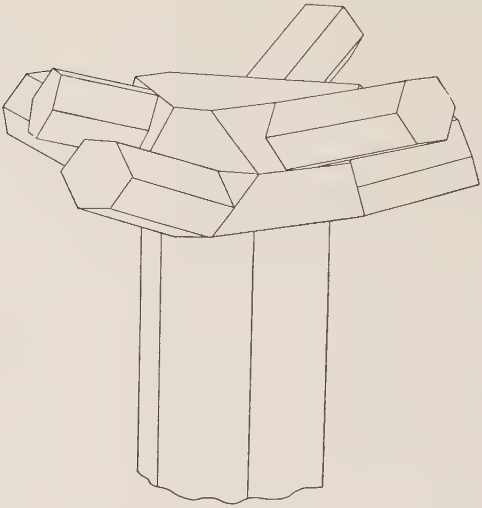

FIG. 5. Idealized drawing of a complex wurtzite-sphalerite group showing wurtzite prisms extending from positive tetrahedral faces of twinned sphalerite. (See Fig. 3*b*.)

second order prisms as well as basal pinacoids are present. Most of the wurtzite prisms are somewhat triangular in shape. This is probably a result of the fact that the prisms are, in a sense, extensions of the original triangular tetrahedral faces. No pyramidal faces were observed. Only rarely could the tetrahedron nuclei be seen.

Because of the well-developed nature of the basal pinacoids and prism faces, the spatial relationships within these groups were readily determined with the use of the optical goniometer. The angular values between the basal pinacoids of the prisms are equal to the angles between the tetrahedral faces of the isometric system (70° 32′).

X-ray rotation photographs proved the coexistence of wurtzite* and sphalerite. The fact that all the hexagonal prisms *x*-rayed show excellent birefringence indicates that the cubic form exists only in the nucleus of the crystal group.

Figure 6 is a cross section of the crystal group shown in Fig. 2. The section is parallel to the plane formed by the *c* axes of any two of the prisms. The relationship of this to Fig. 1 is clearly seen. Portions *AEFB* and *DHGC* are $11\cdot0$ planes through the wurtzite structure, while *ABCD*

---

* The *x*-ray data indicate that the wurtzite prisms are composed primarily of the 2*H* polymorph (Ramsdell nomenclature, 1947). Some crystals also show evidence of the existence of other polytypes with a higher number of layers. Müller (1952) has shown that these can coexist. As yet no intensive investigation of these forms has been carried on in connection with the crystal groups.

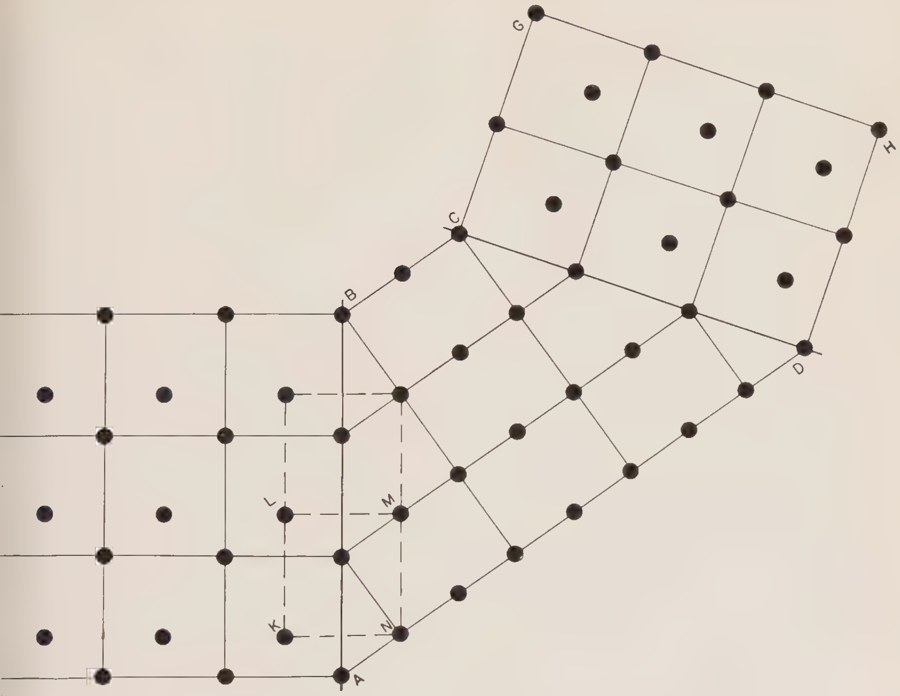

FIG. 6. Cross section of a simple wurtzite-sphalerite group parallel to the plane formed by the *c* axes of any two prisms. Only the Zn (or S) atoms are designated.

is the 110 plane through the sphalerite structure. Lines *AB* and *CD* represent twinning boundaries. The unit cell outlined by *KLMN* represents a second choice for the wurtzite unit cell which exists partially above and partially below the twinning boundary.

The investigators have encountered much difficulty in finding a name which adequately describes the crystal groups. They have hesitated to call them *twins* because the geometrical relationships involved are based upon two crystal systems. Moreover, the term *polymorphic twin* does not describe them. As was pointed out earlier in this paper, wurtzite is a polymorphic twin of sphalerite because of its similar structure, but this term does not indicate that both structures coexist in an individual unit. A single wurtzite prism can be considered a polymorphic twin of sphalerite. In reality the wurtzite prisms are *oriented overgrowths*, but calling them only this does not adequately bring out the structural and chemical similarity that exists between the two forms. The writers believe that the term *oriented polymorphic twin overgrowth*, which is a combination of these above names would adequately describe the crystal groups.

Method of Preparation of the Zinc Sulfide Crystals

The crystals were made by a method described by Lorenz (1891) in which hydrogen sulfide is allowed to react with zinc vapor. A porcelain boat containing 30 mesh granular C.P. metallic zinc was placed in a hydrogen sulfide-filled Vycor U-tube which was preheated to 900° C. Hydrogen sulfide was passed over the boat at this temperature for six hours, a period of time arbitrarily chosen for this experiment. At the end of this period the U-tube was quickly removed and allowed to cool. The hydrogen sulfide atmosphere was maintained during the cooling.

General Appearance and Physical Properties of the Crystals

The zinc sulfide crystals covered the boat, as well as the walls of the portion of the tube surrounding the boat. Masses of the wurtzite-sphalerite groups occurred as segregations in the midst of simple hexagonal wurtzite prisms and fine crystalline masses. No detailed investigation of these latter types has been undertaken. The individual wurtzite-sphalerite groups in these segregated masses are attached perpendicularly to a groundmass by a vertical hexagonal prism which acts as a stem as shown in Figs. 2 and 5. Generally the stem, which may be up to one millimeter in length, is much longer than the other hexagonal prisms which also may vary in length. The crystals are colorless. Under ultraviolet radiation they exhibit strong light blue fluorescence and phosphorescence.

A Discussion of the Growth of the Wurtzite-Sphalerite Groups

It was mentioned above that a hexagonal prism acts as a stem by which the wurtzite-sphalerite group is attached to the groundmass. From this fact it seems logical to conclude that the stem grew first. Next the tetrahedron developed on top of this stem. Finally prisms proceeded to grow out from the remaining three faces of the tetrahedron. No doubt the factors which controlled this growth sequence are numerous. Probably one of the most important factors was a variation in temperature. Müller (1952), who has done considerable work on the tempering of wurtzite crystals at different temperatures, found that hexagonal zinc sulfide transforms completely to the cubic modification when tempered below 870° C. Tempering in the range 870–905° for 10 hours produces a coexistence of cubic and the hexagonal types 2*H*, 4*H*, 6*H*, and 15*R*. Type 2*H* predominates at all temperatures above 905°. From these results it appears that temperatures in the neighborhood of 870° are of special importance in determining if zinc sulfide will crystallize in the cubic or hexagonal system. The temperatures in the Vycor tube probably dropped below 870° during the process of crystal growth, thus producing sphalerite tetrahedrons on top of the primary wurtzite prisms. When higher temperatures were re-established, wurtzite formed on the sphalerite faces. The temperature variation may be attributed to a variation in the flow of the unheated hydrogen sulfide that was passed into the tube during crystal growth or to lack of delicate controls on the muffle furnace.

The significance of the time element is not known. In succeeding experiments simple hexagonal prisms were grown in as short a time as 15 minutes.

So far the writers have been unable to duplicate the results of this experiment. This suggests that the conditions for the formation of this peculiar type of coalescence are very critical.

Other Intergrowths of Sphalerite and Wurtzite

Another type of coalescence of sphalerite and wurtzite was produced at this laboratory which consists of isotropic layers or knobs of sphalerite in what appears otherwise to be a continuous hexagonal wurtzite prism (Fig. 7). It can be seen in Fig. 6 that the wurtzite prisms of the crystal groups described in the previous section were formed by twinning along different sphalerite [111] axes, producing two hexagonal units whose *c* axes are related to each other by an angle of 70° 32′. However, it is also possible for the twinning to occur along the same sphalerite [111] axis

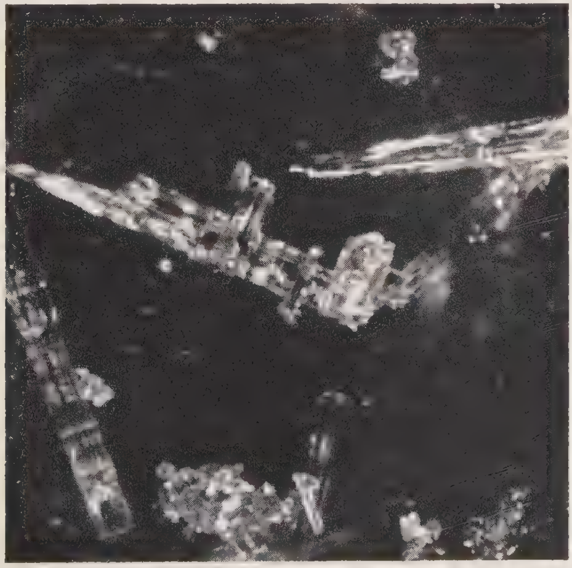

Fig. 7. Photomicrograph of wurtzite prism interrupted by layers or knobs of sphalerite (×92).

extending from opposite sides of a cubic unit. In this case the two hexagonal prisms would be parallel to a common line, and would have a layer of sphalerite separating them. If the conditions changed a number of times during growth, many cubic layers may develop in what appears to be a continuous hexagonal prism. These crystals were grown in the same manner as those first described in this paper, except that the hydrogen sulfide was passed over the boat at 900° for 12 hours.

The coexistence of sphalerite and wurtzite in nature is well known from schalenblende, which consists of an intimate intergrowth of the two forms. The crystallographic relationships of the two modifications are not well known in this association.

Natural sphalerite is frequently found in multiple contact twins and in complicated lamellar intergrowths. In a special sense a sphalerite twin might be considered as having the wurtzite arrangement in the twin boundary. The twin boundary would be a wurtzite crystal two layers high ($2H$)[*] in the direction of its c axis ([111] axis of sphalerite). In other words the wurtzite crystal would be one unit cell high and would extend almost indefinitely in its other directions. This is clearly seen in Fig. 8 where $ABCD$ and $AEFB$ are two portions of sphalerite connected by the twinning boundary AB. $FK'N'M$ outlines a portion of the "two dimensional" wurtzite crystal existing at the twin boundary. Multiple contact twins would contain many of these hexagonal levels. Slawson and Kohn (1950) have suggested that the anomalous double refraction commonly observed in cubic zinc sulfide is due to twinning, since the twinning introduces a distortion at the twinning boundary in the otherwise optically isotropic cubic structure.

Similar Coalescence as Exhibited in Related Substances

Aminoff and Broomé (1936) performed an experiment directly related to the present discussion. They heated crystallized sphalerite in air until it was covered by a thin film of zinc oxide. The resulting film was studied by electron diffraction. It had the hexagonal zinc oxide structure, which is the same as that of wurtzite, and it was so oriented that the c axis was perpendicular to the sphalerite (111) and the a axes were parallel to the

---

[*] The wurtzite layer at the twin boundary would generally be considered as being two layers high because this is the common wurtzite structure. However, with the discovery of wurtzite types $4H$ and $6H$ (Frondel and Palache, 1948, 1950), one might consider that these exist at the twin boundary. In Fig. 8 $OPRQ$ outlines a $4H$ unit cell while $STVU$ outlines $6H$. The twin boundary might also be considered to represent the "two dimensional" wurtzite types $8H$ ($WXZY$), $10H$, $12H$, $\cdots$, $2nH$. As a matter of fact a sphalerite twin with exactly n layers on each side of the twin boundary would be a hexagonal polymorph $2nH$ one unit cell high. One could easily see this c_0 dimension macroscopically if n were sufficiently large.

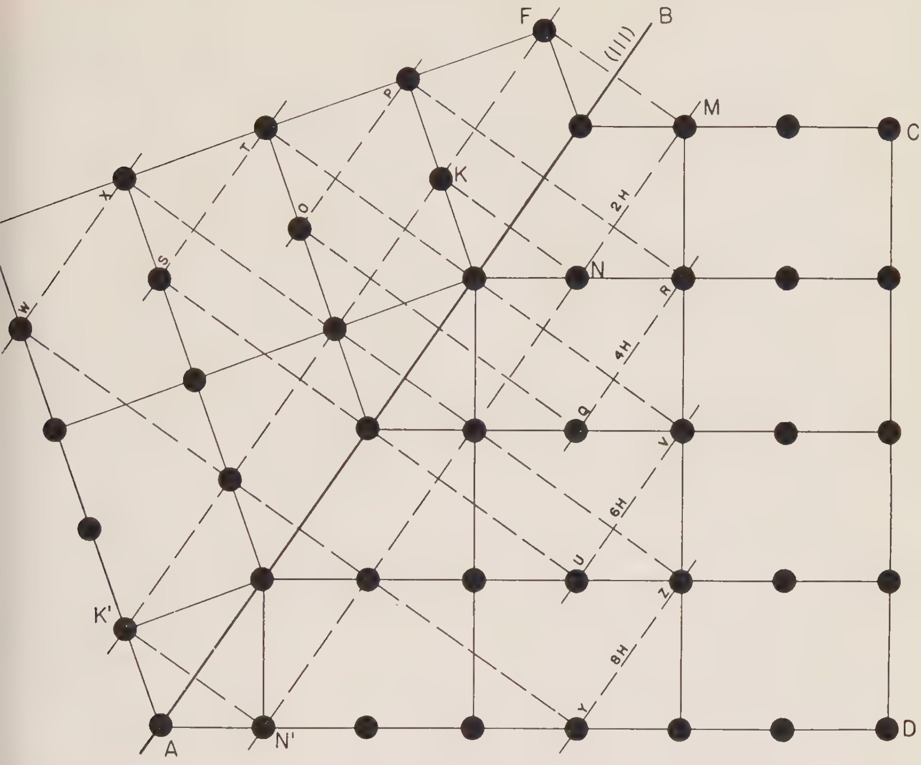

FIG. 8. 110 cross section through a simple sphalerite twin showing the different "two dimensional" hexagonal crystal unit cells that exist at the twin boundary. Only the Zn (or S) atoms are designated.

edges formed by the intersections of tetrahedral faces. This is the same orientation the wurtzite had in relationship to the sphalerite (111) faces. The similarity between the axial ratios of hexagonal zinc oxide and zinc sulfide also show how closely these structures are related: ZnO $a:c=1:1.608$; ZnS, $a:c=1:1.635$ (after Bragg, 1920).

Silicon carbide possesses a twinning property somewhat similar to that of the isostructural zinc sulfide. Cubic crystals have been observed by Thibault (1944) which contain thin plates of α silicon carbide parallel to adjacent faces of the positive and negative tetrahedrons. These plates are inclined to one another 70° 32′ which is the octahedral angle. This is the same angle at which the wurtzite prisms in Figs. 2, 3*a*, and 4 are inclined to each other. If two of these plates of α silicon carbide continued to grow until their size completely hid the cubic section, one would observe a twinning arrangement of them in which the basal pinacoids of the individuals are inclined to each other at an angle of 70° 32′. Numerous examples of silicon carbide twins have been observed with angles approaching this value (Thibault, 1944; Padurow, 1952). Thibault has suggested that this twinning angle is related to the octahedral angle in the manner described above. However, he suggests that the cubic section has reverted to hexagonal silicon carbide at an elevated temperature. From our knowledge of the coexistence of the zinc sulfide forms, the writers feel that with more investigation it may be proven that the cubic modification still exists at the "twinning" boundary.

Slawson and Kohn (1950) have pointed out that diamond, which is isostructural with sphalerite, may possibly have a hexagonal modification similar to the structure of wurtzite. They have pointed out that it would have a low double refraction, a density of approximately 3.50, and a hardness nearly equal to that of the cubic modification. In a sense this modification actually exists as a "two dimensional" crystal at the twinning boundary in a spinel twin of diamond (the same situation discussed earlier for twinned sphalerite, Fig. 8). This hexagonal modification is one unit cell high in the direction of its c axis (diamond [111]) and in the other two directions, extends to the bounds of the crystal. It can be considered $2H$, $4H$, $6H$, $\cdots$, $2nH$ (see footnote, page 780). Slawson and Kohn (1950) have suggested that the anomalous double refraction in diamond may be due to the presence of many of these hexagonal levels caused by repeated twinning in the diamond. A real three dimensional modification would not exist, however, unless the twinning occurred by rotating every other layer of atoms in diamond 180° around the diamond [111] axis. The study of diamond flats (crystals flattened along (111)) showing double refraction should eventually result in the identification of this predicted form.

REFERENCES

AMINOFF, G., AND BROOMÉ, B. (1931), *Zeit. Krist.*, **80**, 355–368.

——— (1936), *Nature*, **137**, 995.

BRAGG, W. L. (1920), *Phil. Mag.*, **39**, 650.

FRONDEL, C., AND PALACHE, C. (1948), *Science*, **107**, 602.

——— (1950), *Am. Mineral.*, **35**, 29.

LORENZ, R. (1891), *Ber. deut. chem. Ges.*, **24**, 1507.

MÜLLER, H. (1952), *Neues Jahrb. Mineral., Geol.*, **84**, 1, 43–76.

PADUROW, N. N. (1952), *Tschermak's Mineralog. u. Petro. Mitt.* (3), **3**, 1, 10.

RAMSDELL, L. S. (1947), *Am. Mineral.*, **32**, 64–82.

SLAWSON, C. B., AND KOHN, J. A. (1950), *Am. Crystal. Assoc.*, abstracts of first meeting, Penn. State College, p. 15.

THIBAULT, N. W. (1944), *Am. Mineral*, **29**, 269.

Manuscript received June 6, 1953

THE BONDING ENERGIES OF SOME SILICATE MINERALS

W. D. KELLER, *University of Missouri, Columbia, Missouri.*

ABSTRACT

The bonding energies of some silicate minerals may be computed by adding the energies of the bonds between their constituent cations and oxygen, starting with the elements in the gaseous ionic state. Data from Huggins and Sun are used in the computations.

After adjusting the bonding energies of the minerals to a standard mineral cell containing 24 oxygens, they are compared for the minerals in the Bowen reaction series, for some micas and mica-like minerals found in sedimentary rocks, and for some common metamorphic minerals. Fair agreement, but not complete, between the order of bonding energy and that of mineral occurrence is observed.

It is concluded that the genesis of a mineral involves the energy balance present in its environment during formation, as well as the availability (concentration and activity) of its constituent elements, their ionic size, electronegativity, force fields, coordination and other factors.

INTRODUCTION

A mineral may be thought of as being the product of a chemical reaction which took place in a geological system; or as being the product of the response of certain elements occurring in a geological system to the energy relationships in the system at that time. The energetics of mineral genesis and stability have been considered in recent years by Fairbairn (1943), Buerger (1948), Gruner (1950), Osborn (1950), Ramberg (1952), and others. Each of these papers has treated the subject from one or more viewpoints, but still a slightly different approach may be made by utilizing data on the ionic bonding energies of simple and complex oxides (including silicates) published by Huggins and Sun (1946, 1945), and Sun and Huggins (1946).

Huggins and Sun computed the decrease in energy which follows when cations and oxygen as gaseous ions form oxides at 18° C. These energies of formation are additive for those substances where the oxygens and cations are nearest neighbors, a category which includes silicate and oxide minerals.

The energy of formation of a silicate mineral may be computed therefore, by adding the energies accruing to the individual ions—oxygen (oxides) making up the mineral. In turn, the energies of formation of different minerals may be compared quantitatively if they are put on a uniform reference basis; this has been done by multiplying the molal energy for each mineral by a factor which adjusts the number of oxygen atoms in each mineral formula to a uniform "mineral cell" containing 24 oxygen atoms.

The energy values given are not the ultimate in accuracy, for as Huggins and Sun (1946) point out, "we emphasize the fact that the ϵ_M values computed in this paper are only approximate average values and that theoretically they *should not* and experimentally they *do not* give accurate energies of of formation by simple additivity. Nevertheless, the approximate constancy and additivity of the ϵ_M values are useful, and comparisons of their magnitudes show correlations with the structures of atoms, crystals, and glasses which, in our opinion, are not as well shown in any other way."

Another factor of inaccuracy results as energy differences are not shown between polymorphic forms of minerals having the same chemical composition. Dickite and kaolinite, for example, possess the same computed energy values, but it is not expected that the energies are the same in those minerals because dickite is usually much better crystallized than is kaolinite. The members of the Al_2SiO_5 group of minerals, and others, are not differentiated in the energy computation.

Despite these shortcomings, the application of Huggins and Sun's data to minerals shows some interesting relationships, and stimulates furthe thinking on the chemistry and thermodynamics of mineral formation

Source of Data Used

Because this paper builds directly on the work of Huggins and Sun (1946), the manner by which they obtained their fundamental data will be quoted verbatim from their article.

"For our data we use the values (Qf) of molal heats of formation (from the elements in their standard states) of the oxides and gaseous ions collected by Bichowsky and Rossini (1). These are all for a temperature of 18° C. The molal energy of formation of a compound from the simple gaseous ions we shall designate by the symbol E_i. For a simple crystalline oxide, M_mO_n, E_i is related to the Qf values according to the equation:

$$E_i[M_mO_n, \text{crystal}] = Qf[M_mO_n, \text{crystal}] - m\,Qf[M^{(2n/m)+}, \text{gas}] - n\,Qf[O^{--}, \text{gas}] - (m+n)RT \qquad (1)$$

The corresponding relations for vitreous oxides and for complex oxides (containing more than one non-oxygen element) are obvious.

It may be noted that the sign of E_i is so chosen as to make E_i greater the greater the stability of the substance, that is, the lower its actual content of energy. This convention as to the sign conforms to the convention adopted by Bichowsky and Rossini with regard to Qf values and to the universal custom in calculating and using "bond energies."

We realize that for some purposes *free energies* are of more interest than total *energies*, but calculation of the former involves complications with regard to the entropy contributions, into which we do not care to go at this time.

From the results of x-ray diffraction studies of crystals and glasses it seems certain that, with very few exceptions, each non-oxygen atom or ion, in any of the oxides we are considering, is surrounded by oxygen atoms or ions. Most of the ionic formation energy, E_i, of such a solid results from the attractions between closest neighbors—that is, from the attractions between each positive atom (Na, Ca, Si, P, $\cdots$) and the surrounding oxygens. One might expect the attraction energy between positive atoms and the surrounding shell of oxygen atoms to vary but little from compound to compound or from glass to glass. This is especially likely if the coordination number stays the same, but even with a change of coordination number the energy change should not usually be large. The energy contributions of pairs of atoms which are not closest neighbors are relatively small, and the summation of these may be assumed to be roughly the same in the compounds being considered. It is reasonable, therefore, to expect approximate additivity of energies, the E_i values being the sum of energy contributions resulting from the attraction of each positive atom for its surroundings. The calculations reported here show this to be the case. Significant departures from additivity do occur, however. In most cases they can be attributed to differences in the number or arrangement of closest neighbors.

The additivity assumption can be expressed mathematically in the following way. For a glass or compound of formula $M_m M'_{m'} M''_{m''} \cdots O_n$,

$$E_i = \sum_{M} m_M \epsilon_M. \tag{2}$$

The m_M values are the relative numbers of metal (non-oxygen) atoms, as expressed by the formula. The ϵ_M values are constants characteristic of these elements, deduced from the experimental E_i values. Each ϵ_M is a measure of the decrease in energy when one gram-atom of the ion M and the equivalent number of oxide ions (O^{--}) are transferred from the gaseous state to an average simple or complex oxide in the solid state, in which each M has as near neighbors only oxygens and each oxygen has as near neighbors only more electropositive atoms (M, M′, M″ $\cdots$)."

Individual ϵ_M values which are listed in Table 1 are selected from a larger list in Table 1 of the article by Huggins and Sun.

Computed Energies of Silicate Minerals

To compute the molal energy of formation of forsterite, Mg_2SiO_4, for example, one simply adds:

2× 912 kg. cal. (Mg^{++})	1,824
1×3,142 kg. cal. (Si^{4+} in SiO_4)	3,142
Bonding energy, 1 mol Mg_2SiO_4	4,966 kg. cal.

The energy of formation of enstatite, $MgSiO_3$, 912+3,131, equa 4,043.

The energy of orthoclase formation is computed:

1× 299 kg. cal. (K^+)	299
1×1,793 (Al^{3+} in silicates)	1,793
3×3,110 (Si^{4+} in SiO_2 group)	9,330
Bonding energy, 1 mol KSi_3AlO_8	11,422 kg. cal..

TABLE 1. ENERGY CONSTANTS FOR VARIOUS IONS IN SIMPLE AND COMPLEX OXIDES

Ion, M	ϵ_M in kg. cal.
Ca^{++}	839
Mg^{++}	912
Fe^{++}	919
Na^+	322
K^+	299
H^+ (in OH)	515
Ti^{4+}	2,882
Al^{+++} (in aluminates)	1,878
(in Al silicates)	1,793
Si^{4+} in $MSiO_4$	3,142
in MSi_2O_7	3,137
in M SiO_3	3,131
in M Si_4O_{11}	3,127 (computed by the writer
in M Si_2O_5	3,123
in SiO_2	3,110

To provide a basis for comparing the energies of different minera species, a "cell" containing uniformly 24 oxygens has been adopted. Th adjusted bonding energy for the above minerals are accordingly expresse as follows:

Forsterite, as 6× 4,966 kg. cal.: 29,796 kg. cal.
Enstatite, as 8× 4,043 kg. cal.: 32,344 kg. cal.
Orthoclase, as 3×11,422 kg. cal.: 34,266 kg. cal.

The computed bonding energies, adjusted to a 24-oxygen cell, of som common silicate minerals are listed in Table 2.

MINERAL-ENERGY RELATIONSHIPS

The relation between energy and mineral genesis is not easily see in an alphabetized table—smaller related groups should be selected fo comparison. Before examining individual groups it is of interest to ob serve that within the silicates (and alumino-silicates), the bond whic

Table 2. Common Minerals and Their Additive Bonding Energies

Mineral		Additive energy of mineral formula	Bonding energy adjusted to 24 O's
Akermanite	$Ca_2Mg_2Si_2O_7$	8,864 kg. cal.	30,391 kg. cal.
Albite	$NaSi_3AlO_8$	11,445	34,335
Almandite	$Fe_3Al_2Si_3O_{12}$	15,939	31,878
Analcime	$NaSi_2AlO_6 \cdot H_2O$	9,450	32,400
Anorthite	$CaSi_2Al_2O_8$	10,645	31,935
Augite	$Ca_4Mg_2Fe_2Si_7AlO_{24}$	30,729	30,728
Biotite	$K(Mg, Fe)_3(OH)_2Si_3AlO_{10}$	30,475	30,475
Dickite	$Al_4(OH)_8Si_4O_{10}$	24,124	32,165
Diopside	$CaMg(SiO_3)_2$	8,013	32,052
Enstatite	$MgSiO_3$	4,043	32,344
Epidote	$Ca_2(Al_2Fe_1)(OH)Si_3O_{12}$	16,261	30,020
Forsterite	Mg_2SiO_4	4,966	29,796
Gehlenite	$Ca_2AlSiAlO_7$	7,593	26,890
Hornblende	$Ca_2(Mg, Fe)_5(OH)_2Si_7AlO_{22}$	31,883	31,883
Idocrase	$Ca_{10}(MgFe)(OH)_2Al_4Si_9O_{34}(OH)_2$	48,071	30,360
Muscovite	$K_2Al_4(OH)_4Si_6Al_2O_{20}$	32,494	32,494
Nepheline	$NaSiAlO_4$	5,310	31,860
Orthoclase	KSi_3AlO_8	11,422	34,266
Pyrophyllite	$Al_2(OH)_2Si_4O_{10}$	16,270	32,558
Quartz	SiO_2	3,110	37,320
Sillimanite	Al_2SiO_5	6,866	32,957
Spinel	$MgAl_2O_4$	4,668	28,008
Staurolite	$H\ Fe_2Al_9O_8Si_4O_{16}$	31,823	31,823
Talc	$Mg_3(OH)_2Si_4O_{10}$	16,258	32,516
Topaz	$Al_2(F, OH)_2SiO_4$	7,928	31,712
Tremolite	$Ca_2Mg_5(OH)_2Si_8O_{22}$	32,284	32,284

contributes most to the bonding energy, and therefore to the range in values, is the high-energy Si—O bond. A pronounced increase in bonding energy occurs in the sequence neso- < soro- < ino- < phyllo- < tectosilicate. This relationship is shown in Table 3, below. Ramberg (1952) found by another approach a parallel relationship.

The bonding energy for Si—O bonds, where 24 O's are concerned, is shown as being almost 8,500 kg. cal. greater for SiO_2 than for SiO_4^{4-}. This difference is unrealistically large for the silicate minerals, because cations will replace the (−) valences of the SiO_4 and increase the bonding energy for all groups other than SiO_2. Nevertheless, no other M—O bond energy is as large as Si—O, and therefore the tectosilicate always has the largest bonding energy within any specific M—Si—O group. Where Al occurs tetrahedrally vicarious for Si, its bonding energy is less than if all tetrahedral cations are Si; indeed, the sum of the bonding energies of vicarious tetrahedral Al with O, with that of another monovalent

TABLE 3. ENERGY SEQUENCE FROM NEOSILICATE TO TECTOSILICATE, 24 OXYGENS

Type	Factor	Adjusted bonding energy: 24 O's
Nesosilicate	$6 \cdot SiO_4$	18,852 kg. cal. plus that of 12 M^{++} bridges
Sorosilicate	$24/7 \cdot 2 \cdot Si_2O_7$	21,511 kg. cal. plus that of $10\frac{2}{7}$ M^{++} bridges
Inosilicate	$8 \cdot SiO_3$	25,048 kg. cal. plus that of 8 M^{++} bridges
Inosilicate	$\frac{24}{11} \cdot 4 \cdot Si_4O_{11}$	27,290 kg. cal. plus that of 7 M^{++} bridges and $2H^+$ (commonly)
Phyllosilicate	$\frac{24}{5} \cdot 2 \cdot Si_2O_5$	29,981 kg. cal. plus that of 6 M^{++} bridges and $4H^+$ (commonly)
Tectosilicate	$12 \cdot SiO_2$	37,320 kg. cal. plus that of 0 M^{++} bridges

cationic bond with O, is commonly less than that of unsubstituted Si—O

The Bowen reaction series, or the Rosenbusch "decreasing basicity" series is one of neosilicate to tectosilicate. Accordingly, it might be expected that energy requirements would be the controlling factor in establishing that series, and that correspondingly the bonding energies of the minerals which actually make up the rocks exhibiting such a series would increase regularly from neosilicate to tectosilicate. This expectation appears to hold for the simple case where only one set of cations are in the minerals compared. It holds also where moderate diadochy prevails.

The uniform increase in bonding energy within mineral sequences does not follow rigorously where compound diadochy of bridging cations, and simultaneously Al for Si, come into play in some minerals but not into others. The effect of OH entering a mineral introduces complications of energy which are not understood by the writer. Minor variations in bonding energy occur between varieties of amphibole, mica, etc., so that for any stipulated energy, the formula for that individual mineral must also be expressed; a "biotite" of one composition may have more or less bonding energy than that of "hornblende." It is not surprising therefore that "exceptions" or "reversals" to the "normal order" of crystallization occur; actually their "abnormal order" may be entirely consistent with the energy balance. See Table 4 for a list of minerals from the Bowen series arranged in order of increasing bonding energy adjusted to 24 O's.

One looks askance at the low energy of formation of biotite and perhaps of augite, and at their positions higher in the table than expected. Is something wrong with the energy values; are the formulas (composition) assigned to the minerals (and from which the energies were computed) inconsistent with the true compositions of these minerals which

TABLE 4. ENERGY RELATIONSHIPS OF MINERALS IN THE BOWEN REACTION SERIES

(Adjusted to 24 O's)
Spinel, $MgAl_2O_4$—28,008

Forsterite, Mg_2SiO_4—29,796	
(Akermanite, $Ca_2MgSi_2O_7$—30,390)	
Biotite, $K(Mg, Fe)_3(OH)_2Si_3AlO_{10}$—30,475	
Augite, $Ca_4Mg_2Fe_2Si_7AlO_{24}$—30,728	
	Anorthite, $CaAl_2Si_2O_8$—31,935
Diopside, $CaMg(SiO_3)_2$—32,052	
Enstatite, $MgSiO_3$—32,344	
Hornblende, $Ca_2(Mg, Fe)_5(OH)_2Si_7AlO_{22}$—31,883	
Muscovite, $K_2Al_4(OH)_4Si_6Al_2O_{20}$—32,494	
Orthoclase, KSi_3AlO_8—34,266	
	Albite, $NaSi_3AlO_8$—34,335
Quartz, SiO_2—37,320	

actually crystallize during cooling of a magma? Or, are the values computed correctly, but is the sequence of crystallization (appearance) of minerals in a cooling magma co-controlled by a critical concentration of specific elements as well as by energy requirements. A conclusive, rigorous answer to these questions is not at hand, but it appears that the minerals (and the sequence of their appearance) which crystallize from a magma are the result of interplay, coordinated in time and space, of two factors, (1) the proper energy balance, and (2) the availability of an adequate concentration of appropriate elements.

To visualize the interplay of those last two factors it is of interest to trace the probable course of crystallization in model of a hypothetical "ordinary average" magma.

An ordinary silicate magma is rather certainly a liquid composed of —O—Si,Al—O—tetrahedra bridged, in three dimensional space, largely by alkali and alkaline earth cations, fluorine, phosphate, hydroxyl and water (Buerger, 1948), which are abundantly hydrogen-bonded (Keller and Pickett, 1954), and scantier accessories. Support is given to the above description from work done on perlite, which is a rapidly undercooled liquid magma (Keller and Pickett, 1954), and inferred from the structure proposed for artificially prepared glass (Zachariasen, 1932; Warren, 1934; Warren and Loring, 1935; Warren and Biscoe, 1938).

At the high temperature of liquidity of the magma the kinetic energy of the magma constituents is high, and the bonds within the —O-Si,Al—O—tetrahedra, and to the bridging cations, are non-uniform, changing, extended, and moderately weak.

As the magma cools it obviously loses thermal (kinetic) energy to its surroundings. After the temperature falls to a certain point a nesosilicate like forsterite can crystallize as far as the energy balance between liquid and solid is concerned. But another condition must be met before forsterite *actually* does crystallize—a high enough ratio of Mg to SiO_4 must prevail for Mg_2SiO_4 to develop. If adequate Mg is lacking, forsterite can not crystallize although the energy balance within the magma is adequate.

As the magma continues to cool and lose energy to its surroundings, the gap widens between the reference level of gaseous ion energy and the energy in the magma. When the energy of the magma lowers to that consistent with the crystallization of enstatite, for example, it (enstatite) can then develop, provided of course that the ratio of Mg to SiO_4 is appropriate. Enstatite has a higher energy of crystallization and has higher stability than forsterite, for enstatite formation is farther removed from its gaseous ions, in terms of energy, than is olivine.

The same line of reasoning carries on downward in the scale to quartz. Always two requirements must be met for a mineral to form: (*a*) the proper energy balance, and (*b*) an adequately abundant supply of appropriate elements in the magma at that time so as to produce a solid mineral containing constituent elements in the ratio demanded by the formula. In mineral families where elements are diadochous, the element, or the distribution between vicarious elements, which enter the mineral may be expected to be governed similarly by the energy and statistical abundance of ions available.

Osborn (1950) emphasized the composition of the liquid as being more significant then the temperature in determining the type of crystal structure which will form. He related the size of cation, its coordination, and its field strength to its segregation in the crystallization history of a magma.

All of these factors are vitally important, and may modify the order of crystallization from what has been set up as "normal." When viewed in this light, the presumably anomalous positions of some minerals in the sequence in Table 3 may not be out of place so seriously after all.

MICAS AND MICA-LIKE MINERALS

Bonding energies of the micas and mica-like minerals show small differences between large quantities. They are listed in Table 5.

Although the micas and mica-like minerals are listed in order of increasing bond energy, the arrangement of the bottom four has little quantitative meaning because the differences between varieties are slight in comparison to the large total energies; a slight error in the values might

TABLE 5. MICAS AND MICA-LIKE MINERALS

Mineral	Bonding energy adjusted to 24 O's
Biotite	30,475 kg. cal.
Dickite	32,165
Muscovite	32,494
Talc	32,516
Pyrophyllite	32,558

result in an interchange of position. Furthermore, the composition of dickite is the same as that of nacrite, kaolinite and halloysite, which have different stability ranges.

Muscovite and illite may have nearly the same chemical composition but their environments of genesis can differ appreciably. The same may be said of pyrophyllite and its sedimentary derivatives, the montmorillonite-group minerals.

Perhaps it is unfair to imply that the bonding energies of dickite and halloysite, or muscovite and illite, should be computed by the same procedure when it is known that halloysite and illite are not nearly so well crystallized as are dickite and muscovite.

Considerable overlap does occur in the environments of formation of these mineral groups. Dickite is found in hydrothermal ore deposits, but it also occurs in sedimentary rocks which show no proven high temperature history (Tarr and Keller, 1936). Talc likewise commonly has a hydrothermal lineage, but it forms under sedimentary evaporite conditions (Stewart, 1949). Thermal energy and temperature may not be the sole controlling energy factor in the genesis of these minerals; the chemical energy present in a concentrated evaporite environment, or the ratio of activities of reactants to those of products (as expressed in the oxidation-reduction potential equation) may influence the mineral formation drastically.

COMMON METAMORPHIC MINERALS

The bonding energies of some metamorphic minerals are listed in Table 6.

Epidote and sillimanite are outstandingly out of the positions expected for them from their occurrence in rocks. The stability of Al_2SiO_5 must certainly be modified by factors extraneous to simple bonding energy because of its trimorphic possibilities, and furthermore because it inverts to mullite and silica upon artificial heating. Why epidote should have such low bonding energy is not clear to the writer.

TABLE 6. BONDING ENERGIES OF SOME METAMORPHIC MINERALS

Mineral	Bonding energy adjusted to 24 O's
Gehlenite, $Ca_2AlSiAlO_7$	26,890
Epidote, $Ca_2(Al_2Fe)(OH)Si_3O_{12}$	30,020
Idocrase, $Ca_{10}(MgFe)(OH)_2Al_4Si_9O_{34}(OH)_2$	30,360
Biotite, $K(Mg, Fe)_3(OH)_2Si_3AlO_{10}$	30,475
Staurolite, $HFe_2Al_9O_8Si_4O_{16}$	31,823
Almandite, $Fe_3Al_2Si_3O_{12}$	31,878
Hornblende, $Ca_2(Mg, Fe)_5(OH)_2Si_7AlO_{22}$	31,883
Sillimanite, Al_2SiO_5	32,957
Orthoclase, KSi_3AlO_8	34,266
Albite, $NaSi_3AlO_8$	34,335
Quartz, SiO_2	37,320

SUMMARY

The bonding energies of some common silicate minerals have been computed by adding the bonding energies of their constituent elements, utilizing data compiled by Huggins and Sun. The notably high-energy Si—O bond dominates the bonding of the silicates.

The bonding energies of silicate mineral assemblages show fair correlation with their occurrence in rocks, but some pronounced exceptions stand out.

The approach used in these computations shows some merit, but refinements are needed to make the results more meaningful. It stresses the fact that other physical and chemical factors, such as availability (concentration and activity) of elements, their size, electronegativity, force fields, coordination, etc., enter, along with the energy balance, into the reaction from which a mineral is a product.

REFERENCES

Buerger, M. J. (1948), The role of temperature in mineralogy: *Am. Mineral.* **33,** 101–124.

Buerger, M. J. (1948), The structural nature of the mineralizer action of fluorine and hydroxyl: *Am. mineral.*, **33,** 744–747.

Fairbairn, H. W. (1943), Packing in ionic minerals: *Geol. Soc. Am., Bull.* **54,** 1305–1374.

Huggins, M. L., and Sun, K.-H. (1945), Energy additivity in glasses: *Jour. Am. Ceram. Soc.*, **28,** 149–151.

Huggins, Maurice L., and Sun, Kuan-Han (1946), Energy additivity in oxygen-containing crystals and glasses: *Jour. Phys. Chem.*, **50,** 319–328.

Keller, W. D., and Pickett, E. E. (1954), Hydroxyl and water in perlite from Superior, Arizona: *Am. Jour. Sci.*, **252,** 87–98.

Osborn, E. F. (1950), Segregation of elements during the crystallization of a magma: *Jour. Am. Ceram. Soc.*, **33,** 219–224.

Ramberg, Hans (1952), Chemical bonds and distribution of cations in silicates: *Jour. Geol.*, **60,** 331–355.

Stewart, F. H. (1949), The petrology of the evaporites of the Eskdale No. 2 boring east Yorkshire: *Mineral. Mag.*, **28,** 621–672.

Sun, Kuan-Huan, and Huggins, Maurice L. (1946), Energy additivity in oxygen-containing crystals and glasses II: *Jour. Phys. Chem.*, **50,** 439–443.

Tarr, W. A., and Keller, W. D. (1936), Dickite in Missouri: *Am. Mineral.*, **21,** 109–114.

Warren, B. E. (1934), *X*-ray determination of the structure of glass: *Jour. Am. Ceram. Soc.*, **17,** 249–254.

Warren, B. E., and Biscoe, J. (1938), Fourier analysis of *x*-ray patterns of soda-silica glass: *Jour. Am. Ceram. Soc.*, **21,** 259–265.

Warren, B. E., and Loring, A. D. (1935), *X*-ray diffraction study of the structure of soda-silica glass: *Jour. Am. Ceram. Soc.*, **18,** 269–278.

Zachariasen, W. H. (1932), The atomic arrangement in glass: *Jour. Am. Chem. Soc.*, **54,** 3841.

Manuscript received July 3, 1953

A NEW VARIETY OF ANTIGORITE (ORTHO-ANTIGORITE) FROM UNST, SHETLAND ISLANDS

G. W. Brindley* and O. von Knorring†

Abstract

Chemical, x-ray and thermal analyses together with petrographical data are given for specimens of antigorite from Unst, Shetland Islands. The x-ray powder diagrams are indexed on the basis of an ortho-hexagonal cell and the mineral is therefore named "ortho-antigorite" to distinguish it from the monoclinic varieties hitherto described. Evidence is obtained for a superlattice similar to that described by Aruja. The unit cell contains two structural layers and their relative orientation is probably similar to that of the kaolin-type layers in amesite. Structural formulae are derived.

Occurrence and General Characters (O. v. K.)

The antigorites described in this investigation were collected during a geological excursion in Unst, the northernmost of the Shetland Islands, in August 1950. The minerals come from the Nikka Vord chromite quarries north of Baltasound. Attention was attracted particularly to two green resinous-looking serpentine minerals forming irregular veinlets in the chromite-bearing serpentine rock, one associated with magnetite, the other with kämmererite (Cr-chlorite).

Antigorite No. 1, is of olive-green color containing scattered well-developed magnetite crystals as striated dodecahedrons. The surrounding rock is an almost black variety of rock-serpentine with chromite.

Antigorite No. 2, is greenish-yellow in color and usually associated with large, perfect crystals of kämmererite, the latter occurring as six-sided, slightly barrel-shaped prisms. Phillips (1927) describes this latter variety "as a pale lemon-yellow serpentine, apparently of secondary origin." The host rock in this case is a yellowish serpentine, with a moderate chromite content.

In hand specimens both minerals have a massive resinous appearance, without any structural features; they are translucent with a conchoidal fracture, and using the old nomenclature could be classed as precious serpentines.

Thin section examination of antigorite No. 1 revealed no significant textural features, the mineral being too fine-grained.

Antigorite No. 2 appeared to be patchy in ordinary light. In thin section the wavy patches are of brownish shade, whereas on a polished surface they are of a lighter color. With crossed nicols an intricate fine banded texture could be seen, in places as wavy fibrous bands, as shown in Pl. I, Fig. 1. The birefringence is very low and sometimes thicker sections are almost isotropic.

---

* Physics Department, University of Leeds, England. Present address, Dept. of Mineral Industries, The Pennsylvania State University, State College, Pa.

† Geology Department, University of Leeds, England.

The axial figure is obtained with difficulty, but where it is seen the sign is always negative.

The relation between the greenish-yellow antigorite and the surrounding chromite-bearing serpentine rock is of some interest. The vein antigorite is separated from the host rock by a margin of graded kämmererite, relatively coarsely crystalline against the antigorite and becoming gradually finer grained towards the country rock. Large crystals of kämmererite, up to 2 cm. in length, are scattered in the middle of the antigorite vein (Pl. I, Fig. 2). In some specimens brucite is developed to a large extent in this marginal zone, partly replacing kämmererite. Chromite, however, is absent in this zone and the nearest chromite grains are in the host rock facing the kämmererite fringe. They are partly or completely replaced by kämmererite (Pl. I, Fig. 3).

The surrounding chromite-serpentine is otherwise of an antigorite type, with outlines of olivine still clearly visible (Pl. I, Fig. 4).

CHEMICAL ANALYSES (O. v. K.)

The two antigorites and the kämmererite were analyzed. The results are shown in Table 1, together with earlier analyses for comparison. The

TABLE 1. CHEMICAL ANALYSES OF ANTIGORITE AND KÄMMERERITE

	1	2	3	4	5
SiO_2	41.65	38.40	41.46	33.23	32.31
TiO_2	none	none	—	—	—
Al_2O_3	0.10	0.10	0.01	10.44	7.50
Fe_2O_3	2.88	3.42	2.42	2.52	—
Cr_2O_3	—	—	—	3.22	7.89
FeO	0.16	none	1.16	—	2.08
MnO	0.05	0.05	0.23	0.02	—
MgO	41.06	41.91	41.76	36.31	32.15
CaO	none	none	tr.	none	3.83
H_2O+	13.10	15.03	12.43	13.40	14.25
H_2O-	1.12	1.26	—	1.22	—
	100.12	100.17	99.47	100.36	100.01

1. Antigorite, No. 1, Nikka Vord quarries, Unst. Analyst, O. v. Knorring.
2. Antigorite, No. 2, same loc. Analyst, O. v. Knorring.
3. Precious serpentine, Niddister, Hillswick Ness. Analyst, M. F. Heddle.
4. Kämmererite, Nikka Vord quarries, Unst. Analyst, O. v. Knorring.
5. Kämmererite, same loc. Analyst, M. F. Heddle.

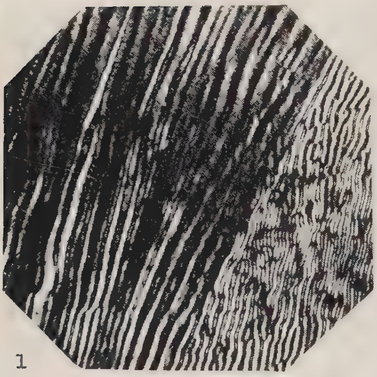

1

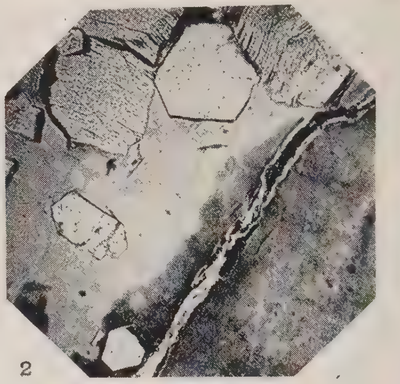

2

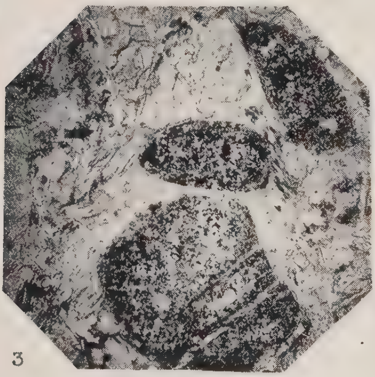

3

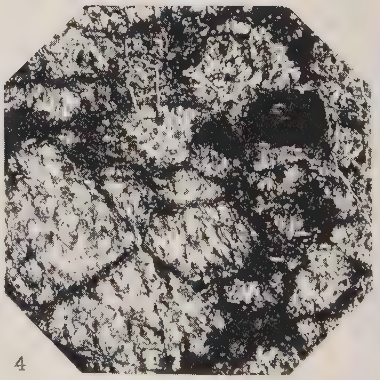

4

5a

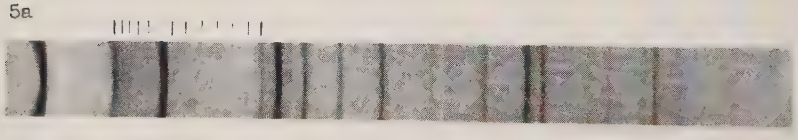

5b

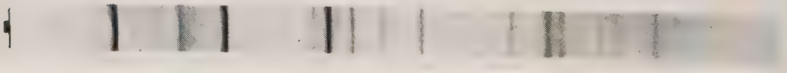

EXPLANATION OF PLATE I

FIG. 1. Wavy thread-like bands of antigorite, No. 2. Crossed nicols. ×33.

FIG. 2. Kämmererite crystals in vein antigorite, No. 2. ×20.

FIG. 3. Chromite crystals replaced by kämmererite. ×33.

FIG. 4. The antigorite rock-serpentine. ×20.

FIG. 5. *X*-ray powder diagrams of ortho-antigorite, No. 2. (*a*) 19 cm. Unicam camera, CoK_α radiation; the positions of the superlattice lines are indicated. (*b*) 20 cm. semi-focusing camera, CuK_α radiation; the imprint of the incident *x*-ray beam appears on the left-hand side.

most striking feature is that the iron is trivalent in these antigorites. In antigorite No. 2 further hydration has occurred with a consequent higher water content and much smaller silica. This agrees reasonably well with the patches observed in the mineral. The contents of Cr and Ni were not determined, but judging from the rather small Al value obtained by difference the amounts of Cr and Ni must be rather small.

The kämmererite was analyzed mainly to check an old analysis of the mineral from the same locality. The analysis is far from complete but the result already obtained differs considerably from that of Heddle (1924). The Cr content is much smaller and no Ca was found.

As to the origin of these secondary vein minerals it is usual to consider them as late products, belonging to a hydrothermal phase in connection with the serpentinization of former ultra-basic rocks. In this particular case the original rock was a dunite. The vein antigorites, however, are of primary origin, i.e., crystallized from Mg-rich solutions at a late stage, and are not the result of the serpentinization of olivine.

STRUCTURAL FORMULAE FOR ORTHO-ANTIGORITES, NOS. 1 AND 2

From the analyses in Table 1, Columns 1 and 2, structural formulae may be evaluated. The most reasonable basis of calculation is, in the first place, to assume that O and (OH) ions fill completely the 9 positions assigned to them in the ideal structure, and on this basis, the following formula is obtained:

Antigorite No. 1

$$\underbrace{(\mathrm{Mg}_{2.869}\mathrm{Mn}_{0.002}\overset{2+}{\mathrm{Fe}}_{0.006}\overset{3+}{\mathrm{Fe}}_{0.060})}_{2.937\text{ atoms}}\quad\underbrace{(\mathrm{Si}_{1.954}\mathrm{Al}_{0.005}\overset{3+}{\mathrm{Fe}}_{0.041})}_{2\text{ atoms}}\quad\underbrace{\mathrm{O}_{4.898}(\mathrm{OH})_{4.102}}_{9\text{ atoms}}$$

The Si is almost sufficient to fill the tetrahedral positions; the vacancies are filled mainly by Fe^{3+} ions since Al is almost absent. The octahedral ions number almost 3. Alternatively, the Al and Fe^{3+} ions may be placed wholly in octahedral positions, bringing the total still nearer to 3 (actually 2.983), with 0.046 tetrahedral vacancies. It is usual, however, to consider the tetrahedral positions fully occupied. The main points of interest are: (i) the presence of some tetrahedral Fe^{3+} ions, (ii) a slight excess of (OH) above the theoretical value of 4.0.

The evaluation of the formula for antigorite No. 2 is less straightforward. On the basis of $O+(OH)=9$ atoms, we arrive at the formula:

$$\underbrace{(\mathrm{Mg}_{2.905}\mathrm{Mn}_{0.002})}_{2.907\text{ atoms}}\quad\underbrace{(\mathrm{Si}_{1.786}\mathrm{Al}_{0.005}\overset{3+}{\mathrm{Fe}}_{0.120})}_{1.911\text{ atoms}}\quad\underbrace{\mathrm{O}_{4.338}(\mathrm{OH})_{4.662}}_{9\text{ atoms}}$$

The Si content appears very low and there is insufficient Al and Fe^{3+} to fill the tetrahedral positions. The (OH) content is considerably in excess of 4.0 atoms. An alternative approach may be made on the basis of 2 Si atoms per formula unit and the excess Mg and (OH) may be present as an impurity, $\mathrm{Mg(OH)_2}$. This leads to the following:

Antigorite No. 2

$$(\underbrace{\mathrm{Mg_{2.716}Mn_{0.002}Al_{0.006}Fe^{3+}_{0.134}}}_{2.858\text{ atoms}})\mathrm{Si_{2.00}}(\underbrace{\mathrm{O_{4.857}OH_{4.143}}}_{9\text{ atoms}} + 0.537\ \mathrm{Mg(OH)_2}.$$

Some justification for this procedure is provided by the presence of brucite associated with the kämmererite, but there is no *x*-ray or thermal evidence for its presence in the antigorite. The O/OH ratio now tends more nearly to the ideal 5/4 ratio. The deficiency of octahedral ions below 3 is not remarkably low. Without further data, this seems to be the most reasonable interpretation of the chemical analysis of the antigorite No. 2.

X-RAY POWDER ANALYSIS (G. W. B.)

X-ray powder diagrams were obtained with a 19 cm. diameter Unicam instrument and a 20 cm. diameter semi-focusing camera, using CoK_α and CuK_α radiations. In addition to the two antigoirites already described, a further specimen, antigorite No. 3, from the same locality, was also examined. This had a coarsely columnar appearance and a turquoise green color. The specimens were crushed to a fine powder and mounted either dry or with gum tragacanth.

The powder diagrams of the three materials are closely similar. The lines are moderately sharp but at high angles the K_α doublet is not resolved. Some 50 lines could be accurately measured. Antigorite No. 2 gave the clearest diagrams and most of the detailed *x*-ray analysis has been made on this material; typical diagrams are reproduced in Pl. I, Fig. 5. The measured lattice spacings in Å, referred to a mean CoK_α wavelength 1.79020 Å, are listed with their visually estimated intensities in Table 2. The results show very little agreement with powder data previously published by Selfridge (1936) and by Gruner (1937).

An important feature of the diagram which attracts immediate attention is a series of closely and regularly spaced lines of weak intensity extending from about 4.6 Å down to about 2.7 Å; their positions in Fig. 5*a* are indicated. This series is shown particularly well by specimen No. 2, less clearly by No. 3, and is scarcely visible in the diagram of No. 1. Apart from this series, which will be discussed in detail later, all other features of the diagrams are the same for the three specimens and these will be considered first.

TABLE 2. *X*-RAY POWDER DATA FOR ORTHO-ANTIGORITE

I=intensity, estimated visually; B signifies head of a continuous band of scattering.
d=spacing in Å based on $\lambda(\text{CoK}_\alpha)=1.79020$ Å.
hkl=indices based on the cell $a=b/\sqrt{3}$, $b=9.219$, $c=14.53$ Å.
$N20$ or $02N$ series calculated for superlattice parameter $S=43.8$ Å.

I	*d* (Obs.)	*d* (Calc.)	*hkl*	*N*20 or 02*N* series	
				d (Calc.)	*N*
10	7.33	7.265	002		
6 *B*	4.597	4.610	020	4.610	0
				4.584	1
				4.511	2
1	4.403			4.395	3
1	4.250			4.249	4
1	4.088			4.079	5
½	3.903			3.897	6
10	3.662	3.632	004	3.711	7
½	3.528			3.526	8
½	3.348			3.347	9
½	3.172			3.185	10
½	3.015			3.014	11
½	2.865			2.862	12
½	2.720			2.720	13
3	2.623	2.618	201	2.589	14
10	2.502	2.499	202		
1	2.450			2.467	15
1	2.425	2.422	006		
7	2.335	2.332	203		
6	2.149	2.147	204		
				|Δ*d*|/*d*	
7	1.9629	1.9626	205	0.0002	
½	1.8154	1.8162	008	.0005	
1	1.7905	1.7911	206	.0003	
1 *B*	1.7392	1.7424	240	.0018	
4	1.6360	1.6368	207	.0005	
8	1.5354	1.5367	060	.0008	
7	1.5013	1.5033	062	.0003	
		1.5002	208		
¼	1.4520	1.4530	00, 10	.0007	
2	1.4148	1.4152	064	.0003	
2	1.3793	1.3803	209	.0007	
1	1.3271	1.3252	401	.0014	
5	1.3092	1.3090	402	.0001	
¼	1.2958	1.2975	066	.0013	
½	1.2832	1.2832	403	.0000	
½	1.2759	1.2752	20, 10	.0006	
1	1.2100	1.2108	00, 12	.0003	
		1.2100	405		
¼	1.1819	1.1832	20, 11	.0011	
½	1.1677	1.1664	406	.0011	
½	1.1207	1.1203	407	.0003	
1	1.0736	1.0734	408	.0002	
1	1.0553	1.0558	06, 10	.0005	
½	1.0277	1.0269	409	.0008	
2	0.9963			Mean |Δ*d*|/*d*=0.0006	
1	0.9763				
2	0.9511				

Unit cell dimensions

The powder diagram bears some resemblance to those of amesite and chamosite, and suggests an hexagonal rather than monoclinic or triclinic cell. Preliminary estimates of the lattice parameters were made as follows: Prominent reflections at 7.26 and 3.63 Å and their higher orders were used to obtain the layer thickness. The b-parameter was obtained by taking the strong 1.535 Å reflection as the 060. The base of the cell was assumed to be centered and ortho-hexagonal in shape, so that $a=b/\sqrt{3}$. Similarities with the powder diagram of amesite (Brindley, Oughton and Youell, 1951), suggested that the unit cell may contain two layers. With these parameters the observed reflections, apart from the closely spaced series, were indexed in a convincing manner. The full range of experimental data was now used to determine as accurately as possible the lattice parameters, the final values of which are as follows:

$$\begin{aligned} a &= b/\sqrt{3} = 5.322 \text{ Å} \\ b &= 9.219 \text{ Å} \\ c &= 2 \times 7.265 = 14.53 \text{ Å}. \end{aligned}$$

The calculated spacings, with their *hkl* indices, are compared with the measured spacings in Table 2. The agreement is everywhere close, particularly for spacings below 2 Å where the agreement is of the order of 0.05%. Many reflections are recorded with the l index an odd number, thereby confirming that the unit cell has a c parameter of 14.53 Å. It must, therefore, contain two structural layers.

The k index, with two exceptions, is 0 or 6. When account is taken of the equivalent ortho-hexagonal indices (see footnote to Table 3), it is seen that k takes the values 0, 3 or 6. Absence of other values for k may be attributed partly to the small structure factors of many of these reflections, but probably arises largely from random layer displacements parallel to b of $nb/3$. The "lines" indexed as 020 and 240 appear to be the terminations of *hk* diffraction bands. A few of the closely spaced lines following the 020 could be indexed as 02l lines, but their interpretation is dealt with later.

Comparison with amesite

The unit cell of amesite (Brindley, Oughton and Youell, 1951) has $a=b/\sqrt{3}$, $b=9.17$ and $c=13.98$ kX. The similarity of the x-ray reflections from the two minerals is shown by the comparison set out in Table 3. The intensities of overlapping lines in the ortho-antigorite diagram are placed in parentheses. The composition of amesite, as indicated by the formula $(Mg_{1.50}Fe_{0.41}{}^{2+}Al_{1.06})(Si_{1.01}Al_{0.99})O_5(OH)_4$, differs somewhat from that of antigorite and in particular it has a higher iron content. When account is taken of these points, the close similarity between the results leaves little doubt that ortho-antigorite and amesite have very similar and probably identical types of structure.

TABLE 3. COMPARISON OF INTENSITIES OF X-RAY POWDER LINES FROM ORTHO-ANTIGORITE, O, AND AMESITE, A

Indices	Intensities		Indices	Intensities	
hkl	*O*	*A*	*hkl*	*O*	*A*
002	10	10	060	8	6
4	10	10	1	0	0
6	1	2*	2	(7)	2
8	½	1*	3	0	0
10	¼	3½*	4	2	2½*
12	(1)	2	5	0	0
			6	¼	0
			7	0	0
			8	0	0
			9	0	0
200	0	0	10	1	2
1	3	2			
2	10	6	400	0	0
3	7	3*	1	1	0
4	(6)	3	2	5	1
5	7	7	3	½	1
6	1	4*	4	0	0
7	4	6	5	(1)	1
8	(7)	6+	6	½	0
9	2	5	7	½	1
10	½	3	8	1	1
11	¼	2	9	½	—

Equivalent indices: $20l \equiv 13l$; $06l \equiv 33l$; $40l \equiv 26l$.

( ) Indicate overlapping ortho-antigorite reflections.

* Overlapping amesite reflections, the observed intensities being shared in the ratio of the calculated intensities.

The closely spaced series of lines

The appearance of this series suggests a long spacing or superlattice such as Aruja (1945) found in his study of single crystals of antigorite. Since the series proceeds from the 020 position, the lines may be of the general type $H20$ or $02L$, the indices H and L corresponding to superlattice parameters along the a and c axes respectively. Both groups of reflections are calculated from an expression of the type

$$(1/d)^2 = (2/b)^2 + (N/S)^2$$

where N stands for H or L, and S is the super-spacing along a or c. Close agreement is obtained with the observed spacings with $S = 43.8$ Å and acceptable agreement is obtained with

$$43.5 < S < 44.0.$$

Table 2 gives the calculated $N20$ or $02N$ spacings for $S=43.8$, with N ranging from 0 to 15.

The nature of the superlattice

Aruja (1945) gave for the a parameter of an antigorite from New Zealand the value $a=43.39=8\times 5.42$. Since his measurements were made on single crystals, it was clear that the superlattice parameter was in the direction of the a-axis and equal to $8a$. The present value for S, 43.8, is so close to Aruja's value that there is little doubt that it arises in a similar way. However, the present value of a is 5.322 Å and the 8-fold value, 42.58 Å, lies outside the acceptable limits of S. Onsager (1952) suggested an undulating structure with a superlattice parameter of $8\frac{1}{2}a$, in which the additional $\frac{1}{2}a$ is a necessary feature of the undulations. With $a=5.322$ Å, $8\frac{1}{2}a=45.24$ Å which is also well outside the limits for S. For the present ortho-antigorite, the ratio $S/a=8.23$ which is near to $8\frac{1}{4}$. Onsager's model is then applicable if we take $S=16\frac{1}{2}a$ and use even values only for the index H.

An alternative hypothesis is that the superlattice is related to the c parameter, a possible interpretation being

$$S = 3c = 3 \times 14.53 = 43.59 \text{ Å}.$$

A superlattice parameter of $3c$ corresponds to a 6-layer structure, a result which recalls the 6-layer structure of nacrite and the 6-layer mica structures. On this basis, it is evident that superlattice reflections with N a multiple of 3 could be indexed as $02l$ reflections with respect to the small cell.

The available data provided by x-ray powder analysis are insufficient to distinguish between these alternative interpretations of the superlattice parameter S. From a purely numerical standpoint $S=3c$ is the simpler interpretation, but in the light of the unambiguous single-crystal data of Aruja it seems very probable that we have observed a similar superlattice with $S=8\frac{1}{4}a$ or $16\frac{1}{2}a$.

A COMPARISON OF ANTIGORITE STRUCTURES

Four closely related structures have now been suggested for antigorite, namely by Aruja (1945), by Ito (1950), by Midgley (1951), and in the present work. Their principal features are compared in Table 4. While the present structure may be referred to hexagonal axes, it seems preferable to retain the ortho-hexagonal cell and indices to facilitate compari-

TABLE 4. STRUCTURE DATA* FOR ANTIGORITE

	1	2	3	4
a	43.39=8×5.42 kX	5.32 Å	5.29 kX	5.322 Å
b	9.238	9.50	9.18	9.219
c	7.265	14.90	7.45	14.53
β	91.40°	101.9°	91.4°	90.0°
Layer thickness	7.262	7.29	7.45	7.265
Space group	—	Cm	$C2/m, Cm, C2$	$C6_3cm$ (?)
Supperlattice parameter	43.39	—	—	43.8
Texture	b=fibre axis	b=fibre axis	Platy	Massive

* The lattice parameters are given in kX and in Å units; values in kX are converted to Å units by multiplying by 1.002.

(1) Aruja (1945), *Mineral. Mag.*, **27,** 65–74.
(2) Ito (1950), "*X*-ray Studies on Polymorphism" (Tokyo), 160–167.
(3) Midgley (1951), *Mineral. Mag.*, **29,** 526–530.
(4) Present paper.

son between these structures. The probable space group for the ortho-antigorite is that determined for amesite, namely $C6_3cm$.

THERMAL ANALYSIS (G. W. B.)

Differential thermal analysis curves of antigorites, Nos. 1, 2, and 3, are shown in Fig. 6 together with a comparison curve for kaolinite from Cornwall. Specimens No. 1 and No. 2 give closely similar curves with endothermic peaks at 685° and 690° C. and exothermic peaks at 825° and 840°C. respectively. Specimen No. 3 gives a somewhat different curve with peaks at 720° C. and 845° C., with a marked arrest in the curve at about 790° C. The results are broadly in agreement with data by Caillère and Hénin (1947) for their α-antigorite, by Kauffman and Dilling (1950), by Kiefer (1951), and by Midgley (1951). Kiefer has shown that the exothermic peak tends to be suppressed in unground materials (the so-called β-antigorite of Caillère and Hénin) and to appear prominently after grinding. The materials used in the present work were lightly ground.

The products obtained after heating in the thermal analysis unit to 1000° C. followed by slow cooling in the furnace have been identified by x-ray analysis as principally olivine. Additional lines in the powder diagram of the product from specimen No. 3 may be due to enstatite. The agreement with the data for enstatite in the *A.S.T.M.* Index is not exact and rests on three lines only.

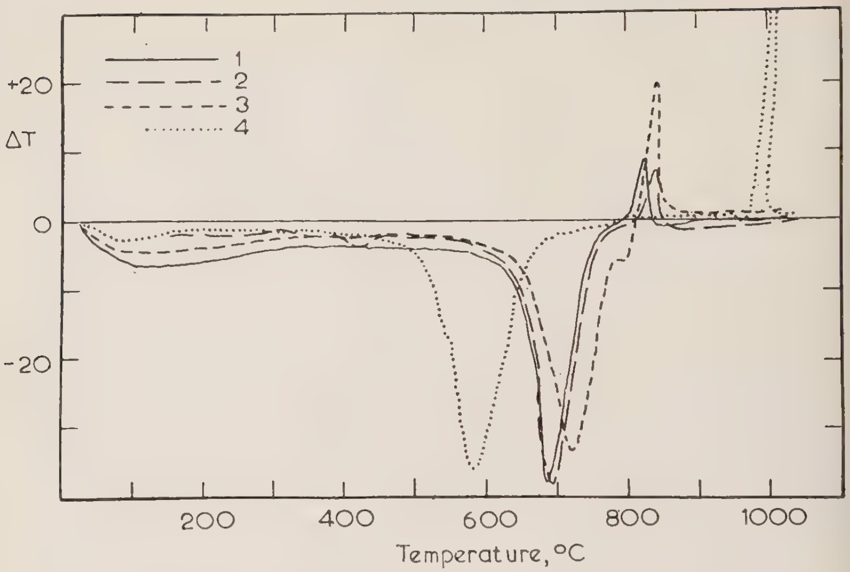

FIG. 6. Differential thermal analysis curves for ortho-antigorites and kaolinite.
———— ortho-antigorite, No. 1; 1.01 gm. specimen.
— — — ortho-antigorite, No. 2; 1.08 gm. specimen.
– – – – – ortho-antigorite, No. 3; 0.89 gm. specimen.
.... kaolinite (Cornwall); 0.36 gm. specimen.

REFERENCES

ARUJA, E. (1945), An x-ray study of the crystal-structure of antigorite: *Mineral. Mag.*, **27**, 65–74.

BRINDLEY, G. W., OUGHTON, B. M., AND YOUELL, R. F. (1951), The crystal structure of amesite and its thermal decomposition: *Acta Cryst.*, **4**, 552–557.

CAILLÈRE, S., AND HÉNIN, S. (1947), Application de l'analyse thermique différentielle à l'étude des argiles des sols: *Ann. Agronom.*, **17**, 23–72.

GRUNER, J. W. (1937), Notes on the structure of serpentines: *Am. Mineral.*, **22**, 97–103.

HEDDLE, M. F. (1924), The Mineralogy of Scotland, vol. II, Henderson and Son, St. Andrews.

ITO, T. (1950), X-ray Studies on Polymorphism, Maruzen and Co. (Tokyo), pp. 160–167.

KAUFFMAN, JR., A. J., AND DILLING, E. D. (1950), Differential thermal curves of certain hydrous and anhydrous minerals, with a description of the apparatus used: *Econ. Geol.*, **45**, 222–244.

KIEFER, C. (1951), Contribution à l'étude de la stabilité et de la classification des minéraux phylliteux. Thesis (Paris).

MIDGLEY, H. G. (1951), A serpentine mineral from . . . Cornwall: *Mineral. Mag.*, **29**, 526–530.

ONSAGER, L. (1952), See report of a conference on structures of silicate minerals, by K. Robinson and E. R. S. Shaw (1952): *J. Sci. Instr.*, **3**, 281–282.

PHILLIPS, F. C. (1927), The serpentines and associated rocks and minerals of the Shetland Islands: *Quart J. Geol. Soc.*, **83**, 622–652.

SELFRIDGE, G. C. (1936), An x-ray and optical investigation of the serpentine minerals: *Am. Mineral.*, **21**, 463–503.

Manuscript received June 9, 1953

DETERMINATION OF THE CRYSTAL STRUCTURE OF NEPHELINE

M. J. BUERGER, GILBERT E. KLEIN,† AND GABRIELLE DONNAY,§
Massachusetts Institute of Technology, Cambridge, Massachusetts.

ABSTRACT

The structure of nepheline has been determined by the implication method followed by Fourier synthesis. The dense atoms were all located with the aid of Harker syntheses and implication maps. With these atoms located, the oxygen atoms were found by successive electron density projections. Nepheline is based upon the tridymite framework in which all silicon atoms in tetrahedra pointing toward one end of the c axis are replaced by aluminum atoms, and the valence is compensated by adding alkali atoms to the voids. The true formula of nepheline is not $NaAlSiO_4$, but $KNa_3Al_4Si_4O_{16}$. The alkali atoms occur in two sets, one set occupying a larger void than the other. The smaller void is produced by a twisting of the tridymite framework about the sets of three-fold axes. The oxygen atoms on the three-fold axes are probably in motion, at least at elevated temperatures, and make contact with the surrounding sodium atoms only part of the time.

INTRODUCTION

There have been several x-ray diffraction investigations of the mineral nepheline.[1–7] All except Gossner and Jaeger agree on assigning nepheline to the space group $P6_3$ (C_6^6) with 8 $NaAlSiO_4$ per hexagonal cell. The structure has not been determined, although Schiebold[4,5] suggested that it is based upon a tridymite structure in which Al atoms were substituted for half the total Si atoms, Na being added to the voids of the structure to balance valances. This suggestion was accepted by Bannister and Hey[6] as well as by Nowacki.[7]

---

† Now at Oak Ridge National Laboratory, Oak Ridge, Tennessee.

§ Now with the U. S. Geological Survey, Washington, D. C.

[1] Gottfried, C., Über die Struktur des Nephelins: *Zeits. Krist.*, **65**, 100–109 (1926).

[2] Gossner, B., Über die Symmetrie von Nephelin: *Central. Mineral., etc.*, **A-1927**, 150–158 (1927).

[3] Jaeger, F. M., Westbrink, H. G. K., and van Melle, F. A., The structure of artificial ultramarines; a relation between these and the minerals haüynite, noselite, sodalite, lazurite, and nepheline: *Verslag. Akad. Wetenschappen Amsterdam*, **36**, 29–47 (1927).

[4] Schiebold, E., Zur Struktur von Nephelin und Analcim: *Naturwiss.*, **18**, 705–706 (1930).

[5] Schiebold, E., Über die Isomorphie der Feldspatmineralien: *Neues Jahrb. Min., etc. Bl. Bd.* **64A**, esp. pp. 312–313 (1931).

[6] Bannister, F. A., and Hey, M. H., A chemical, optical, and x-ray study of nepheline and kaliophilite: *Mineral. Mag.*, **22**, 569–608 (1931).

[7] Nowacki, W., Beziehungen zwischen $K[AlSiO_4]$ (Tief-Kaliophilit), $Ba[Al_2O_4]$, $K[LiSO_4]$, $Na[AlSiO_4]$ (Nephelin) und $[Si_2O_4]$ (β-Tridymit): *Naturwiss.*, **30**, 471–472 (1942).

We have carried out an investigation of the crystal structure of nepheline. This has proved to be a tedious task, largely because the structure lacks inversion centers and has little symmetry, and because the cell is moderately large.

We are indebted to Dr. Frederick H. Pough, formerly of the American Museum of Natural History, for a gift of several small nepheline crystals from Monte Somma, Vesuvius. Our first problem was the choice of a suitable small untwinned crystal. Since the point-group symmetry of nepheline is merely 6, it tends to twin into composites whose *c* axis Weissenberg photographs have diffraction symmetry 6*mm*. A number of crystals which were suitable from point of size proved to be twinned in this way, so that we finally used a somewhat irregular, small fragment broken from a larger crystal which gave diffraction symmetry 6. We believe the fragment we used to be untwinned, since we tested the diffraction symmetry in several stages as the fragment was being reduced in dimensions and we failed to find any increase in contrast in the relative intensities of reflections which would be identical in intensity in a twin

CELL AND SPACE-GROUP STUDY

Preliminary Weissenberg photographs showed that the diffraction symbol of nepheline is $6/mP6_3/-$. This embraces the two space groups $P6_3$ and $P6_3/m$. Since nepheline is known not to have a symmetry plane normal to the hexagonal axis, the space group is uniquely fixed as $P6_3$. This confirms the space group determination of earlier investigators.

The preliminary Weissenberg study provided the following cell dimensions:

$$a = 10.01 \text{ Å}$$
$$c = 8.405$$

This cell contains 8 $NaAlSiO_4$. The atoms must be accommodated by the following sets of equipoints in space group $P6_3$:

2(*a*) along the 6_3 screw,
2(*b*) along the trigonal rotation axes,
6(*c*) in the general position.

INTENSITY DETERMINATION

For the subsequent quantitative work on the structure of nepheline it was necessary to have reasonably reliable estimates of the intensities of the spectra. For this purpose we used the Dawton[8] process modified so as to take advantage of the characteristics of photographic materials available in America.

---

[8] Dawton, Ralph H. V. M., The integration of large numbers of *x*-ray crystal reflections: *Proc. Phys. Soc.*, **50**, 919–925 (1938).

For the determination of the nepheline intensities, we used Weissenberg photographs made with crystal-monochromatized copper radiation. The Lorentz and polarization factors were allowed for in a manner described elsewhere.[9] Absorption was assumed to be negligible because of the small size of the crystal, and no further allowances were made in transforming intensities to $|F_{hkl}|$.

General Outline of the Structure Determination

Before proceeding to a detailed discussion of the determination of the crystal structure, the general plan of the structure determination is given here in bare outline.

The two possible Harker syntheses were first prepared and these were studied with the aid of their implication diagrams. By combining two mplication diagrams, all the dense (metal) atoms could be located in xy projection.

Assuming that the diffraction phases were dominated by these metals alone, a preliminary electron density projection $\rho(xy)$ was prepared which showed not only the metals already located, but other dense areas, attributed to oxygen locations. The total number of oxygen atoms was distributed over these dense areas, and from their x,y coordinates, a new set of phases was computed and a new electron density projection $\rho(xy)$ was prepared. By repeating this procedure a number of times, an electron density projection was finally attained which required no further change n phases. The rough x,y projection of the structure was now known.

In order to determine the z parameters, several one-dimensional Patterson syntheses of the Harker type, namely $P(x_1y_1z)$, were prepared with strategic horizontal components x_1, y_1. A study of these made it evident that the nepheline structure is indeed based upon a stuffed tridymite framework, as suggested by Schiebold. The deviations of the z parameters from the ideal tridymite parameters could then be determined.

We were then in a position to prepare the electron density projection $\rho(xz)$ from the $h0l$ reflections and their phases computed with the aid of the parameters determined as above. This projection was refined by repetition until the last projection required no further phase changes.

The rough structure of nepheline was now determined. The structure type and approximate parameters were known, but the exact parameters were not known because of the lack of resolution in the electron density projection. To refine the structure requires the preparation of electron density sections. These are exceedingly tedious to prepare, because the phases of all reflections must be computed, and because each section in-

---

[9] Buerger, M. J., and Klein, Gilbert E., Correction of x-ray diffraction intensities for Lorentz and polarization factors: *J. Appl. Phys.*, **16**, 408–418 (1945).

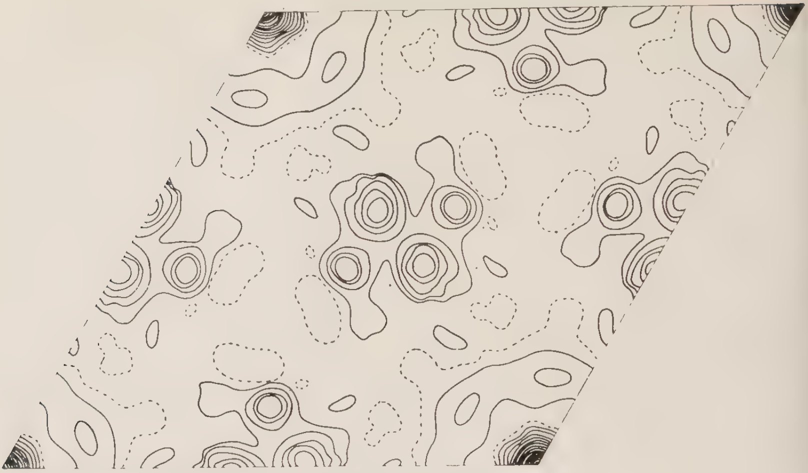

FIG. 1. Nepheline, $P(xy0)$.

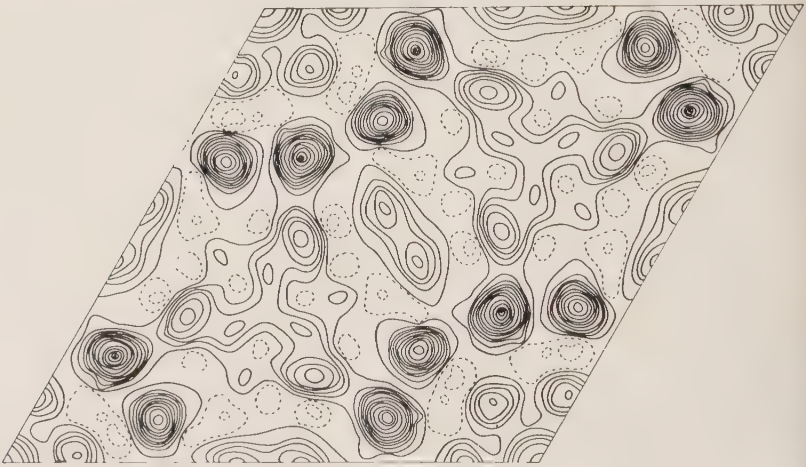

FIG. 2. Nepheline, $P(xy\frac{1}{2})$, also implication map $I6(xy\frac{1}{2})$.

volves four separate two-dimensional Fourier syntheses for the preparation of the coefficients of the two-dimensional syntheses.

HARKER SYNTHESES AND IMPLICATION MAPS

The symmetry of nepheline permits making Harker sections[10] of the Patterson[11,12] function on two levels, namely $P(xy0)$ and $P(xy\frac{1}{2})$. These were accordingly prepared from the available $\left|F_{hkl}\right|^2$ values. The Harker sections are shown in Figs. 1 and 2, respectively. The first of these can be transformed into only one *implication* map,[13] namely $I3(xy0)$

while the second can be transformed into two implication maps, namely $I6(xy\frac{1}{2})$ and $I2(xy\frac{1}{2})$. These implication maps locate the dense atoms with the following ambiguities:

	Implication	*Ambiguity factor*
Fig. 2	$I6(xy\frac{1}{2})$	1
Fig. 3	$I3(xy0)$	3
	$I2(xy\frac{1}{2})$	4

The first and second of these were prepared and are shown in Figs. 2 and 3, respectively. The first implication, having an ambiguity factor of unity (i.e., no ambiguity) is identical with the Harker synthesis $P(xy\frac{1}{2})$.

Implication $I6(xy\frac{1}{2})$ contains satellitic peaks which are valuable in authenticating genuine Harker peaks (i.e., peaks due to "interaction" between symmetrically equivalent atoms). Each authentic Harker peak is accompanied by a satellitic peak of half the height of the Harker peak and located at twice its vector distance from the origin.[14] The authentic

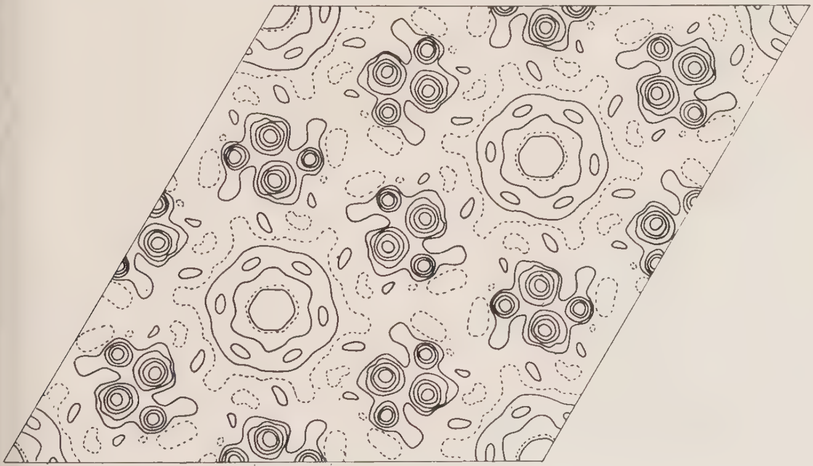

Fig. 3. Nepheline, $I3(xy0)$.

---

[10] Harker, David, The application of the three-dimensional Patterson method and the rystal structure of proustite, Ag_3AsS_3, and pyrargyrite, Ag_3SbS_3: *J. Chem. Phys.*, **4,** 81–390 (1936).

[11] Patterson, A. L., A Fourier series method for the determination of the components of nteratomic distances in crystals: *Phys. Rev.*, **46,** 372–376 (1934).

[12] Patterson, A. L., A direct method for the determination of the components of inter-tomic distances in crystals: *Zeits. Krist.* **(A)90,** 517–542 (1935).

[13] Buerger, M. J., The interpretation of Harker syntheses: *J. Appl. Phys.*, **17,** 579–595 1946).

[14] Reference 13, page 586.

peaks and their satellitic peaks are the following:

Peak	*Satellitic peak*	*Attributed to*
0, 0	0, 0	Na_1
0, .43	0, .86	Na_2
.09, .33	.18, .66	Si_2+Al_2

The atoms to which the peaks are to be attributed can be interpreted upon the assumption that nepheline is based upon a tridymite framework, Fig. 4. The other major peak of $I6(xy\frac{1}{2})$ is without an implication satellite and is therefore a non-Harker peak due to pairs of non-equivalent atoms.

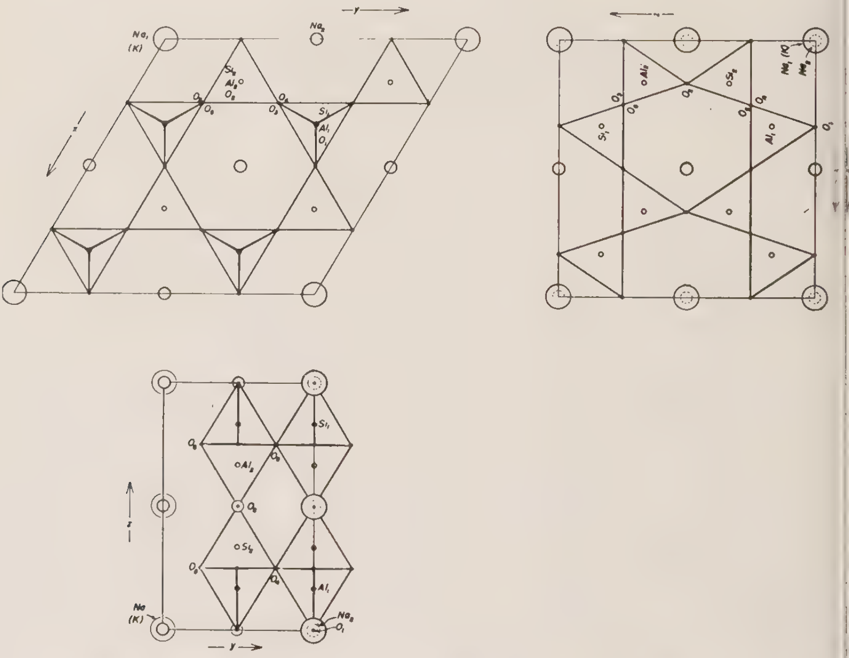

FIG. 4. Plan and elevation of ideal high tridymite referred to nepheline cell and symmetry, showing labeling of representative atoms.

On superposing the implication $I3(xy0)$ on the implication $I6(xy\frac{1}{2})$ the authenticated peaks of the latter, just listed, are found to coincide with certain of the peaks of the former. This further affirms the correctness of the positions of the atoms already located. The atoms listed in the foregoing table account for 8 Na, 6 Al, and 6 Si, out of a total of 8 Na, 8 Al, 8 Si, and 32 O. This leaves 2 Al, 2 Si, and 32 O still to be placed. Since 2 and 32 are not divisible by 6, the 2 Al, 2 Si, and at least 2 of the O's must be on either the 6-fold screw or the 3-fold axis. The former is already occupied by Na_1 atoms, which take substantially all the available space. This requires 2 Al_1, 2 Si_1, and 2 O_1, to be on the 3-fold axis. The implication peak for atoms in this location is peculiarly blurred. This is attributed to motion of the atoms so that they occupy the axis only statistically.

DETERMINATION OF *xy* COORDINATES OF THE OXYGEN ATOMS

The reasoning discussed in the last section provides the *xy* parameters of the atoms of nepheline as shown in column *B* of Table 1. The Na_1 atoms were interpreted as K atoms since the number corresponds closely to the amount of potassium in nepheline analyses.[7] The locations of thirty oxygens are unknown.

TABLE 1. STAGES IN THE DETERMINATION OF THE PARAMETERS OF THE ATOMS IN THE NEPHELINE STRUCTURE

Atom	Coordinates of atoms						
	A Deduced from implication diagrams		*B* From implication diagrams plus equipoint reasoning		*C* From electron-density projection, $\rho(xy)$		*D* From lines through the Patterson function
	x	y	x	y	x	y	z
2 Na_1 (=2 K)	0	0	0	0	0	0	0
6 Na_2	0	0.43	0	0.43	0.01	0.43	0.00
2 Al_1			$\frac{1}{3}$	$\frac{2}{3}$	$\frac{1}{3}$	$\frac{2}{3}$	0.18
6 Al_2	0.09	0.33	0.09	0.33	0.09	0.33	0.67
2 Si_1			$\frac{1}{3}$	$\frac{2}{3}$	$\frac{1}{3}$	$\frac{2}{3}$	0.82
6 Si_2	0.09	0.33	0.09	0.33	0.09	0.33	0.33
2 O_1			$\frac{1}{3}$	$\frac{2}{3}$	$\frac{1}{3}$	$\frac{2}{3}$	
6 O_2			?		0.02	0.33	
6 O_3			?		0.18	0.50	
6 O_4			?		0.17	0.53	
6 O_5			?		0.23	0.28	
6 O_6			?		0.23	0.28	

In order to locate the remaining thirty oxygen atoms it was assumed that the phases of the $hk \cdot 0$ reflections are determined, to first approximation, by the locations of the known atoms. (Fortunately, the *xy* projection of the space group $P6_3$ is centrosymmetrical, so the phases must be 0 or π, i.e., the signs of the *F*'s are either positive or negative.) With this assumption, the phases of all $hk \cdot 0$ reflections were computed, and using these phases, an electron density projection, $\rho(xy)$ was prepared by the Fourier summation

$$\rho(xy) = \frac{1}{A} \sum_h \sum_k F_{hk0} \cos 2\pi(hx + ky).$$

The summation was carried out with the aid of the Patterson-Tunell method.[15] This electron density projection not only returned the atoms which were used to determine the phases, but also revealed other regions of high electron density which were interpreted to be due to the remaining oxygen atoms.

Oxygen atoms O_2, O_3, O_4, O_5, and O_6 were then distributed on these regions of high electron density and, with these new atoms located, the phases were computed again. Several sign changes occurred due to the new oxygen atoms. Utilizing these new signs, the electron density projection was again computed. The second approximation showed the new oxygen locations more clearly. Using this second electron density projection, a new set of signs for the F_{hk0}'s was computed, and the electron density projection again prepared.

This process was repeated until finally an electron density map was obtained, Fig. 5, which gave oyxgen atoms in locations such that the signs of the computed F's were the same as those which had been used for the preparation of the final electron density projection. The final set of parameters so determined is given in column C of Table 1.

This set of parameters provides a fairly good explanation of the $hk\cdot 0$ intensities. The discrepancy factor,

$$R = \frac{\sum \left| \, |F_{\text{observed}}| - |F_{\text{calculated}}| \, \right|}{\sum |F_{\text{observed}}|},$$

has a value of 0.34 for the $hk\cdot 0$; reflections, with no allowance being made for a temperature factor. That the parameters do not provide a perfect explanation of the intensities is to be expected because the parameters are approximate. This is partly because pairs of atoms which overlap in projection are unresolved, or poorly resolved, and consequently the location of each of the pair is in doubt. This kind of overlap is most annoying in derivative structure,[16] and nepheline is a derivative structure of tridymite in which the following sets of atoms overlap (see Fig. 4): Al_1, Si_1, O_1; Al_2, Si_2, O_2; O_3, O_4; O_5, O_6. The atoms in these sets are unresolved, and their parameters as determined above are probably subject to small but annoying errors.

A second reason why the discrepancy factor, R, is high, is that Al_1, Si_1, and O_1 are assumed to occupy the 2-fold equipoint, namely the 3-fold axis. There are several reasons which suggest that this is not the precise distribution of these atoms. These reasons are noted at the end of this paper.

---

[15] Patterson, A. L., and Tunell, George, A method for the summation of the Fourier series used in the x-ray analysis of crystal structures: *Am. Mineral*, **27,** 655–679 (1942).

[16] Buerger, M. J., Derivative crystal structures: *J. Chem. Phys.*, **15,** 1–16 (1947).

DETERMINATION OF Z PARAMETERS

In order to determine the z parameters of the atoms, several lines through the three-dimensional Patterson function parallel to the c axis were computed. These lines were chosen to have vector components in the XY plane, equal to the vector from the K atom at the origin to each of the metal peaks. The following syntheses were made:

	to determine z parameters of
$P\left(\frac{2}{3}\ \frac{1}{3}\ z\right)$	Al_1, Si_1, O_1
$P(0.09, 0.33\ z)$	Al_2, Si_2, O_2
$P(0, 0.43, z)$	Na_2

The interpretation of these syntheses was again made difficult because nepheline is a derivative structure of tridymite. Nevertheless, prominent peaks were found on these lines which were consistent with the vector distances from K to the several metal atoms expected from a derivative structure of ideal high tridymite. The z coordinates so found as listed in Table 2.

PROJECTIONS OF THE STRUCTURE INVOLVING z

In order to refine the structure as much as possible, the phases of the 62 observed $h0{\cdot}l$ reflections were computed based upon the x, y param-

TABLE 2

	Idealized derivative of tridymite z	Nepheline, as determined from one-dimensional Harker syntheses z
Na_1 (=K)	0	0
Na_2	0	0.00
Al_1	$\frac{1}{6}$	0.18
Al_2	$\frac{2}{3}$	0.67
Si_1	$\frac{5}{6}$	0.82
Si_2	$\frac{1}{3}$	0.33
O_1	0	—
O_2	$\frac{1}{2}$	—
O_3	$\frac{3}{4}$	—
O_4	$\frac{1}{4}$	—
O_5	$\frac{1}{4}$	—
O_6	$\frac{3}{4}$	—

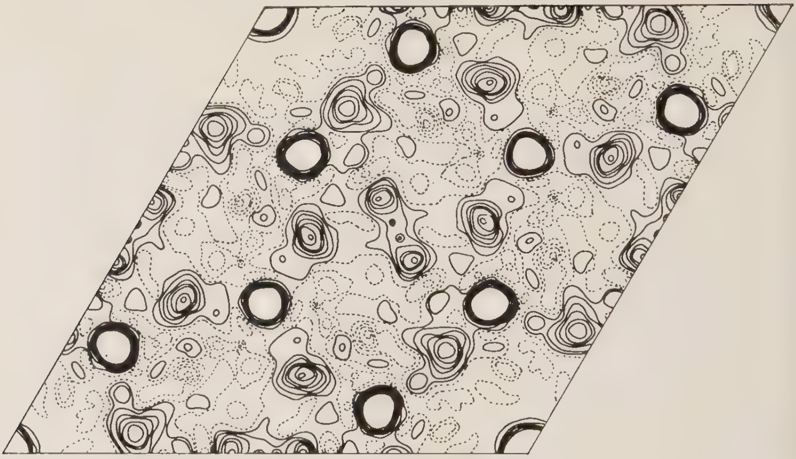

FIG. 5. Nepheline, $\rho(xy)$. The interpretation of this electron density projection is shown below in Fig. 6.

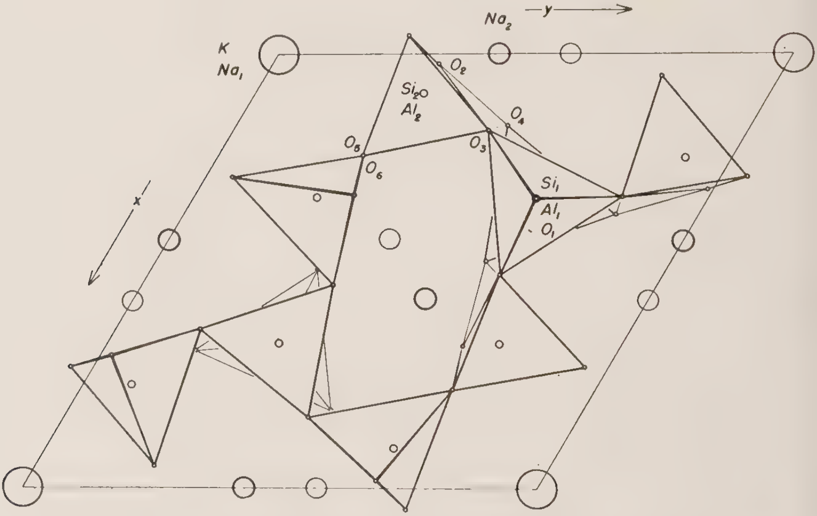

FIG. 6. Interpretation of electron density map, shown above in Fig. 5, giving designations of representative atoms.

eters determined from the $\rho(xy)$ electron density projection, and the z parameters determined from the one-dimensional Harker syntheses, plus idealized values of the z parameter for the oxygen atoms. This provided data for the determination of the electron density $\rho(xz)$ as projected parallel to a_2 onto the plane $(1\bar{2}10)$. Such a preliminary projection was prepared, and this was subsequently refined exactly as in the case of the

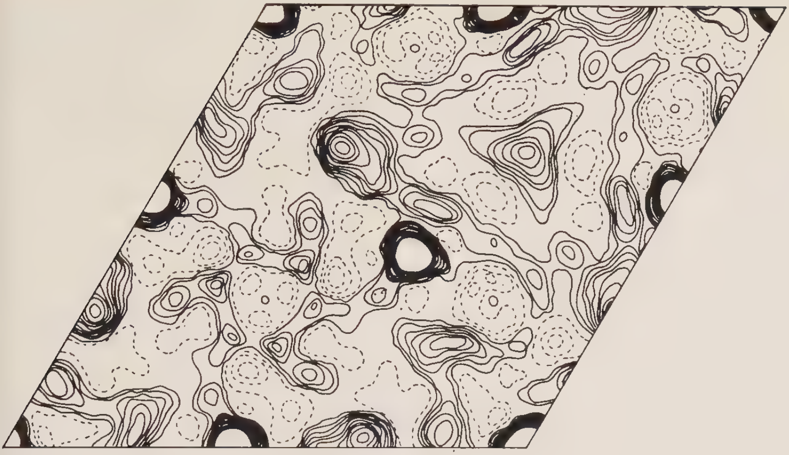

FIG. 7. Nepheline, electron density section $\rho(xy0)$.

$\rho(xy)$ projection. Unfortunately, in the $\rho(xz)$ projection no peaks corresponding to the oxygen atoms O_3, O_4, O_5, or O_6 are sufficiently resolved to permit an adequate determination of the parameters. Finally the $hh \cdot l$ reflections were used to prepare a Fourier synthesis of the electron density projected parallel to [210] onto plane (100).

FINAL ROUGH PARAMETERS

The final parameters of tridymite as determined by the study just described, are listed in Table 3. These parameters should be regarded as approximate and subject to further refinement for the following reasons:

(1) The parameters of the atoms other than K and Na are determined from electron density projections in which there is overlapping of atoms.

(2) There are reasons for believing that the Al_1, Si_1, and O_1 atoms, which were taken to occupy the equipoint 2 (*b*) because of the numbers of atoms involved, do not actually occupy this equipoint in a strict sense.

(*a*) The fundamental evidence for this is that the peak corresponding with this position on the implication map, Fig. 2, is not as high as that corresponding to the similar group of atoms, Al_2, Si_2, and O_2. This means that the density at the position accepted for Al_1, Si_1, O_1, is not as high as at the position for Al_2, Si_2, O_2. The density deficiency can be accounted for if one or more of these atoms, supposed to occupy the three-fold axis, do so only statistically, i.e., if they are actually off the axis but assume positions with time whose averages lie on the three-fold axis.

(*b*) We made an electron density section $\rho(xy0)$, Fig. 7. In this section the oxygen on the three-fold axis is more diffuse than the other oxygens in the section, and, furthermore, it is smeared so as to look like the projection of a three-bladed propeller, with the blades directed halfway between pairs of the three surrounding sodium atoms. We interpret this to mean that the oxygen is not actually on the three-fold axis,

TABLE 3. COORDINATES OF ATOMS IN NEPHELINE, COMPARED WITH THOSE OF IDEAL HIGH TRIDYMITE

Atom	Coordinates in ideal high tridymite			Coordinates in nepheline			Remarks
	x	y	z	x	y	z	
2 Na_1 (=K)	0	0	0	0	0	0	(void in tridymite
2 Al_1	$\frac{1}{3}$	$\frac{2}{3}$	$\frac{1}{6}$ (.167)	$\frac{1}{3}$	$\frac{2}{3}$	.18	
2 Si_1	$\frac{1}{3}$	$\frac{2}{3}$	$\frac{5}{6}$ (.833)	$\frac{1}{3}$	$\frac{2}{3}$	.82	
2 O_3	$\frac{1}{3}$	$\frac{2}{3}$	0	$\frac{1}{3}$	$\frac{2}{3}$	.00	
6 Na_2	0	$\frac{1}{2}$	0	$.00_8$	$.43_2$	.00	(void in tridymite
6 Al_2	$\frac{1}{6}$ (.167)	$\frac{1}{3}$ (.333)	$\frac{2}{3}$ (.667)	$.09_2$	$.33_0$	.67	
6 Si_2	$\frac{1}{6}$ (.167)	$\frac{1}{3}$ (.333)	$\frac{1}{3}$ (.333)	$.09_2$	$.33_0$	.33	
6 O_2	$\frac{1}{6}$ (.167)	$\frac{1}{3}$ (.333)	$\frac{1}{2}$ (.500)	$.02_0$	$.33_0$	.50	
6 O_3	$\frac{1}{4}$ (.250)	$\frac{1}{2}$ (.500)	$\frac{3}{4}$ (.750)	.18	.50	~.75	
6 O_4	$\frac{1}{4}$ (.250)	$\frac{1}{2}$ (.500)	$\frac{1}{4}$ (.250)	.17	.53	~.25	
6 O_5	$\frac{1}{4}$ (.250)	$\frac{1}{4}$ (.250)	$\frac{1}{4}$ (.250)	.23	.28	~.25	
6 O_6	$\frac{1}{4}$ (.250)	$\frac{1}{4}$ (.250)	$\frac{3}{4}$ (.750)	.23	.28	~.75	

except statistically. At any one time, it is coordinating with only two of the thre surrounding sodium atoms, and this connection varies with time. In other words the oxygen atom is undergoing a kind of a rotation or gyration about the three-fold axis.

(*c*) The gyration of the oxygen atom about the three-fold axis is not unexpected. It is well-known that there is a bend in the alignment of the three atoms Si-O-Si in the silica structures, and it should be expected in the alignment Al-O-Si also. This bent alignment cannot occupy a three-fold axis, unless it does so statistically. The meaning of the three-fold axis is then that the bend takes three equivalent positions with time.

The gyration of the oxygen atom about the three-fold axis must be accompanied by a gyration of the silicon and aluminum atoms about the same axis. This would explain why the peak on this axis in the implication map $I6(xy\frac{1}{2})$ is low and propeller-shaped. Unless such deviation occurs for the silicon and aluminum atoms there is no explanation for the character of this Harker projection.

It is interesting to note that only 2 of the 32 oxygen atoms of the cell appear to gyrate. It is known that nepheline undergoes a reconstructive transformation to an isometric form, carnegieite at 1248° C. Presumably, at this temperature, all the oxygen atoms begin to gyrate with consequent increase in symmetry.

DISCUSSION

In spite of the fact that only rough parameters for the nepheline structure can be given at this time, a number of interesting mineralogical conclusions can be drawn. In the first place, as Schiebold predicted[4], the structure of nepheline is indeed based upon a generalization of the tridymite structure. If all the silica tetrahedra in the tridymite structure which point, say, up, are replaced by alumina tetrahedra, and if the largest voids are stuffed with alkali atoms to balance the loss of positive charge due to this replacement, a nepheline-like structure results. The replacement of silicon by aluminum gives the hexagonal axis a polar character which is absent in the parent tridymite structure.

The space requirements of the alkali atoms give rise to two interesting features. In the first place, sodium is too small to occupy the voids and at the same time coordinate with the surrounding oxygen atoms. The tridymite framework therefore collapses somewhat by a twisting motion centered about the three-fold axes of the space group, and in so doing clutches the sodium atoms in the general position. This twisting collapse of the framework robs the idealized framework of its vertical symmetry planes, and therefore nepheline has no symmetry planes whatever (the horizontal plane having been lost by replacings ilicon with aluminum, as discussed above). Since the twisting motion may be either right or left, a right-or left-handed nepheline results.

The twisting motion does not significantly reduce the size of the void occupied by the alkali atom in the special position on the 6_3 axis to the same extent that it reduces the general-position void, just discussed. As a consequence, a large symmetrical hole capable of supplying a nine-fold oxygen coordination remains to be occupied by two of the eight alkali atoms of the cell. Since potassium is better suited by size to occupy such a void, it does so, provided that the nepheline crystallizes from an environment capable of supplying potassium. For this reason, natural nepheline invariably has this site substanitally filled with potassium instead of sodium. The symmetry of the nepheline structure requires that the alkali atoms be divided into two sets of 2 and 6. These two sets may, but need not, be occupied by the same chemical element, and, indeed, in general, K and Na may be expected to separate into the 2-fold and 6-fold sites respectively. Pure sodium nepheline is formed only when there is no potassium present in the environment of crystallization. Thus the ideal chemical formula for nepheline is not the currently quoted $NaAlSiO_4$, but rather $KNa_3Al_4SiO_{16}$. The analyses collected by Bannister and Hey[6] confirm this view. Since calcium is about the right size to proxy for potassium, it also may be found in the 2-fold site, thus either reducing the amount of the 2-fold alkali metal, or increasing the aluminum:silicon ratio.

Further Investigation in Progress

The members of the group which undertook the original investigation of the nepheline structure, as discussed in this paper, now reside in three different locations. The refinement of the structure is now being continued at the Crystallographic Laboratory of the Massachusetts Institute of Technology by M. J. Buerger and Theodor Han. It is expected that this refinement process will reveal more exact coordinates of the atoms, and specifically provide detailed information on the coordinates of the sodium atoms and the possible gyration of the atoms in the neighborhood of the three-fold axis.

Acknowledgment

This investigation was generously supported by the Owens-Illinois Glass Company.

Manuscript received Oct. 2, 1953

MORDENITE AS AN ALTERATION PRODUCT OF A PITCHSTONE GLASS

P. G. Harris* and G. W. Brindley†

Abstract

A hydration product formed from the glass of a pitchstone (Judd's No. 1 dike, Isle of Arran, Scotland) is identified by *x*-ray analysis as the zeolite mordenite. Chemical analysis shows some removal of alkalis in the change from the original glass to the final product.

Introduction (P.G.H.)

In the course of an investigation by one of us (P.G.H.) of the composition of co-existing phases from glassy rocks, a pitchstone, labelled as Judd's No. 1 dike, Tomore Shore, Arran, Scotland, in the collections of the Geology Department of the University of Leeds, was separated with heavy liquids into its components. A fraction lighter than the glassy groundmass and derived from it by hydration, is shown by *x*-ray analysis to be the zeolite mordenite.

Although alteration of volcanic glasses generally results in the formation of clay minerals such as montmorillonite (Hauser and Reynolds, 1939), nontronite (Allen and Scheid, 1946) and sericite (Norton, 1941), other products have been described, notably zeolites. Coombs (1952) describes the alteration of the more acid glasses in a series of andesite tuffs to laumontite, with some evidence of an intermediate stage of alteration to heulandite or analcime. Analcime of similar origin has been described by Ross (1941).

Occurrence (P.G.H.)

The parent material is a quartz-fayalite pitchstone occurring as a dike in the shore at Tomore, Arran, Scotland (see Tyrrell, 1928). The glassy groundmass is more abundant than usual (96% of the volume of the rock) and is comparatively free from crystallites which form long green needles. The alteration product (about 1% of the rock) is not identifiable in thin section. As a powder, it is readily distinguished from the clear glass, being of a buff yellow color, due perhaps to ferric oxide. Between crossed nicols the yellow color masks any optical characteristics. Most of the separated grains contain both glass and the alteration product, while the crystallites occur in both phases.

---

* Formerly Geology Department, University of Leeds, England; now at Dominion Laboratory, Wellington, New Zealand.

† Formerly Physics Department, University of Leeds, England; now Research Professor of Mineral Sciences, Pennsylvania State University, Pa., U.S.A.

CHEMICAL ANALYSES (P.G.H.)

Chemical analyses of the pure glass and of the alteration product are given in Table 1.

TABLE 1. CHEMICAL ANALYSES OF A PITCHSTONE GLASS AND OF ITS HYDRATION PRODUCT

	1	2
SiO_2	73.41	68.24
TiO_2	0.14	0.11
Al_2O_3	11.65	11.04
Fe_2O_3	0.28	1.74
FeO	1.09	n.d.
MnO	0.03	n.d.
MgO	0.02	0.23
CaO	0.75	1.31
Na_2O	3.63	3.19
K_2O	3.63	2.45
H_2O+	4.76	6.59
H_2O-	0.10	5.02
P_2O_5	0.03	n.d.
Others	0.28*	n.d.*
	99.80	99.92

1. Glass from pitchstone, Judd's No. 1 Dike, Tomore, Arran. Analyst, P.G.H.
2. Alteration product of glass. Analyst P.G.H.

* In analysis 1, this item represents the difference between $H_2O\pm$ by the Penfield method and the total loss on ignition corrected for oxidation of FeO. It may be due to other volatiles in the glass, such as non-carbonate CO_2. In analysis 2, any such component is included in H_2O+, which is based on the loss on ignition.

The analysis of the mordenite fraction may be recalculated in conformity with the theoretical mordenite structure $(Ca,Na_2,K_2)_4Al_8Si_{40}O_{96}\cdot 28H_2O$.

Disregarding the titanium and iron oxide contents, the analysis gives a formula $(Mg_{0.2}Ca_{0.8}Na_{3.7}K_{1.8})Al_{7.7}Si_{40.3}O_{96}\cdot 22.9H_2O$, which is reasonably close when the possible presence of unaltered glass is considered.

The analyses show that the main changes are small removals of alkalis and a considerable increase of water content. These resemble the changes accompanying palagonitization (cf. Hoppe, 1941). The latter, however, differ in several respects.

(*a*) The alteration products of palagonitization are amorphous and give no *x*-ray powder diagram.

(*b*) Palagonitization is accompanied by a greater decrease in alkalis and in CaO content.

(*c*) Palagonite forms from basaltic glass. More acid glasses seem to result in zeolites or clays.

(*d*) The water content is significantly different.

Palagonite, even after washing with acetone, during its separation, still retains more than 10% of H_2O- (unpublished analysis), while analyses by Hoppe and others have H_2O- contents as high as 14%. This content of H_2O- may be as diagnostic a feature of a true palagonite as the amorphous character shown by *x*-rays.

X-RAY EXAMINATION (G.W.B.)

X-ray powder diagrams of the alteration product were taken with 19 cm. and 20 cm. diameter cameras and filtered CoK_α radiation ($\lambda = 1.79020$ Å). The material is well crystallized and gives fifty or more easily measurable lines. Diagrams taken with a stationary powder specimen show smooth and continuous diffraction lines without obvious broadening; the crystal size is, therefore, estimated to be about 1–5μ. The high order reflections do not resolve the K_α doublet.

The occurrence of a long spacing, about 13.7 Å, is noteworthy but the material is clearly not a clay mineral of any known type. Data for a number of zeolites in the *A.S.T.M.* index show some similarities with the observed results, but no satisfactory agreement was obtained. A search through crystallographic literature showed that Waymouth, Thornely and Taylor (1938) had measured the cell dimensions of a mordenite from Aros, Isle of Mull, Scotland (British Museum Cat. No. 47614) which were consistent with a (110) spacing of 13.6 Å, but no powder data are given in their paper. Powder data for natural and synthetic mordenites have been recorded by Barrer (1948) which confirm the long spacing of about 13.5 Å and show general agreement with the present data.

To confirm the identification of the alteration product as mordenite, a specimen from the same sample of Mull mordenite which Taylor and his colleagues had previously studied was obtained from the British Museum with the assistance of Dr. G. F. Claringbull. Its powder diagram is more clearly defined than that of the alteration product and many weak lines are recorded which are not measureable from the alteration product, but in all essential respects the diagrams are identical. While the powder diagrams of the zeolites as a group tend to have certain similarities, which in fact were sufficient to suggest that the alteration product was probably a zeolite, the differences between them are such that no doubt attaches to the identification of the alteration product as mordenite.

Table 2 compares the powder data for the Mull mordenite (B.M. 47614), for the alteration product from Arran, and a natural mordenite examined by Barrer; the intensities listed by Barrer are transcribed to a numerical basis as follows *s*,10; *ms*,8; *m*,6; *mw*,4; *w*,2; *vw*,1; *vvw*,$\frac{1}{2}$.

TABLE 2. *X*-RAY POWDER DATA FOR MORDENITE

1				2		3	
$d_{obs.}$	I	$d_{calc.}$	hkl	$d_{obs.}$	I	$d_{obs.}$	I
13.7	5	13.58	110	13.7	6	13.5	10
9.10	9	9.080	200	9.10	9	8.66	10
6.61	9	6.592	111	6.60	8	6.54	10
6.38	4	6.383	130	6.39	5	—	
6.10	5	6.070	021	6.09	2		
5.79	5	5.801	201	5.80	5	5.72	6
5.03	1	5.046	221	—		—	
4.871	2	4.872	131	—		—	
4.525	8	4.527	330	4.535	8	4.50	10
4.143	3	4.150	420	—		—	
3.999	9	3.991	150	4.008	9	3.99	10
3.842	6	3.836	241	3.854	4	—	
3.763	2	3.770	002	3.778	4	—	
3.624	1	3.633	112	—		—	
3.563	1	3.576	510	—		—	
3.483	10	3.482	202	3.486	10	—	
3.393	9	3.409	060	3.398	9	3.40	10
3.308	1	3.296	222	3.315	1	—	
3.222	10	3.206	530	3.224	9	3.15	10
3.103	2	3.096	441	—		—	
2.946	2	2.950	531	—		—	
2.896	6	2.900	402	2.899	7	2.90	8
2.743	1	2.741	152	2.746	1	—	
2.700	3	2.709	621	2.707	1	2.70	1
2.639	1	2.632	370	—		—	
2.560	4	2.564	461	2.569	3	—	
2.522	5	2.523	442	2.534	5	2.50	6
2.465	2			2.469	1	—	
2.437	2			2.440	1	2.43	2
2.343	2			—		—	
2.299	1			—		—	
2.275	1			—		—	
2.228	2			2.234	½	—	
2.162	2			2.165	½	—	
2.123	1			2.124	½	—	
2.047	4			2.051	3	2.02	4
2.019	4			2.019	½	—	
1.998	4			2.001	½	—	
1.953	4			1.955	4	1.94	4
1.936	1			—		—	
1.917	2			1.922	1	—	
1.883	4			1.884	4	—	
1.865	1			1.857	2	1.855	4
1.850	1						
1.813	3			—		—	
1.795	3			1.795	2	1.785	4
1.765	1			—		—	
1.738	1			1.746	½?	—	
1.720	2			1.722	½	—	
1.698	1			1.697	½	1.687	½
1.686	2			—		—	
1.665	2			—		—	
1.647	1			—		1.646	½
1.622	2			1.621	½	—	
1.597	3			1.597	1	1.585	1
1.546	2			1.548	1	—	
1.527	3			1.528	2	1.527	2

TABLE 2 (Cont'd)

1				2		3	
$d_{\text{obs.}}$	I	$d_{\text{calc.}}$	hkl	$d_{\text{obs.}}$	I	$d_{\text{obs.}}$	I
1.508	1				—	—	
1.492	½			—		—	
1.478	1			1.479	½	1.477	2
1.445	3			1.447	2	1.439	6
1.426	2			1.427	½	—	
1.412	3			1.413	½	1.415	½
1.401	2			1.401	½	—	
1.386	3			1.387	1	—	
1.375	3			1.376	½	1.376	1
1.354	1			—		—	
1.334	1			—		—	
1.318	1			—		1.311	½
1.300	2*b*			1.301	½	1.291	1
1.278	1			1.281	½	—	
1.266	2			1.267	1	1.262	1
1.245	2			1.245	½	1.238	1
1.228	1			1.228	½	—	
1.217	1			1.216	1	1.211	½
1.209	½			—		—	
1.1955	½			—		—	
1.1856	1			1.1858	½	1.180	½
1.1731	½			—		—	
1.1568	½			1.1587	½	1.154	½
1.1445	1			1.1447	½	—	
1.1285	2			1.1285	½	1.125	½
1.1061	½			—		1.095	½
1.0642	½						
1.0217	½						
0.9802	½						
0.9580	½						
0.9386	½						
0.9324	½						
0.9288	½						
0.9192	½						
0.9171	½						
9.9128	½						
0.9098	½						
0.9047	½						

1. Mordenite from Aros, Isle of Mull, Scotland (B.M. Cat. No. 47614).
2. Alteration product from Tomore, Isle of Arran, Scotland.
3. Natural mordenite, examined by Barrer (1948).

b signifies broad line.

The powder data have been indexed for the lower order reflections and the orthorhombic cell dimensions derived therefrom are given in Table 3 where they are compared with those given by Taylor and his colleagues.

CONCLUSIONS

The chemical and x-ray data combine to show that the alteration product is the zeolite mordenite. The close similarity in chemical composition of the original glass and the resultant zeolite suggests that the nature

TABLE 3. UNIT CELL DIMENSIONS OF MORDENITE

	1	2
a	18.25±0.1 Å	18.16+0.10Å
b	20.35±0.1	20.45±0.10
c	7.50±0.05	7.54±0.05

1. Data by Waymouth, Thornely and Taylor (1938).
2. Present data: camera diameter 19 cm. filtered CoK_α radiation, $\lambda = 1.79020$ Å.

of the zeolites which form by alteration of glasses, depends largely on the composition of the original material.

Zeolites, as intermediate products in the breakdown of volcanic material, may be more common than is thought.

Finally, we wish to thank Dr. G. F. Claringbull and the Trustees of the British Museum for Natural History for the specimen of mordenite from Mull. One of us (P.G.H.) is indebted to Professor W. Q. Kennedy, in whose laboratories the chemical work was done, to the D.S.I.R., New Zealand, for a National Research Scholarship, and to Dr. D. S. Coombs, University of Otago, for his advice.

REFERENCES

ALLEN, V. T., AND SCHEID, V. E. (1946), Nontronite in the Columbia River Region: *Am. Mineral.*, **31,** 294–312.

BARRER, R. M. (1948), Syntheses and reactions of mordenite: *J. Chem. Soc.*, 2158–2163.

COOMBS, D. S. (1952), Cell size, optical properties and chemical composition of laumontite and leonhardite: *Am. Mineral.*, **37,** 812–830.

HAUSER, E. A., AND REYNOLDS, H. H. (1939), Alteration of glasses to montmorillonite: *Am. Mineral.*, **24,** 590–597.

HOPPE, H. J. (1941), Untersuchungen an Palagonituffen und über ihre Bildungsbedingungen: *Chem. der Erde*, **13,** 484–514.

NORTON, F. H. (1941), Hydrothermal formation of clay minerals in the laboratory, Part II: *Am. Mineral.*, **26,** 1–17.

ROSS, C. S. (1941), Sedimentary analcite: *Am. Mineral.*, **26,** 627–629.

TYRRELL, G. W. (1928), Geology of Arran: *Mem. Geol. Survey, Scotland.*

WAYMOUTH, C., THORNELY, P. C., AND TAYLOR, W. H. (1938), An *x*-ray examination of mordenite (ptilolite): *Mineral. Mag.*, **25,** 212–216.

Manuscript received July 16, 1953

WISAKSONITE IS METAMICT URANOAN THORITE

C. Osborne Hutton, *Stanford University, California.*

Abstract

On very slender evidence Druif has given the name wisaksonite to green isotropic euhedra of what he believed to be a new mineral species. Work just completed leads one to suggest that this name be abandoned since the results of *x*-ray diffraction and other determinations have shown that the mineral in question is undoubtedly metamict uranoan thorite.

Data Reported by Druif

During a study of a heavy mineral residue from a sand sample from Pekoeringan River in Central Celebes, Druif (1948) observed crystals of what he believed to be a new mineral—wisaksonite.[1] In an attempt to identify the green more or less isotropic euhedra, Druif considered in turn the properties of zircon, malacon, and other altered forms of zircon, vesuvianite, nageite,[2] and oyamalite, and in his opinion the properties of his wisaksonite were distinct from those of the minerals just listed. Undoubtedly he was justified in setting aside identification as true or normal zircon on the basis of the isotropy of the mineral, but less so with malacon since he was under the misapprehension that a green color is never found in the latter.

It might be pertinent to list the properties of wisaksonite as determined or estimated by Druif, since it was on the basis of these that he felt justified in adding a new mineral to the literature:

1. Tetragonal morphology; with considerable similarities to zircon.
2. Green color.
3. Brittleness; that is, apparently, in contra-distinction to what is found for zircon.
4. Refractive index is in excess of 1.80.
5. Isotropic or nearly so, with positive elongation parallel to the longer dimension (*c* axis) of those crystals with faint but perceptible birefringence.
6. Intergrown with zircon.
7. Density about 4.
8. The properties of naegite and wisaksonite were considered to have certain features in common; however, Druif believed that absence of cassiterite in the heavy mineral assemblage that included wisaksonite excluded this possibility, apparently because cassiterite is always associated with naegite in Japan!

It will be noted that Druif has not made available any exact physical datum for his green mineral although such is usually deemed necessary as a basis on which to establish satisfactorily any new mineral species.

---

[1] In his review of Druif's paper, Fleischer (1948, p. 787) expressed the opinion that the mineral in question was "low-density zircon."

[2] Naegite was described by Shibata and Kimura (1923, pp. 3–5) as similar to zircon except that rare earths, thorium, and uranium were important constituents. In the analysis of oyamalite on the other hand, Kimura (1925, pp. 84–85) reported both phosphorus and rare earths in addition to zirconia and silica. Both of these minerals require further study.

The description of wisaksonite interested the present writer to the extent that an enquiry was sent to Dr. Druif asking if some material might be made available for further study, but unfortunately the letter was returned stamped "unknown." However, through the splendid efforts of Dr. F. A. van Baren of the Tropical Institute, Amsterdam, the writer was able to secure a Canada balsam preparation that contained eight minute crystals of wisaksonite. These crystals, none of which exceeded 0.2 mm. in length, were freed from their mounting medium by treatment with xylol; of these, four were set aside for determination of refractive index and specific gravity, and four were segregated for *x*-ray study.

X-RAY INVESTIGATION

Employing a camera of 57.3 mm. diameter and copper radiatio filtered by nickel, three rotation photographs were taken. A euhedr crystal that measured 0.2 by 0.04 mm. was set up on the end of a glas fiber in such a manner that the longer axis, the *c* crystallographic direction, was made the axis of rotation. After an exposure of ten hours a 30 KV. and 20 MA. the crystal yielded only diffuse powder haloes wit no evidence of orientation. This crystal was now unmounted, heated fo four hours at 860° C., being placed in a fully heated electric furnace after air-quenching the crystal was mounted as before. A ten-hour exposure now yielded faint but well defined lines, namely those of the face-centered cubic lattice of ThO_2; there were no traces of lines due t any crystalline modification of SiO_2.

Once again the same crystal was unmounted but this time it was heated to 1250° C. for four hours, and then remounted. In this instance the ThO_2 pattern was barely detectable and instead lines corresponding to those of the monoclinic modification of thorium silicate—huttonite— were strongly evident. A second crystal was heated for four hours at 860° C., but this time an exposure of twenty-five hours produced lines of better density for evaluation purposes. This film has been measured and the spacings (Table 1) compare satisfactorily with those of ThO although the length of the cell-side, $a = 5.52$ Å, is distinctly smaller than that for pure ThO_2 (*vide* Arnott, 1950, pp. 388–390); this departure is possibly due to replacement of thorium by smaller uranium atoms.

PHYSICAL PROPERTIES

The results of the determinations of refractive indices on heated and unheated crystals may be summed as follows:

TABLE 1. POWDER PATTERNS OF THORITES HEATED TO 860° C. FOR FOUR HOURS. Cu/Ni radiation with $\lambda = 1.5418$ Å

A			B	
$d_{obs.}$	I^*	*hkl*	$d_{obs.}$	I^*
3.16	10	111	3.23	10
2.75	6	200	2.78	6
1.95	7	220	1.96	7
1.66	8	311	1.69	8
1.60	2	222	1.62	2
1.38	2	400	1.40	2
1.27	4	331	1.29	4
1.23	4	420	1.26	3
1.13	4	422	1.15	3
1.06	4	511 333	1.08	3
0.98	v. faint	440	0.99	v. faint
0.93	2	531	0.95	2
0.92	2	600 442	0.94	2
0.87	1	620	0.885	1

A. "Wisaksonite," Celebes.
B. Uranoan thorite, mouth of Año Nuevo Creek, San Mateo Co., California.
* Intensities were determined visually.

1. Clear green isotropic crystal: $n = 1.88 \pm 0.005$.
2. Green crystal with some opacity due to alteration or inclusions: $n = 1.795$.
3. Green crystal, slightly more translucent than crystal 2: $n = 1.82$.
4. A clear green isotropic crystal with semi-translucent patches ($n = 1.87$ but with some parts of the crystal with $n = 1.84$ *ca.*) became opaque after heating to 860° C for four hours. On fracturing, however, the grain was found to be quite heterogeneous and to be composed of deep reddish-brown areas, with $n = 1.79$, that are intimately associated with dark greenish-brown material with $n = 1.835$; the latter material was quite translucent, whereas the former was heavily clouded with minute dust-like particles. It is suggested that the dark greenish-brown phase is derived from the clear portions of the original crystal and the reddish-brown portions from the altered or inclusion-bearing zones. It is not known whether these two phases taken separately would give distinct *x*-ray patterns but it does remind one of a similar situation found in priorite (Hutton, 1953, p. 7). Heating of wisaksonite, that is uranoan thorite, in this instance appears to bring about a lowering of refractive index.

It is interesting to note that thorites of initially low refractive index exhibit a distinct rise in the value of that property when heated (Pabst, 1952). The rise of refractive index in one instance and the decrease in another might be due in some measure to the water content of the metamict minerals. Thorites with initially a high percentage of water could be expected to show an increase of refractive index with dehydration, for certainly, originally anhydrous metamict thorites, the California type, show the reverse effect.

The minute quantity of the mineral did not permit determination of specific gravity; however, each of four crystals was found to sink quite rapidly in a melt of thallous formate and thallous malonate. Therefore all that one is prepared to say in this connection is that the specific gravity of each of these crystals is considerably in excess of 5.

URANIUM CONTENT

Two euhedra of wisaksonite, a grain of monazite ($U_3O_8 = 1.23$ per cent), and a crystal of metamict uranoan thorite ($UO_2 = 6.95$ per cent), each of the two latter had particle sizes approximately equivalent to that of wisaksonite, were placed on the surface of a thin film of solidified $Na_2CO_3 \cdot NaF$ fusion mixture. The film was heated carefully to permit momentary melting and then quickly cooled. When this preparation was obliquely illuminated with short-wave ultraviolet light and viewed with a binocular microscope a fluorescent halo was noted surrounding wisaksonite, and this was comparable in intensity to that surrounding the thorite with a known content of uranium, and yet distinctly stronger than that adjoining monazite.

SUMMARY

The *x*-ray study of crystals of a mineral named wisaksonite by Druif leaves no doubt that this mineral is metamict thorite. The physical data, although not conclusive when taken alone, are in support of this opinion. Finally a not inconsiderable content of uranium would seem to be present. Therefore the mineral is considered to be metamict uranoan thorite, and it is suggested that the name wisaksonite be deleted from mineralogical literature.

ACKNOWLEDGMENT

I wish to express my indebtedness to Dr. F. A. van Baren of the Tropical Institute, Amsterdam, for his kindness in securing the material that formed the basis of this study.

REFERENCES

ARNOTT, R. J. (1950), *X*-ray diffraction data on some radioactive oxide minerals: *Am. Mineral.*, **35**, nos. 5–6, 386–400.

DRUIF, J. H. (1948), On the occurrence of a new mineral species in the deposits of the River Pekoeringan, District Masamba, Celebes: *Meded. van het Algemeen Proefstation voor de Landbouw, Buitenzorg, Java, No.* **69**, pp. 3–8.

FLEISCHER, M. (1948), Wisaksonite, review of the paper by Druif: *Am. Mineral.*, **33,** nos. 11–12, 787.

HUTTON, C. O. (1952), Accessory mineral studies of some California beach sands: *U. S. Atomic Energy Commission, RMO*—**981,** 3–112.

——— (1953), Annual technical report for April 1, 1952 to March 31, 1953: *U. S. Atomic Energy Commission, RME*—**3045,** 3–9.

KIMURA, K. (1952), The chemical investigations of Japanese minerals containing rarer elements. Part V. Analyses of fergusonite of Hagata, hagatalite of Hagata, and oyamalite of Oyama, Iyo Province: *Jap. Jour. Chem.*, **2,** no. 3, 81–85.

PABST, A. (1952), The metamict state: *Am. Mineral.*, **37,** 137–157.

SHIBATA, Y., AND KIMURA, K. (1923), The chemical investigation of Japanese minerals containing rarer elements. Part I. Analyses of fergusonite, naegite, and monazite of Naegi, Mino Province: *Jap. Jour. Chem.*, **2,** no. 1, 1–6.

Manuscript received Sept. 14, 1953

NOTES AND NEWS

ORTHO-ANTIGORITE AND THE TETRAHEDRAL CONFIGURATION OF HYDROXYL IONS

DUNCAN MCCONNELL, *College of Engineering, The Ohio State University, Columbus, Ohio.*

Elsewhere in this issue of *The American Mineralogist* Brindley and von Knorring (1954) have described a new variety of antigorite from the Shetland Islands. The purpose of my remarks is to show the applicability of my hypothesis for the structure of montmorillonite (McConnell, 1950) to the unusual chemical composition of their "antigorite No. 2."

As their results indicate, difficulties arise from an attempt to obtain a reasonable structural formula by conventional methods of calculation on the basis $O+OH=9$ atoms. The (OH) content calculates to be 4.66 instead of 4.00 atoms and there is a deficiency for the two silicon positions even after all aluminum and iron atoms have been allocated to these positions. In another attempt to resolve this enigma, they calculated approximately 20 per cent of the total magnesium as though it occurred in the form of a brucite impurity. They do not present a strong justification for this procedure and indicate that the powder diffraction lines and the *d.t.a.* curve did not show the presence of brucite.

One can proceed on the assumption that brucite is *not* present and obtain satisfactory results. It is merely necessary to assume that the unit of structure contains 9 large anions (O+OH) and to use the chemical analysis as a basis for deciding how many of these anions involve hydrogen. The methods for accomplishing this calculation are described in detail elsewhere (McConnell, 1951). Briefly, it is merely necessary to

TABLE 1. CALCULATION OF THE STRUCTURAL FORMULA OF ANTIGORITE NO. 2
(Analyst: O. von Knorring)

Oxides	Weight Per Cents	Molecular Ratios	Cation Ratios	Ratios of Cationic Charges	Cationic Charges $\Sigma=18$	Cations in Unit Cell (oxygen=9)
SiO_2	38.40	.6394	.6394	2.5576	6.996	1.749
Al_2O_3	0.10	.0010	.0020	.0060	.016	.005
Fe_2O_3	3.42	.0214	.0428	.1284	.351	.117
MnO	0.05	.0007	.0007	.0014	.004	.002
MgO	41.91	1.0394	1.0394	2.0788	5.686	2.846
H_2O+	15.03	.8343	1.6686	1.8084	4.947	4.947*
H_2O-	1.26	.0699	.1398			
	100.17				18.000	

* $4.95 \doteq 4.00+4(0.24)$.

balance the electrical charges of all cations (including hydrogen) in their proper ratios against the 18 negative charges of the 9 oxygen atoms. The calculations are given in Table 1 and can be cast in the form of a structural formula, thus:

$$(Mg, Fe, Mn)_{2.97}[Si_{1.75}Al_{0.01}(H_4)_{0.24}]O_5(OH)_{4.00}.$$

Here it has been assumed that tetrahedral hydroxyl groups substitute for silica tetrahedra. The agreement is exceedingly good inasmuch as the octahedral cations differ from the theoretical requirement by merely one per cent if other constituents exactly match the requirements. To obtain this agreement it is necessary to assume that all of the water shown in von Knorring's analysis is essential to the structure.

These results offer further indirect evidence of the occurrence of hydrogens in substitution for silicon (i.e. tetrahedral hydroxyls) in structures of this general type. Although this hypothesis was originally presented in order to explain certain data for montmorillonite, it has been admitted (McConnell, 1951, p. 188) that the occurrence need not be restricted to montmorillonite.

I am indebted to Brindley and von Knorring for an opportunity to examine their results prior to publication and for their interest and cooperation.

REFERENCES

Brindley, G. W., and von Knorring, O. (1954), A new variety of antigorite (orthoantigorite) from Unst, Shetland Islands: *Am. Mineral.*, **39**, 794–804.

McConnell, Duncan (1950), The crystal chemistry of montmorillonite: *Am. Mineral.*, **35**, 166–172.

——— (1951), The crystal chemistry of montmorillonite. II—Calculation of the structural formula: *Clay Minerals Bull.*, **1**, 179–188.

ALLANITE PEGMATITE, SAN GABRIEL MOUNTAINS, LOS ANGELES COUNTY, CALIFORNIA*

George J. Neuerburg, *U. S. Geological Survey,*
Pasadena, California.

This short note is intended to bring to the attention of mineral collectors an intriguing locality for pegmatite minerals.

Pre-Cretaceous pegmatites, generally of simple mineralogy and of small size, abound in and near the anorthosite massif in the San Gabriel Mountains, Los Angeles County, California. One of these pegmatites is exceptional for its content of well-formed crystals of allanite, apatite, beryl, uranothorite, and zircon. This pegmatite occurs in a norite facies of the anorthosite massif, in a small land-slide-scar amphitheater on the south wall of the South Fork of Pacoima Canyon. A well-maintained Forest Service road is in the bottom of the canyon. The pegmatite is in the northwest portion of the 6-minute Trail Canyon quadrangle and is in a land-grant area in what would be Sec. 17, T. 3 N., R. 13 W., S.B.B.M.[1]

---

* Publication authorized by the Director, U. S. Geological Survey.

The pegmatite consists of a number of irregular bulging and fingering lenses along a single, nearly horizontal plane. For the most part the pegmatite consists of very coarse grained subhedral light pinkish-brown perthite and white quartz, containing a few large blobs of quartz and partly replaced by anastomosing veinlets of quartz; no zonal structure is evident. In three places swarms of parallel biotite crystals transect both quartz and perthite; individual biotite crystals measure in cross section from ½ inch by 6 inches to 6 inches by 5 feet. Small amounts of fine grained anhedral oligoclase are present. Red perthite pods and lenses containing the rare minerals are irregularly distributed throughout the pegmatite. A few of these pods occur in the metamorphic aureole. The total volume of red perthite in the pegmatite is probably less than 10 per cent, and in the metamorphic aureole the volume is less than 1 per cent. Both ends of the pegmatite are fault contacts.

The wallrock of the pegmatite is a medium-grained uralitized ilmenite-bearing norite of the kind assigned to the border facies of the San Gabriel anorthosite massif (Higgs, 1950). Locally, a banded structure, striking N. 65° W. and dipping 80° S., is present in the norite. A discontinuous sheath of metamorphosed norite surrounds the several pegmatite lenses. This sheath is remarkable for its grain size. Grains in places average 1 foot in maximum dimension; they vary irregularly from less than ⅛ inch to 2 feet or more. The metamorphic rock consists largely of hornblende, oligoclase, and biotite. Microscopic constituents include garnet, sphene, zircon, carbonate, allanite, and ilmenite. Generally the crystals of the metamorphic aureole are anhedral, but euhedral prisms of hornblende and euhedral tablets of biotite are common in the coarser-grained parts.

The metamorphic rock is sharply bounded against the pegmatite in most places, but locally it grades into the pegmatite within the space of a few feet by changes in the mineral proportions and in texture. Gradational contacts are most common in the western end of the pegmatite, which is exceptionally rich in oligoclase, hornblende, and biotite. This part of the pegmatite contains remarkably large euhedral hornblende crystals, no one of which is fully exposed. One crystal has exposed dimensions of 3½ feet by 4 feet by 1 foot and two others are larger than 2 feet by 3 feet by 1 foot. The weight of the largest crystal (computed on the basis of the exposed dimensions) is at least 850 pounds; each of the three large crystals might actually weigh in excess of half a ton.

---

[1] I originally mistakenly reported the locality to Murdoch (Murdoch and Webb, 1952' p. 34) as being in section 6.

A 2-foot-thick vein of granular carbonate, seemingly pure, is present in the eastern end of the pegmatite. A swarm of fine-grained hornblende-biotite-plagioclase lamprophyre dikes, 1 to 4 feet thick, transects both the norite and the pegmatite, and parallels the pegmatite. The dikes contain small pegmatitic pods; they also show a banded structure reflected by small variations in grain size. No contact effects are apparent.

The presence of a discontinuous sheath of very coarse grained hornblende-(and/or biotite)-oligoclase metamorphic rock seems to be a common feature of the many small pegmatite bodies in this region. Many of these pegmatites can be seen along the road in the upper reaches of the North Fork of Pacoima Canyon. Short lenses of this metamorphic rock are also present in the norite away from known bodies of pegmatite. Such lenses are common in the vicinity of the allanite pegmatite, where a few contain small pods of red perthite, very rarely with zircon and allanite.

The minerals of special interest are found in the small pods of red perthite in the pegmatite and less commonly in the metamorphic aureole. Allanite, apatite, beryl, and zircon occur together. Except for the smallest of the zircon crystals, crystals of all four minerals are finely and pervasively fractured. All four are found in well-formed euhedral crystals, uncommonly slightly replaced by quartz. Associated with them are small amounts of anhedral oligoclase.

Allanite occurs in thin tabular black crystals, ranging from $\frac{1}{2}$ inch by $\frac{1}{4}$ inch by $\frac{1}{8}$ inch to a known maximum of $\frac{1}{2}$ inch by 10 inches by 18 inches. In thin section, the color is light to dark pinkish orange. It is the most abundant of the unusual minerals. No alterations are evident and powder photographs show very slight evidence of metamict structure (J. Berman, personal communication).

Zircon crystals occur as doubly terminated square prisms that range in size from those barely visible with a hand lens to a known maximum of 1 inch by 8 inches. Despite the intense fracturing, no evidence of alteration or metamictization is apparent. The color ranges, according to the extent of fracturing, from purplish white to deep purple. Under the short-wave ultraviolet lamp the crystals fluoresce a deep orange yellow with little variation in the intensity of the color.

Beryl is rare; most of it occurs in one small part of the pegmatite. The crystals, highly fractured, are short prisms, which have a maximum size of $\frac{1}{4}$ inch by $\frac{1}{2}$ inch. They are colored a very light greenish white.

Microscopic crystals of apatite are present in the pegmatite and in all of the surrounding rocks. Apatite is most abundant, and its crystals—

stubby prisms up to $\frac{1}{4}$ inch —are largest in association with allanite and zircon, in both of which it is a common inclusion.

Uranothorite was found in only one small red perthite-quartz pod, where it apparently occurs without allanite, apatite, beryl, or zircon. The largest crystal found measures $\frac{1}{2}$ inch by $1\frac{1}{2}$ inches. It is dark brown with many streaks and irregular masses of orange color. It is apparently completely metamict. Unlike allanite, apatite, beryl, and zircon, the uranothorite crystals are not fractured. Aureoles of the apple-green fluorescence common to secondary uranium minerals surround the crystals; the fluorescing substance is not visible in ordinary light. The identification as uranothorite was kindly checked by Joseph Murdoch.

References

Higgs, D. V. (1950), Anorthosite and related rocks of the western San Gabriel Mountains, Southern California: *Ph.D. thesis*, Univ. Calif., Los Angeles.

Murdoch, J., and Webb, R. W. (1952), Minerals of California: *California Div. Mines, Bull.* **136,** 1952 supplement.

A MODIFICATION OF THE CHAYES POINT COUNTER STAGE

Melvin A. Rosenfeld, *Magnolia Petroleum Company, Dallas, Texas.*

In 1949 Chayes described a point counter suitable for attachment to a standard Spencer or Bausch and Lomb petrographic mechanical stage. In this device leaf springs mounted on the stage engage click wheels mounted on the horizontal and vertical shafts to furnish the point stops used in count analysis (see Chayes' description).

The present modification, designed and made by Mr. W. F. Mueller,* is an improvement over the original in three respects:

1. Lighter clicking action requiring less work for each point change.
2. Positive centering at each point (*i.e.*, no play when the plunger is engaged in the click wheel).
3. A simple arrangement for disengagement of the point-counting device so that the stage may be used for ordinary traversing.

The point counter stage is shown in Fig. 1; a cross-sectional diagram of the working mechanism is presented in Fig. 2. A pointed plunger (*a*) is mounted in a housing (*b*) containing a light coil spring. The plunger point is sharper than the indentation in the leaf spring of the original design; this permits deeper and narrower slots in the click wheel (*c*) and thus reduces play. The shoulders of the slots are slightly rounded as is

---

* Supervisor, Instrument Shop, Magnolia Petroleum Co., Field Research Laboratories. The stage is a Bausch and Lomb model 31-59-54.

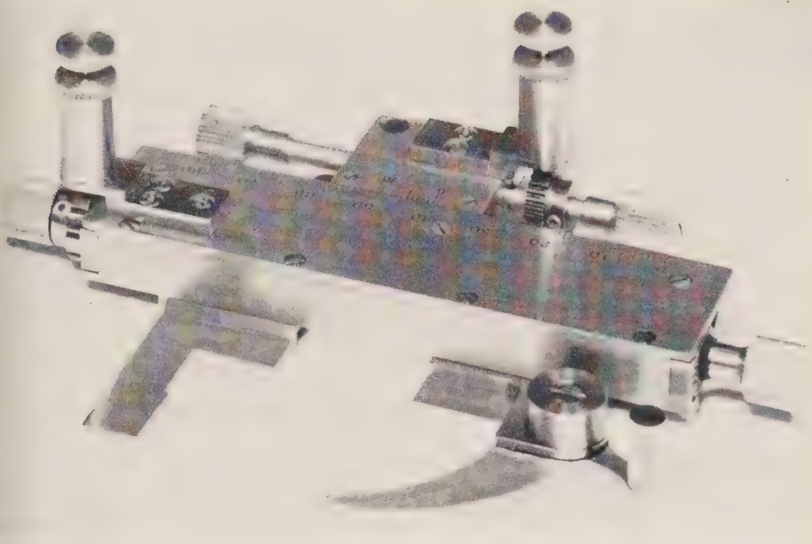

FIG. 1. The point counter stage.

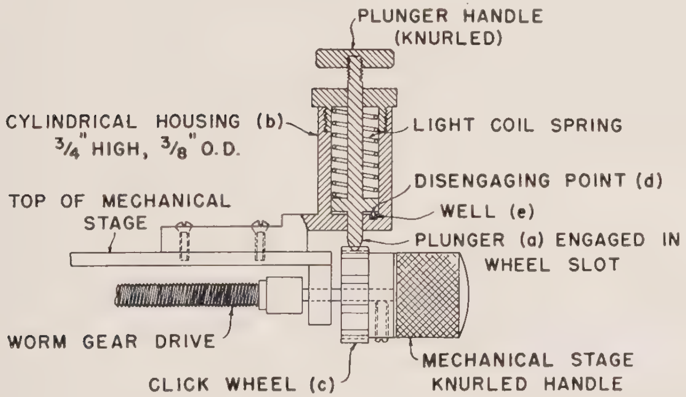

FIG. 2. Cross sectional view of point counter.

the plunger point; these features make for a light touch in operation. The purely vertical motion of the plunger eliminates horizontal drag and the consequent "settling" encountered when a leaf spring is used. The stage may be used for non-point traversing by retracting the disengaging point (*d*) from its well (*e*); this pulls the plunger point clear of the click wheel.

The stage described herein has 0.25 mm. spacing for horizontal traverses and 0.5 mm. spacing for vertical traverses. It is somewhat more expensive to make than the leaf-spring type but the advantages gained in the ease and speed of operation will soon offset the original cost.

REFERENCE

CHAYES, F., A simple point counter for thin-section analysis: *Am. Mineral.*, **34,** 1–12 (1949).

THE CHEMICAL FORMULA OF CLARKEITE[1]

JOHN W. GRUNER, *University of Minnesota, Minneapolis, Minnesota.*

The mineral clarkeite in pegmatites from Spruce Pine, N. C., when first described by Ross, Henderson, and Posnjak (1931) was given the formula $RO \cdot 3UO_3 \cdot 3H_2O$. In their paper (p. 214) they state: "Alkalies are the essential RO constituents and sodium predominates over potassium. Analysis No. 1 is closely similar to No. 2, the only essential difference being a slight excess of calcium in the former. The quantity of lead and alkalies is nearly the same in the two analyses and the uranium contents agree very closely. Both analyses contain only small quantities of iron and aluminum oxides but there is a difference in the water content." They also give a diagram of an x-ray picture which agrees with one obtained by Frondel of the same material. A film (Table 1) obtained by us from a sample received from the Trace Elements Laboratory of the U. S. Geological Survey which is labelled *TE-1334* also agrees within reasonable limits.

The author was able to synthesize clarkeite in a number of experiments (Gruner, 1952) from uranyl nitrate solutions and $CaCO_3$ or CaO. While the x-ray patterns unquestionably agreed with the natural material there was reason to suspect judging by the orange buff color that the synthetic clarkeite was mechanically mixed with uranyl hydroxides and possibly uranyl silicates and carbonates. Therefore, no analyses were made of these synthetics. It is evident, however, that no Pb, Na, or other alkalies are contaminants in them, as they were absent in the experiments.

Among our older chemical reagents we found a container with orange buff $Na_2U_2O_7$ (Uransaures Natrium) made by A. C. F. Kahlbaum, Berlin. This material gave a very faint x-ray pattern of clarkeite. But on heating, the pattern improved and reached near-perfection after heating the sample five hours over the Bunsen burner at low redness. Table 1 gives the spacings and intensities of its lines compared with those of the natural and synthetic products. From the similarity of them and the

---

[1] Research done in connection with a contract of Division of Raw Materials of the U. S. Atomic Energy Commission.

Table 1. *X*-Ray Data for Clarkeite and $Na_2U_2O_7$
Unfiltered Fe-radiation, Camera Radius = 57.3 mm.

Clarkeite U.S.G.S. *TE 1334*		Clarkeite Synthetic *JO-155*		$Na_2U_2O_7$ Heated to Low Redness *A-105a*	
d	*I*	*d*	*I*	*d*	*I*
5.75	5	5.76	5	5.80	7
3.66	f	3.66	f	3.66	1
3.48	f	3.46	1	3.49	1
3.339	6	3.337	6	3.323	8
3.156	10	3.138	10	3.156	10
2.920	2	2.912	4	2.945	3
2.683	5	2.662	5	2.689	4
2.435	1	2.423	4	2.444	2
2.164	1	2.152	1	2.165	1
		2.012	1	2.029	2b
1.960	6	1.942	7	1.965	7
1.845	5b	1.838	8	1.856	8
				1.694	2
1.673	1	1.674	1		
		1.650	1	1.668	2
1.633	4	1.619	3	1.635	6
1.550	f	1.556	2b	1.557	2b
1.526	f	1.517	1	1.535	2
				1.484	1
		1.443	1	1.458	1
				1.415	1
1.386	1	1.379	2	1.393	3
1.350	1	1.344	1	1.352	1
1.275	2b	1.259	1	1.273	2b

b = broad line.

fact that shrinkage on heating of these compounds is almost negligible, it is evident that they have essentially the same structures and that H_2O is not required in them though always present in the material unless heated to a relatively high temperature. As there was the possibility that the Na compound might be Na_2UO_4, an analysis for Na_2O was made on the heated sample in the Rock Analysis Laboratory of the University of Minnesota. It gave 8.8%. K_2O was about 0.1%. Theoretically, the percentages of Na_2O are:

in $Na_2U_2O_7 = 10.36$
in $Na_2UO_4 = 18.78$

It is obvious that the analysis agrees fairly well with $Na_2U_2O_7$. Complete agreement had not been expected in a complex compound of U prepared more than 30 years ago. The corresponding Ca synthetic uranate is $CaU_2O_7 \cdot xH_2O$. The natural mineral is essentially a Na-Ca uranate. K and Pb are considered "impurities" in the sense that their ions are too large to occupy Ca or Na positions. They could, however, be in the H_2O positions if these are more or less fixed. The formula would be $(Na, K)_{2-2x}(Ca, Pb)_xU_2O_7 \cdot yH_2O$. The material of Ross, Henderson, and Posnjak indicates that they probably had a mixture of U-minerals. Also, the dark brown color of their material as compared with the lighter colored synthetics suggests this.[2] Such mixtures are almost the rule instead of the exception in U-minerals, as more recent work has indicated. Ross, Henderson, and Posnjak state that clarkeite is of hydrothermal origin, that is, of a late stage in pegmatite formation. Our synthesis at 258° C certainly supports this claim. In many experiments which we have made below 100° C we have never obtained the mineral.

The following recent paper dealing with synthetic diuranates has come to the writer's attention too late to be included in the discussion (Hoekstra, Henry R., and Katz, Joseph J., Studies on the alkaline earth diuranates: *Jour. Am. Chem. Soc.*, **74,** 1683 (1952)).

REFERENCES

Ross, C. S., Henderson, E. P., Posnjak, E. (1931), Clarkeite, a new uranium mineral: *Am. Mineral.*, **16,** 213–220.

Hintze, Carl (1938), Handbuch der Mineralogie: Ergänzungsband, p. 117.

Dana's System of Mineralogy (1944), 7th Edition, p. 624.

Gruner, J. W. (1952), New data of syntheses of uranium minerals: *Atomic Energy Commission* **RMO-983,** Part I. Annual Report July 1, 1951, to June 30, 1952, page 9.

---

[2] As the minerals are extremely fine grained, indices are difficult to obtain. Ca-clarkeite after heating has a mean index above 2.00 while that of Na-clarkeite is around 1.84.

THE INDIRECT DETERMINATION OF β AND 2V

P. McL. Swift, *Welwyn Garden City, England.*

The following method is suggested for the indirect determination, using the polarizing microscope, of β and 2V for crystals capable of being mounted so that they can be rotated around the β direction. β and 2V are determined concurrently with the indirect determination of α and γ by the method of Wood and Ayliffe (*Phil. Mag.* (1936) (7) **21,** 324). Hippuric acid is cited as an example.

The apparatus used was a rotation apparatus in which the crystal, 0.5 2 mm. long, mounted on a needle with β lying in the direction of the needle, could be rotated through 360° while immersed in a liquid held in a glass cell (see Hantshorne and Stuart, Crystals and the Polarising Microscope, p. 214). The crystal was observed through an 8 mm. objective

TABLE 1

	from Fig. 1	from Winchell
α	1.537	1.535
β	1.594	1.592
γ	1.762	1.760
2V	65° 45′±15′	65° 49.5′

with β at right angles to the vibration direction of the polarizer and the four angular positions found in which the refractive indices of liquid and crystal were matched, as in Wood and Ayliffe's method. The stage was then turned to the 45° position, the interference figure observed using the Bertrand lens, and the four angular positions were found at which the optic axes were apparently vertical. This gives the apparent optic axial angle 2V in the liquid used, of refractive index μ. This apparent optic axial angle is determined for each liquid used.

In Wood and Ayliffe's method, $\cos^2\theta$ is plotted against $1/\mu^2$, to give a straight line, θ being the angle between the position in which α is horizontal, and the position in which the refractive index of the crystal is matched by that of the liquid. When $\mu=\beta$, $2\theta=2V$, the true optic axial angle. Thus if $\cos^2V^1$ (for positive crystals: for negative crystals plot $\sin^2V^1$) is plotted against $1/\mu^2$ on the same axes as $\cos^2\theta$ vs $1/\mu^2$, $1/\beta^2$

FIG.I

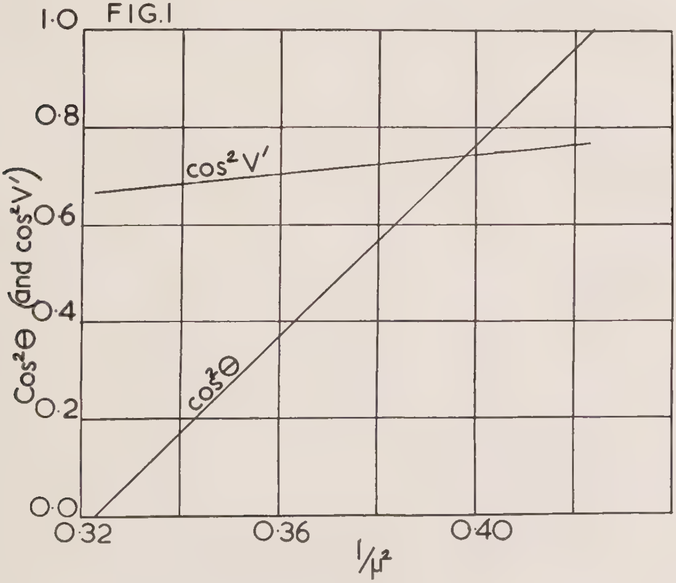

and $\cos^2 V$ are given by the point of intersection of the two curves. $\text{Cos}^2 V^1$ vs $1/\mu^2$ is not in general far from being a straight line, particularly if points lying at either end are neglected in favor of those lying nearer the intersection. Figure 1 gives the curves obtained for hippuric acid, and Table 1 the values for α, β, γ, and 2V obtained from this figure and as given in Winchell's Optical Properties of Organic Compounds.

The Institute of Silicate Research at the University of Toledo was dedicated on May 15. The Institute is a center for basic research in physical chemistry, colloid chemistry, *x*-rays, microphotography, microscopy, refractometry and interferometry. It is supported by the University, Libbey-Owens-Ford Co., Owens-Corning Fiberglas Corporation, Owens-Illinois Glass Co., Pittsburgh Plate Glass Co., and Columbia-Southern Chemical Corporation. Dr. Wilhelm Eitel is the director of the Institute.

The Twelfth Annual Pittsburgh Diffraction Conference will be held at the Mellon Institute, Pittsburgh, Pennsylvania, on Nov. 3, 4, and 5, 1954. This will be a joint meeting with the American Crystallographic Association. Technical sessions are being arranged on Instrumentation and Methods, Metals, Neutron Diffraction, Small-Angle Scattering, and Silicates and Related Structures. Titles of papers should be submitted to Professor G. A Jeffrey, University of Pittsburgh, Pittsburgh 13, Pennsylvania, before Sept. 1, 1954. Abstracts should be submitted by Sept. 20, 1954.

The Society for Experimental Stress Analysis will hold its annual meeting and exposition in conjunction with The First International Instrument Congress and Exposition on Sept. 21, 22, and 23, 1954, at the Bellevue-Stratford Hotel, Philadelphia, Pennsylvania. Information regarding this meeting may be obtained by writing to General Chairman, Mr. Frank G. Tatnall, P.O. Box 4034, Chestnut Hill, Philadelphia, Pennsylvania.

The 8th Annual Midwestern meeting of the Society of Exploration Geophysicists will be held November 18 and 19 at the Adolphus hotel in Dallas, Texas. Registration will begin November 17 for exploration scientists from Texas, Louisiana, Oklahoma and New Mexico. Meeting committees are headed by members of the Dallas Geophysical Society, assisted by members of five other participating SEG local sections in Fort Worth, Midland, Shreveport, Oklahoma City and Tulsa.

Corrections

The word *ferroan* in the title of the note starting on p. 676 of the July–August issue of this journal should read *ferro;* the same change should be made just above the *Note* near the middle of p. 680. In Table 2 on p. 677 the gravity values are reversed.

MINERALOGICAL SOCIETY (LONDON)

A meeting of the Society was held on Thursday, June 10th, 1954, at 5 P.M., in the apartments of the Geological Society of London, Burlington House, Piccadilly, W.1 (by kind permission).

The following papers were read:

(1) Truscottite

By Dr. A. L. Mackay and Dr. H. F. W. Taylor

A new chemical analysis of the mineral truscottite confirms its formula as $CaO \cdot 2SiO_2 \cdot \frac{1}{2}H_2O$. *X*-ray examination of powdered and single-crystal material, the latter somewhat disoriented flakes, gives a hexagonal unit-cell with $a = 9.72 \pm 0.01$ and $c = 18.71 \pm 0.03$ Å which has c perpendicular to the principal cleavage and contains 12 formula units. The structure is stable up to 700° C., although the dehydration curve shows some loss at about 400°. Heating to above 1000° transforms the material first to wollastonite and then to pseudo-wollastonite together with cristobalite in each case. The structure appears to be one of layers, fundamentally similar to those found in gyrolite, but differs from the gyrolite structure in the arrangement of the layers and in the quantities of calcium and water between the silicate sheets.

(2) Direct Measurement of Reflecting Powers with the Microphotometer

By Dr. A. F. Hallimond

By means of an inclined reversible reflecting surface it is possible to measure the incident and reflected intensities at quasi-normal incidence. The device is used on the microscope stage with the ordinary microphotometer arrangement.

(3) A Note on the Relationship between the Precision of Classical Methods of Rock Analysis and the Concentration of each Constituent

By Dr. L. H. Ahrens

Geometric (log) scales clearly reveal a regularity between the concentrations of elements and the precision, expressed as a relative deviation, with which they have been determined in granite and diabase by means of classical methods of chemical analysis. As the regularity is well developed it may be utilized as a rapid and semiquantitative guide for assessing and comparing the precision of silicate rock analyses which have been carried out by means of these methods.

(4) A Further Note on the Presentation of Chemical Analyses of Minerals

By Dr. M. H. Hey

In a previous communication the advantages of presenting chemical analyses, whenever possible, as empirical unit-cell contents were stressed. A simple method is now proposed for calculating the most probable limits of error of the empirical unit-cell contents consequent on any assessed probable limits of error in the chemical analysis, density, and unit-cell dimensions. It is notable that in many minerals, especially silicates and oxides in which oxygen is an important constituent and often occupies an integral number of positions in the crystal structure, the probable error in the oxygen content of the unit-cell is relatively small and varies little for very considerable variations in the assessed analytical error.

The following papers were taken as read:

(1) An Occurrence of Palygorskite in the Shetland Isles

By Dr. I. Stephen

A white to grayish-white material occurring in small pocket-like masses and as veinlets in montmorillonitized syenite has been shown to consist dominantly of the mineral palygorskite. The properties of the mineral have been investigated by optical, chemical and *x*-ray methods, and by *D.T.A.* and electron microscopy.

(2) On the Occurrence of the Rare Copper Molybdate, Lindgrenite, at Brandy Gill, Carrock Fell, Cumberland

By Mr. A. W. G. Kingsbury and Mr. J. Hartley

The occurrence of wulfenite and stolzite among material from an old trial-level on the east side of higher Brandy Gill, Carrock Fell, together with pieces of veinstone, indicated the presence of intersections between an east-west lead-copper vein and one or more of the "granitic" suite of veins that further south in and near Grainsgill carry tungsten and molybdenum minerals. Further careful examination has revealed the presence of small amounts of lindgrenite, hitherto not recorded in Great Britain.

(3) New Occurrences of Vanadium Minerals (Mottramite, Descloizite and Vanadinite) in the Caldbeck Area of Cumberland

By Mr. A. W. G. Kingsbury and Mr. J. Hartley

The finding in 1949 of a single small specimen of mottramite among material from an old trial on the west side of higher Brandy Gill, Carrock Fell, has resulted in the finding of further occurrences of this mineral, in addition to descloizite, and of vanadinite at several localities in the Caldbeck-Carrock area.

(4) Determination of the Composition of Natural Nephelines by an *X*-ray Method

By Dr. J. V. Smith and Prof. Th. G. Sahama

X-ray data obtained for 13 synthetic nephelines and 24 chemically analyzed minerals are plotted against the atomic percentage $K/(K+Na+Ca)$.

(5) Zoisite-Amphibolite with Corundum from Tanganyika

By Mr. P. M. Game

A colorless zoisite, occurring as a monomineralic rock, and a green zoisite, associated with red corundum, iron-poor hornblende and anorthite, occur in lenses in the basement complex of the Northern province of Tanganyika.

Analysis of the green zoisite shows it to be a non-ferriferous variety ($Fe_2O_3 < 2\%$). The values of the optic axial angle (for both green and white varieties) agree with those previously published for iron-poor zoisites, but the orientation ($\alpha \perp (010)$) and the dispersion ($r > v$, strong) are at variance with previous data for non-ferriferous zoisites and conform to the values quoted for zoisites with 5% or more of Fe_2O_3 (β-zoisite of P. Termier).

(*Titles and abstracts kindly submitted by G. F. Claringbull, General Secretary.*)

BOOK REVIEWS

LES MINÉRAUX ET LES ROCHES, ÉTUDES PRATIQUES DE CRISTALLOGRAPHIE, PÉTROGRAPHIE ET MINÉRALOGIE, by H. BUTTGENBACH. 8^e édition établie avec la collaboration de J. Mélon. Paris (Dunod)—Liege (Vaillant-Carmanne), 1953. Printed in Belgium. xii+763 pp., 16 by 24 cm., 613 figs., 4 pls. Bound in cloth. 800 Belgian francs (about $16).

In the preface to the 6th edition,* which appeared in 1935, Professor Buttgenbach commented that this edition was probably going to be the last one he would publish. A 7th edition was nevertheless printed in 1943. Now with the 8th one, coming as it does on his 80th birthday, we are happy to note that his gloomy prediction has twice come untrue!

Dr. Mélon, now a professor at Liège, is a co-author of the new edition. The most notable changes are as follows: The Miller notation is used throughout the text, jointly with the old Lévy form symbols. This will make the book easier to read outside French-speaking countries. So will the comparison between the co-ordinate axes used in the text with those commonly used in America, for the hexagonal and the rhombohedral systems. The presentation of the law of rationality is revised to include one of its important aspects—the simplicity of indices. The description of twinning follows Friedel (exception must be taken to the definition of twinning by merohedry). The law of Bravais is no longer credited to Mallard. The classification of silicates is based on their crystal structures.

A few species have been added, such as pentlandite and kernite. The Dana classification is followed, though not blindly. In a praiseworthy effort to keep the price of the volume from soaring even higher, the authors have kept the traditional crystal settings for descriptive purposes. For about 50 species the structural cell obtained by x-rays differs from the morphological cell; for these the transformation matrices relating the two cells to each other are tabulated in an appendix. More sweeping innovations in matters of symbolism would seem desirable: the Hermann-Mauguin symmetry notation, which has truly become the *lingua franca* of present-day crystallographers, should be adopted. Isomorphism, polymorphism, and alterations have been grouped in a new chapter entitled crystal chemistry. This is a step in the right direction. More will be needed to do justice to the paramount importance of crystal chemistry in modern mineralogy.

The 8th edition remains faithful to the teaching philosophy that made the success of its predecessors. The Liège textbook is here to stay. We are looking forward to its 9th edition!

J. D. H. DONNAY,
The Johns Hopkins University, Baltimore, Maryland

SPEZIELLE MINERALOGIE AUF GEOCHEMISCHER GRUNDLAGE, by FELIX MACHATSCHKI, Vienna, Springer-Verlag, 1953, vii+378 pages, 228 figures. Price, $8.60.

Machatschki has written a mineralogy which, although at a moderately elementary level, is up-to-date and authoritative. No attempt is made at completeness; about 800 species are described, most of them quite briefly. The more important ones are treated fairly completely, composition, crystallography, hardness, optical properties (including properties by reflected light for opaque minerals), varieties, properties of isomorphous series, and even a summary of the information about their crystal structure, where known, being given. Treatments range from this to a one or two-line statement of composition, color, crystal habit and fracture or cleavage for some of the less common species.

The book begins with a brief discussion of mineral formulae, names, and classification. This is followed by a one-page tabulation of "radii of the building blocks of mineral crystals." A short (11 page), generalized, elementary discussion of the principles of geochemistry and a seven-page outline of the geochemistry of the atmosphere, hydrosphere, and lithosphere complete the 29-page introduction.

---

* Reviewed in *Am. Mineral.*, **21,** 211–213 (1936).

No references to literature are given in the text, but there is a list of references for supplementary reading on pages 354–355.

In the main part of the text the arrangement and treatment emphasize the genetic viewpoint. Under "primary minerals" those of igneous rocks are discussed in 70 pages; pegmatites, 34 pages; hydrothermal (deposits), 34 pages; and volcanic exhalations, 6 pages. Minerals of weathering products and sedimentary rocks are allotted 28 pages; those of metamorphic rocks, 22 pages. The "ore" minerals are not treated genetically, but are classified primarily according to the (principal) heavy metal contained and secondarily by the non-metal or non-metallic radical. These are treated in part four, of 74 pages.

Each of the three "genetic" parts opens with a short discussion of principles and includes a very brief classification of the rocks involved. The book is primarily mineralogy, so the short discussions of rocks are appropriate,—but this very brevity makes it more imperative that the statements on rocks should be accurate and to the point. It is disconcerting, therefore, to find rather serious inaccuracies in the discussion of igneous rocks. It should be noted in the table on page 97, for example, that diabase and proterobase are not extrusive rocks. Picrite, although it is an extrusive rock, is certainly not the extrusive equivalent of anorthosite, as indicated in the table. Kimberlite is a variety of peridotite, not its extrusive equivalent.

While no actual inaccuracy is involved, it is unfortunate to follow in so modern a book the antiquated system of assigning different names to identical extrusive rocks just because they are of different ages.

It should also be noticed that in this table on page 97, in the list of minerals to the lower left, "Peridotit" should read "Olivin."

The table, or diagram, on page 94 also leaves some erroneous impressions. If interpreted strictly it indicates, for example, that peridotite always contains basic plagioclase, and that granite always contains albitic feldspar and muscovite. Neither, of course, is the case. If appropriate parts of some of the lines had been dashed these inconsistencies could have been avoided.

The genetic approach applied in this book gives a geologic setting to the descriptions of minerals and a geologic feel to the reader not ordinarily imparted by systematic treatments of mineralogy. This arrangement could undoubtedly be used very effectively in organizing certain types of courses.

For other purposes, such as reference, however, it has more or less serious drawbacks. In some of the sections mixing of processes with descriptions of minerals is a little confusing. A much more serious difficulty is the very considerable overlap in mineral species among the genetic groups treated. Quartz, for example, is described in considerable detail under magmatic minerals, but is not mentioned in the descriptions of pegmatite or hydrothermal minerals, although for many purposes these varieties are much more important, interesting and impressive than igneous quartz. Careful reading of the introductory remarks of these sections discloses casual, but to the reviewer entirely inadequate, mention of quartz. There is no indication in the index that quartz is mentioned at all as a pegmatitic, hydrothermal, or metamorphic mineral.

Likewise, feldspar is described as a magmatic mineral, but is entirely neglected in the discussion of pegmatites. It can be inferred from the names of the pegmatites mentioned in the introduction of the section, granite pegmatite, syenite pegmatite, and gabbro pegmatite,—that they must contain feldspar, but it is not mentioned specifically either there or in the mineral descriptions that follow.

Some phosphates are described under magmatic, some under pegmatite, and some under hydrothermal minerals. Most of these minerals occur in at least two of these categories, some in all three, and a few also in sedimentary rocks.

The iron oxides are mentioned as igneous accessories, but described under ore-minerals. Their distribution, of course, is much wider than this.

These examples could be multiplied many times. There would be no point, of course, to describing the same mineral in two or more sections. The treatment would have been much more satisfactory, however, if the important minerals that occur in each category, but are described elsewhere, could have been listed, with references to where the descriptions are to be found. This is done in part (minus the references) for the hydrothermal minerals (p. 135).

A 52-page appendix classifies all of the minerals described in the text in a crystal chemical system much like that used in the 7th Edition of Dana's System of Mineralogy. Cell dimensions and space groups are given for all species for which these data were available in the literature by the end of 1952.

Machatschki has produced a textbook of mineralogy with a refreshing point of view and a novel approach. With appropriate explanatory and additional material for beginning students and those who lack geologic background this book should provide much broader and more varied training than that given by more conventional texts.

Earl Ingerson,
U. S. Geological Survey, Washington 25, D. C.

MANUAL OF THE POLARIZING MICROSCOPE, by A. F. Hallimond, second edition, 204 pp., 92 figures, Cooke, Troughton, and Simms, Ltd., York, England, 1953, distributed in the United States by R. Y. Ferner Co., Inc., 110 Pleasant Street, Malden 48, Massachusetts, $3.00.

At the outset Dr. Hallimond, in his Manual of the Polarizing Microscope. reviews briefly the historical development of the polarizing microscope. Following the historical development, the construction of microscopes and microscope accessories is described. Special emphasis is given the Cooke, Troughton, and Simms instruments, which are built with an Abbe condenser, its use made possible by the substitution of polaroid for calcite prisms. Accessories useful in studying opaque as well as transparent crystals are explained.

Methods of accurately determining path-difference and extinction positions are treated in some detail. Certain advantages of making these measurements conoscopically are pointed out. The use of the Koenigsberger and Nakamura plates is described. The accuracy indicated for the measurement of the thickness of a specimen by means of the fine focusing adjustment is somewhat greater than that of the reviewer's experience. It seems that by labeling the ordinate in figure 31 *d* (p. 58), "phase angle of the retarded wave," some confusion is introduced. Perhaps just phase angle would be better. Brief chapters are devoted to the dichroscope, to the dispersion of birefringence, and to binocular and stereoscopic microscopes. Accompanying the chapter on the interference figure and the Bertrand lens is an excellent series of photographs of conoscopic figures of phlogopite, which illustrate not only the effects due to birefringence, but also those due to pleochroism. The photographs show the appearance of figures of phlogopite between crossed polars, with polarizer only, and in ordinary light. The value of these illustrations might be enhanced if the numerical aperture of the objective used and the thickness, indices of refraction, and suitable absorption moduli of the phlogopite were stated.

A very useful summary of the theory and practice of the examination of polished opaque substances in polarized reflected light is given in four chapters. The theoretical treatment is based largely on that of Berek. This section of the book should be of especial interest to students of mineralography. Following the chapters on reflected light is a description of a relatively simple microphotometer.

The use of the three-axis universal stage is simply but adequately described. The author includes in his discussion the extrapolation of a third principal index, Berek's method of determining axial angle, and the Emmons double variation method.

The reader is assumed to have a basic knowledge of crystal optics. The book as a whole is non-mathematical, although a number of important relations are derived. Of particular interest should be the section on strongly absorbing crystals in reflected light. Throughout the book the treatment is concise and accurate. Ample references to the basic literature are provided, and the text is well illustrated. Some of the methods described are more refined than is usual for ordinary work. While the book is not intended to be an elementary or complete text of crystal optics, it contains an uncommonly good treatment of many important aspects of the use of the polarizing microscope.

Although Dr. Hallimond stresses Cooke, Troughton, and Simms instruments, the book should be of considerable interest to all serious students of crystal optics, to students of mineralography, to research workers, and to teachers.

REYNOLDS M. DENNING,
University of Michigan, Ann Arbor, Michigan

EDELSTEINE UND PERLEN, by K. SCHLOSSMACHER. viii+280 pp., 103 illustrations in the text, 3 tables, and 3 plates (2 colored). 16×24.5 cm. E. Schweizerbart'sche Verlagsbuchhandlung (Erwin Nägele) Stuttgart, Germany, 1954. Price, bound, 25 DM.

According to the author, this text is designed for all lovers of gemstones and pearls, but more especially for jewelers, goldsmiths, diamond cutters, lapidaries, and dealers in gemstones and pearls. The book can be considered as an abridged replacement of Dr. Schlossmacher's two-volume revision of Max Bauer's classical *Edelsteinkunde*, published in 1928–32, which is now out of print and cannot be revised on account of its size and present unfavorable economic conditions. The author was for many years professor of mineralogy at the University of Königsberg, East Prussia, and is now director of the Gemological Research Laboratory at Idar-Oberstein, the world-famous gem cutting center.

The book is divided into three parts, designated as *general*, *special*, and *practical*. The general part includes, aside from the foreword and introduction, rather comprehensive descriptions of the various properties of gemstones (58 pages) and of the methods and instruments used in investigating them (16 pages).

The special section, which comprises the bulk of the book (167 pages), contains detailed discussions of the properties, occurrences, production, and imitations of the important inorganic gemstones. Fourteen gemstones not commonly encountered in the trade, such as fluorite, obsidian, euclase, etc., are described briefly. The organic gems—pearls, amber, coral, and jet—are considered next. In twenty pages natural and cultured pearls, including the methods of identification, are treated rather exhaustively. The syntheses of the diamond, corundum, spinel, emerald, rutile, and quartz, as well as reconstructed stones, are amply described. With regard to the synthesis of the diamond, Schlossmacher concludes that thus far the diamond has not been produced in the laboratory, and that the identification of the alleged product is not the determining factor but that the whole process must be critically investigated by competent scientists. It is also pointed out that in some cases there has been evidence of fraud.

In the third section the cutting, engraving, and methods used in obtaining uncut material and in the sale of cut gems are described in considerable detail. There are three tables listing indices of refraction, specific gravity, and hardness. These tables are adapted from the *Handbook of Gem Identification* by R. T. Liddicoat, Jr. The two colored plates add interest to the text. There is a good index.

The treatment throughout is authoritative. The book should appeal strongly to the

German public and gem trade. It can be recommended as a helpful reference work to all interested in gemology.

Edward H. Kraus,
University of Michigan, Ann Arbor, Michigan

THE CHARNOCKITE PROBLEM, by C. S. Pichamuthu. Mysore Geologists' Association, Bangalore, India. 1953, 178 pp.

The main features of this monograph on the characteristics and origins of the charnockites formed the basis for the presidential address delivered at the 1952 annual meeting of the Mysore Geologists' Association by C. S. Pichamuthu, who is director of the Mysore Geological Department. In the 18 chapters the following main topics are treated: nomenclature, occurrence, distribution, petrography, origin and age of charnockites. Considerable detailed information also is presented on charnockites in India, particularly in Mysore, and one chapter is devoted to summaries of the literature on charnockites. Although the study is a thorough one, it presents little new general information on charnockites that was not gathered by Quensel (*Arkiv Min. Geol.* **1** (10), 227–332, 1951). However, the information on Indian charnockites that has accummulated since the classic studies of Holland (*Mem. Geol. Surv. India,* **28,** pt. 2, 1900) is carefully digested and well integrated. After demonstrating that strong arguments may be advanced for both the magmatic and metamorphic genetic hypotheses, the author concludes that there are "charnockites and charnockites" and no one theory of origin adequately explains the formation of all types. According to him, Indian charnockites are of two generations, the older being developed by regional metamorphism and the younger by metasomatism and palingenesis.

E. Wm. Heinrich,
University of Michigan, Ann Arbor, Michigan

SPOMENICA MIŠE KIŠPATICA. Edited by Fran Tućan. Yugoslavian Academy. 247 pp. 1952 (?).

This is a jubilee volume to commemorate the 100th anniversary of the birth of Mišo Kišpatić, the famous Yugoslavian scientist, who was born in 1851 and died in 1926. Kišpatić, who founded the Institute of Petrology and Mineralogy at the University of Zagreb, was a petrologist, mineralogist, crystallographer and seismologist who held advanced ideas in the fields of earth science, many of which have received substantiation in the light of more modern facts and theories. The papers, which are in Serbian and are followed by summaries in German (two in English), include (titles in translation):

1. Luka Marić, Mišo Kišpatić in the light of contemporary petrology.
2. Fran Tućan, A new contribution to the knowledge of the crystalline rocks of Moslavačka gora.
3. Ljudevit Barić, Ludlamite from the Stari Trg (Trepča) mine at Kosovska Mitrovica.
4. Miroslav Tajder, Petrography of the Srebrenica ore district in Bosnia.
5. Vladimir Majer, Chabazite and stilbite from Bor (Yugoslavia).
6. Luka Marić, The extrusive rocks of the ore district between Zletovo and Kratovo.
7. Ivan Jurković, Barite from the Dobrevo mine at Zletovo.
8. Stevan Karamata, General characteristics of the melaphyres in the vicinity of Vareš (Bosnia).

The excellence of the contributions guarantees the quality of the tribute to this remarkable pioneer in the fields of petrology and mineralogy.

E. Wm. Heinrich,
University of Michigan, Ann Arbor, Michigan

NEW MINERAL NAMES

Navajoite

Alice D. Weeks, Mary E. Thompson, and A. M. Sherwood, Navajoite, a new vanadium oxide from Arizona. *Science,* **119,** No. 3088, p. 326 (1954).

Navajoite is dark brown, soft, fibrous, with silky luster and brown streak. G = 2.56. Optically biaxial, probably negative, extinction parallel, α 1.905 ± .003, β about 2.02, γ slightly above 2.02; pleochroic with X and Y yellowish brown, Z dark brown and parallel to the fiber length.

The *x*-ray pattern is distinct from those of hewettite and corvusite. Single crystal measurements could not be made, but a rotation photograph of a small bundle of fibers give the unit cell length along the fibers as 3.65 Å. Study of a zero-layer photograph suggests that navajoite is probably monoclinic with a_0 17.43 ± .1, b_0 3.65 ± .05, c_0 12.25 ± 0.1 Å, β 97° ± 30′. This unit cell would contain approximately 6 ($V_2O_5 \cdot 3H_2O$).

Analysis (Sherwood) gave V_2O_5 71.68, V_2O_4 3.08, Fe_2O_3 3.58, H_2O 20.30, SiO_2 1.20, CaO 0.22; sum 100.06%, indicating the formula $V_2O_5 \cdot 3H_2O$.

Navajoite occurs in a U-V deposit in the Monument no. 2 mine, Navajo Indian Reservation, Apache County, Arizona. The ore impregnates sandstone. Associated minerals are corvusite, tyuyamunite, rauvite, hewettite, steigerite, and limonite.

The name is for the Navajo Indians.

Michael Fleischer

Matteuccite

Guido Carobbi and Curcio Cipriani, Ralstonite e bisolfato sodico (matteuccite) fra i prodotti della fumarole vesuviane. *Rend. accad. nazl. Lincei, Classe sci., fis., mat., e nat.,* **12,** 23–29 (1952).

Analyses are given of stalactites from the 1933 eruption of Vesuvius. These are mixtures: mercallite ($KHSO_4$) was identified optically; ralstonite (hydrated fluoride of Na, Mg, and Al) was identified optically and by its *x*-ray powder pattern. A third component with large 2V is probably $NaHSO_4 \cdot H_2O$ (the synthetic compound has 2V = 86°, positive); the powder pattern shows a strong line at $d = 3.47$, which is interpreted as corresponding to lines at $d = 3.55$ and $d = 3.43$ given for $NaHSO_4 \cdot H_2O$ in the *A.S.T.M.* file.

The name is for Vittorio Matteucci, 1862–1909, Director of the Vesuvius Observatory.

M. F.

Väyrynenite

A. Volborth, Väyryneniiti, [$BeMn(PO_4)(OH, F)$], *Geologi (Finland),* **6,** P. 7 (1954).

Preliminary announcement. The mineral is monoclinic, $\beta = 102°\ 49' \pm 10'$. Optically negative, indices $\alpha = 1.640$, $\beta = 1.662$, $\gamma = 1.667$, all ±.001. G. = 3.183. From the Viitaniemi pegmatite, Eräjärvi, Finland. The name is for Heikki Väyrynen, Finnish geologist.

M. F.

Bøggildite

Richard Bøgvad, Mineralogical observations on the cryolite deposit at Ivitgut, Greenland. *Medd. Dansk. Geol. Fören.,* **12,** 109–110 (1951).

A. H. Nielsen, Chemical analysis of a new mineral, bøggildite, from Ivigtut, Greenland. *Acta Chem. Scandinavica,* **8,** 136 (1954).

Analysis of material containing only traces of quartz and sphalerite gave Al 10.04, Fe 0.06, Sr 31.89, Ba 0.35, Mg 0.18, Ca 0.20, Mn trace, Na 8.60, K 0.15, Li trace, PO_4 17.63, F 31.70, H_2O none, Cl, Zn, Ce not found; sum 100.80%, corresponding closely to $Na_2Sr_2Al_2(PO_4)F_9$. When heated in a glass tube over a Bunsen burner, the mineral melts and gives a small amount of white sublimate. Color flesh-red. Monoclinic (or triclinic) with twinning lamellae. H.=4–5, G.=3.66. Optically biaxial, positive, axial angle rather large, α above 1.46, β and γ below 1.47. Occurs at Ivigtut, Greenland, at the contact of cryolite with greisen. Associated minerals include siderite, fluorite, black cryolite, quartz, green mica, and sphalerite.

The name is for Professor O. B. Bøggild, University of Copenhagen.

M. F.

Tertschite

Heinz Meixner, Neue türkische Boratlagerstätten. *Berg. u. hüttenmann. Monatsh.*, **98,** 86–92 (1953).

Heinz Meixner, Einige Boratminerale (Colemanit und Tertschit, ein neues Mineral) aus der Türkei. *Fortschr. Mineral.*, **31,** 39–42 (1953)

Heinz Meixner, Mineralogische Beobachtungen an Colemanit, Inyoit, Meyerhofferit, Tertschit, und Ulexit aus neuen türkischen Boratlagerstätten Heidelberg. *Beitr. Mineral. Petrog.*, **3,** 445–455 (1953).

The new mineral occurs at the Kurtpinari mine, Faras, Turkey, as snow-white masses that are finely fibrous with silky luster, resembling ulexite. Analysis of air-dried material (W. Zwicker, analyst) gave CaO 22.40, MgO tr., B_2O_3 37.26, H_2O (total) 37.72, gangue 2.68; sum 100.06%, corresponding to $Ca_4B_{10}O_{19}\cdot 20\ H_2O$.

The mineral loses 10.16% H_2O at 50°, 21.24 at 110°, 26.70% at 150°. It is slightly soluble in hot H_2O, easily soluble in dilute HCl. The optical properties are difficult to measure because of the fibrous character. Monoclinic? α' 1.502, γ' 1.517, extinction inclined, γ' to long axis 30–33°. *X*-ray powder data are given; the strongest lines are at 2.83, 2.35, 2.02, 3.12, 2.16, and 1.93 Å. Under ultra-violet light, it fluoresces light to deep blue-violet, the same as ulexite.

The name is for Prof. Hermann Tertsch, Univ. of Vienna.

M. F.

Tavorite

M. L. Lindberg and W. T. Pecora, Tavorite and barbosalite: two new phosphate minerals from Minas Gerais, Brazil. *Science*, Vol. **119,** no. 3099, p. 739 (1954).

Tavorite is the iron analogue of montebrasite, with which it is isostructural. Analysis: Li_2O 7.64, FeO 2.39, MnO 1.47, Fe_2O_3 42.57, P_2O_5 39.78, H_2O^+ 5.76, H_2O^- 0.40; sum 100.01%, formula $LiFe(PO_4)(OH)$. It is yellow, fine-grained, with mean *n* 1.807, sp.gr. 3.29. *X*-ray powder diagrams show principal *d*-spacings at 3.045, 3.285, 4.99, 4.68, and 2.474 Å. Tavorite occurs in the Supucaia pegmatite, Minas Gerais, intimately intergrown with barbosalite, and associated with many phosphates including triphylite and its oxidation products, frondelite, faheyite, variscite, montebrasite, and apatite.

The name is for Professor Elysiario Tavora, Universidade do Brasil, Rio de Janeiro.

M. F.

Barbosalite

M. L. Lindberg and W. T. Pecora, *op. cit.*

Barbosalite is the ferric analogue of scorzalite. Analysis, recalculated after deducting admixed tavorite, gave FeO 13.12, MnO 2.82, Fe_2O_3 41.70, P_2O_5 37.54, H_2O 4.92%, corresponding to the formula Fe'' Fe''' $(PO_4)_2(OH)_2$. It is structurally identical with the synthetic compound described by Gheith (*Am. Mineral.*, **38**, 612–628 (1953)) as ferrous ferric lazulite. It occurs in black, nearly opaque, grains and masses. Thin edges are dark blue-green and show pleochroism. The mean apparent *n* is 1.810, sp. gr. 3.60. *X*-ray powder diagrams show principal *d*-spacings at 3.361, 3.313, 4.84, 3.239, 3.160, and 2.327 Å. For occurrence, see Tavorite above.

The name is for A. L. de M. Barbosa, Professor of Geology, Escola de Minas, Ouro Preto, Brazil.

M. F.

NEW DATA

Lead Selenate ($PbSeO_4$) (=kerstenite?)

J. Goni and C. Guillemin, Données nouvelles sur les sélénites et séléniates naturels, *Bull. soc. franç. mineral. crist.*, **76**, 422–429 (1953).

Lead selenate, $PbSeO_4$, was found in orthorhombic prisms and acicular needles 1 mm. long. at Pacajake, Bolivia, and at Cerro de Cacheuta, Argentina. Colorless to greenish yellow, luster greasy, hardness $=3\frac{1}{2}$. Cleavage imperfect perpendicular to the elongation. Optically biaxial, negative, $\alpha=1.96$, $\gamma=1.98$, 2V about 50°, elongation positive, extinction parallel. Difficulty soluble in warm (1+1) HNO_3. The *x*-ray pattern is given; it is identical with that of synthetic $PbSeO_4$ and very similar to that of anglesite. This may be identical with kerstenite (see *Dana's System*, Vol. II, p. 640), but the properties of the latter are so little known that comparison is not yet possible.

M. F.

Ahlfeldite

J. Goni and C. Guillemin, *op. cit.*

The validity of ahlfeldite, hydrate nickel selenite, is established on material from the type locality, Pacajake, Bolivia. Ahlfeldite is rose-colored, luster vitreous, no cleavage, fracture conchoidal. Hardness $=2\frac{1}{2}$, G. $=3.4\pm.05$. Optically biaxial negative, $\alpha=1.73$, $\gamma=1.76$, 2V about 80°, extinction inclined 16°; strongly pleochroic, X rose, Y pale green, Z brown green. Easily soluble in dilute HNO_3. Gives microchemical reactions for nickel. selenite, and a little Co. *X*-ray powder data are given. Cobaltomenite may be identical with ahlfeldite, but the type material is not available to check this.

M. F.

Molybdomenite

J. Goni and C. Guillemin, *op. cit.*

Molybdomenite, considered to be a dubious mineral (*Dana's System*, Vol. II, p. 640), is confirmed as a valid species by study of type material from Cerro de Cacheuta, Argentina, and from a new find at Trogtal, Harz. It is orthorhombic (?), with one perfect cleavage and another less distinct perpendicular to the first. Colorless to yellowish-white, luster pearly (Cerro de Cacheuta), greasy (Trogtal), hardness $=3\frac{1}{2}$. Optically biaxial, negative, $\alpha=2.12$, $\beta=2.14$, 2V about 80°, extinction parallel, elongation positive. Soluble in cold (1+10) HNO_3; gives qualitative tests for lead and selenite. The *x*-ray powder pattern differs from that of $PbSeO_o$.

M. F.

Churchite

G. F. Claringbull and M. H. Hey, A re-examination of churchite. *Mineralog. Mag.*, **30**, 211–217 (1953).

Churchite from Cornwall, described in 1865 as a hydrated phosphate of Ca and rare earths, is shown by analysis and *x*-ray study to be (Y, Er, La) $PO_4 \cdot 2H_2O$, identical with weinschenkite (Laubmann, 1922). It is urged that the name churchite be retained, since it has priority, the error in the original description by which the yttrium group was overlooked being considered insufficient to cause preference to be given to weinschenkite.

Discussion: This is a hard decision to make; the original description was so incomplete that rather remarkable insight would have been needed by Laubmann to recognize the identity. For the sake of uniformity, the suggestion of the authors should be followed and the name weinschenkite abandoned.

M. F.

Chlorites

M. H. Hey, A new review of the chlorites. *Mineralog. Mag.*, **30**, 277–292 (1954).

From consideration of 117 analyses, a new classification is suggested which retains the following names:

Orthochlorites—corundophilite, pseudothuringite, sheridanite, ripidolite, daphnite, clinochlore, pycnochlorite, brunsvigite, pennine, diabantite, and talc-chlorite. For the oxidized chlorites (Fe_2O_3 more than 4%)—thuringite and its variety klementite, chamosite, and delessite. The following are varieties and the names can be discarded: aphrosiderite (=ripidolite), bavalite and metachlorite (daphnite), berlauite, chloropite, euralite, and hallite (delessite), grochauite (sheridanite), leuchtenbergite (clinochlore), loganite and pyrosclerite (pennine), subdelessite (chamosite), also rumpfite and pseudophite, which fall into two of the new groups. Doubtful species include batavite, epichlorite, epiphanite, moravite, parathuringite, phyllochlorite, steatargillite, and strigovite.

Discussion: We need more of this.

M. F.

DISCREDITED MINERALS

Arnimite (=Antlerite?)

P. Kokkoros, Antlerit aus Lavrion. Eventuelle Identiat des Arnimits mit Antlerit. *Tachermaks Mineralog. petrog. Mitt.*, **3**, 295–297 (1953).

Arnimite (Weisbach, 1886) was described as a calcium-free variety of devillite with formula $Cu_5(SO_4)_2(OH)_6 \cdot 3H_2O$. Frondel (*Dana's System*, 7th Ed., Vol. **2**, p. 592) states that he "found an authentic specimen to be sensibly orthorhombic with *nX* 1.720±0.003. The five darkest powder lines are *d* 4.84, *I* 10; 3.60, 9; 2.68, 8; 2.57, 8; 2.13, 8."

Kokkoros points out that Frondel's *x*-ray data agree well with the strongest lines of the powder diagram given by antlerite, $Cu_3(SO_4)(OH)_4$, which has *nX* 1.724−1.726.

M. F.

Jurupaite (=Xonotlite)

H. F. W. Taylor, The identity of jurupaite and xonotlite. *Mineralog. Mag.*, **30**, 338–341 (1954).

X-ray study of jurupaite and xonotlite, both from the type localities, showed them to be identical with $a=8.50$, $b=7.32$, $c=7.05$ Å, beta 90°±1°. The compositions differ in that jurupaite was reported to contain 4.19% MgO and much more water than xonotlite.

M. F.

Falkenhaynite (=Tetrahedrite)

Jan Kutina, The identity of falkenyaynite with tetrahedrite. *Bull. internatl. Acad. tcheque Sci.*, (**1951**), No. 34, 5 pp.

Falkenhaynite (Scharizer, 1890) has been considered a dubious species, probably tetrahedrite. Spectrographic and *x*-ray study of the type material show it to contain Cu and Sb as essential elements, Ag, As, Fe, and Zn as subordinate to insignificant, and to give a powder pattern (a_0 10.357 Å) identical with that of tetrahedrite.

M. F.